NASA CR-797

PARAMETRIC STUDY OF ADVANCED MULTISTAGE AXIAL-FLOW COMPRESSORS

By M. L. Miller and A. C. Bryans

Prepared under Contract No. NAS 3-7277 by
ALLISON DIVISION
General Motors
Indianapolis, Ind.

for Lewis Research Center

NATIONAL AERONAUTICS AND SPACE ADMINISTRATION

For sale by the Clearinghouse for Federal Scientific and Technical Information
Springfield, Virginia 22151 – CFSTI price $3.00

FOREWORD

The research described herein, which was conducted by the Allison Division, General Motors, was performed under NASA Contract NAS 3-7277. The work was done under the technical management of Mr. William L. Beede, Airbreathing Engines Division, NASA-Lewis Research Center, with Mr. L. Joseph Herrig, Fluid System Components Division, NASA-Lewis Research Center, as research advisor.

ABSTRACT

A parametric study of compressor design parameters was made by analyzing results of compressor flow paths for a 9.0:1 overall pressure ratio and 12.0-inch inlet tip radius. The flow paths were computed on the basis of simple-radial-equilibrium and free vortex design. Energy addition was specified through rotor tip diffusion factor. The rotor tip diffusion factor is reduced if limit values were exceeded on stator hub Mach number, stator hub diffusion factor and rotor relative exit hub flow angle. Effects of independent parameters defined as tip speed, rotor tip diffusion factor, axial inlet velocity, axial velocity ratio, inlet hub-tip radius ratio, stage efficiency and ramp angles were evaluated.

PARAMETRIC STUDY OF ADVANCED MULTISTAGE AXIAL-FLOW COMPRESSORS

by

M. L. Miller and A. C. Bryans

Allison Division, GM

SUMMARY

This technical report presents the results of a parametric multistage compressor study of which the primary objective is to indicate productive areas of study and research development for increasing average stage pressure ratio and reducing compressor overall length. The secondary objective is to correlate compressor design independent parameters and loading parameters to show their effects on average stage pressure ratio and to present them in one compressor design report for reference.

The parametric study is based on simple-radial-equilibrium compressor design philosophy with constant efficiency radially, free-vortex energy addition, and zero whirl velocity into each rotor. A compressor design computer program was specially devised for this study to compute compressor flow paths with the first rotor inlet conditions given in complete detail and also given are arbitrary energy addition, tip speed, axial velocity out of each row, solidities, aspect ratios, hub ramp angle limits, and tip ramp angle limits. The compressor design program has the capability of reducing aspect ratio from initial values if required to reduce the annulus area to satisfy continuity. It also is capable of reducing energy addition from initial values if required to prevent stator hub diffusion factor, stator hub Mach number, or rotor relative hub exit flow angles from exceeding prescribed values. This compressor design program permits the assessment of the effects of design independent parameters on average stage pressure ratio and compressor length as restricted by aerodynamic parameter and geometric limits.

The design program was used in the parametric study by analyzing results of compressor flow paths for a 9.0:1 overall pressure ratio and 12.0-in. inlet radius. Free-vortex energy addition was specified by rotor tip diffusion factors. To study the effects of independent parameters defined as tip speed, rotor tip diffusion factor, axial inlet velocity, rotor tip axial velocity ratio, inlet hub-to-tip radius ratio, stage efficiency, hub ramp

angle, and tip ramp angle, three classes of compressor study were defined. Class I considered the effects of rotor tip diffusion factor, tip speed, axial inlet velocity, and stage efficiency without aerodynamic parameter limits. Class II considered the effects of rotor axial velocity ratio where stage axial velocity ratio was held constant at unity, tip speed, and stage efficiency with two levels of rotor tip diffusion factor and one set of aerodynamic parameter limits. Class III considered the effects of tip speed, axial inlet velocity, hub-to-tip radius ratio, hub ramp angle, tip ramp angle, and stage efficiency with one set of aerodynamic parameter limits.

The principal results of this study are:

1. Significant gains in achieving higher average stage pressure ratio can be made by advancing rotor tip and stator hub diffusion factor technology and employing this capability with state-of-the-art technology of relative inlet Mach number (i.e., tip speed) and stator hub Mach number.

2. Significant gains in achieving higher average stage pressure ratio can be made by advancing rotor relative inlet Mach number technology and employing this capability with state-of-the-art technology of rotor tip diffusion factor, stator hub diffusion factor, and stator hub Mach number.

3. As rotor tip and stator hub diffusion factor technologies are increased to higher levels, a condition will be reached wherein state-of-the-art stator hub Mach number technology must also be advanced.

4. As rotor tip and stator hub diffusion factor technologies are increased to higher levels, a condition will be reached wherein rotor hub turning past the axis will become critical for state-of-the-art tip speed. Further advances will require increases in tip speed and relative Mach number technology.

5. As rotor axial velocity ratio is increased while maintaining unity stage axial velocity ratio, stator hub diffusion factor and stator hub Mach number are increased significantly while rotor hub turning is approximately constant.

6. Compressor overall length is primarily dependent on the number of stages and hence the average stage pressure ratio level for a given overall pressure ratio.

7. Compressor overall length can be reduced significantly by advancing compressor design technology on radial flow effects as a result of higher hub and tip ramp angles.

INTRODUCTION

The work reported herein was performed under contract NAS3-7277 for the NASA-Lewis Research Center to make a parametric compressor study on advanced multistage axial-flow compressors. The purpose of this study is to examine a wide range of design parameters to determine their effects on average stage pressure ratio and compressor length and to indicate significant areas for study and research. No previous work with sufficient completeness and generality has been published to define the design parameter effects which would enable the determination of the significant areas for study and research. A second purpose of this study, therefore, is to present the design parameter results in one compressor design report for reference.

To obtain the effects of the design parameters on average stage pressure ratio and compressor length, it was necessary to devise a compressor design program to compute the flow path for arbitrary specified conditions. Since this program was meant to be useful for rapid and relatively inexpensive screening of designs and for showing the effects of wide variations in values of design parameters, the simple-radial-equilibrium design philosophy was selected. Constant polytropic efficiency radially was selected also to avoid time consuming calculation and analysis of blade element losses in the screening process.

SYMBOLS

Note: The primary symbols are illustrated schematically in Figure 1.

AR	aspect ratio
b	blade row axial length, in.
B, C, D, E	constants in tangential velocity equation
c_p	constant pressure specific heat, $BTU/lb_m-°R$
D	diffusion factor
g_c	gravitational constant, $ft-lb_m/lb_f-sec^2$
H	total enthalpy, BTU/lb_m
J	mechanical equivalent of heat, $ft-lb_f/BTU$
L	compressor length, in.
M	Mach number
$\mathcal{M}$	molecular weight, $lb_m/mole$
n	stage number
N	number of stages
P	total pressure, $lb_f/in.^2$
R	radius, in.
R_c	total pressure ratio
R, θ, z	cylindrical coordinates
T	total temperature °R
U	wheel speed, ft/sec
V	gas velocity, ft/sec
$\dot{w}$	flow rate, lb_m/sec

Greek

α	ramp angle, degrees
β	flow angle, degrees
γ	ratio of specific heats
δ^*	blockage factor
η_{PR}	polytropic rotor efficiency
η_{PS}	polytropic stage efficiency
ω	angular velocity, rad/sec
ρ	gas density, lb_m/ft^3
σ	solidity (chord/spacing)

Subscripts

f	fraction of stage
H	hub
i	inlet
n	stage number
o	outlet
ov	overall
R	rotor or radial direction
S	stator
T	tip
z	axial direction
1	rotor inlet
2	stator inlet
θ	tangential direction

Superscript

'	relative value

DESCRIPTION OF COMPRESSOR DESIGN PROGRAM

A brief description of the compressor design program (described in detail in Reference 1) is given here to provide a better understanding of the analytical approach and of the results obtained. The design program is based on simple-radial-equilibrium flow theory with constant efficiency radially (i.e., zero entropy gradient). The basic equations of motion which lead to the simple-radial-equilibrium flow theory with constant efficiency radially have been derived in many reports such as Reference 2. The resultant equations of motion are:

Continuity Equation

$$\dot{w} = 2\pi \int_{R_H}^{R_T} \rho V_z \, R dR \tag{1}$$

Radial Equation of Motion

$$g_c J \frac{\partial H}{\partial R} = \frac{V_\theta}{R} \frac{\partial (RV_\theta)}{\partial R} + V_z \frac{\partial V_z}{\partial R} \tag{2}$$

Energy Equation

$$\Delta H = \omega \Delta (RV_\theta)/(g_c J) \tag{3}$$

The usual method of solution of this set of equations is to specify an efficiency or total pressure loss, flow path geometry, and energy addition through total enthalpy change or exit tangential velocity. With the blade row inlet conditions known, the exit velocity conditions are then determined iteratively through Equations (1) and (3).

The objectives of this compressor design program, however, are (1) that the flow path of a compressor for a given overall pressure ratio is determined, (2) that resultant aerodynamic parameters (defined as stator hub Mach number, rotor relative hub exit flow angle, and stator hub diffusion factor) must be less than or equal to a specified value, and (3) that blade aspect ratio is equal to or less than an initial value as required by specified limit values of hub and tip ramp angle.

To accomplish these objectives, it is required that energy addition be determined through rotor tip diffusion factor, axial velocity ratio at the tip, and a specified form for tangential velocity distribution. Once the energy addition has been determined, the blade row exit annulus area is determined.

With appropriate hierarchy established on the limit ramp angle, the exit annulus area can be located radially and the aerodynamic parameter values calculated. If the aerodynamic parameter limits are exceeded, the rotor tip diffusion factor must be reduced to lower the aerodynamic parameter values.

Rotor tip diffusion factor and tip axial velocity ratio are two parameters exerting a controlling influence on stage configuration. For the case of a rotor having defined inlet and outlet radii and a defined tip solidity, these two parameters define stage energy addition. With these values known, the equation for diffusion factor at the rotor tip may be resolved to give outlet absolute tangential velocity and, from this, energy addition.

The absolute tangential velocity at the rotor exit is defined by the nonlinear functional relationship:

$$V_{\theta 2} = \frac{B}{R_2} + C + DR_2 + ER_2^2 \qquad (4)$$

where B, C, D, and E are constant coefficients. To use this expression for the radial evaluation of tangential velocity, some arbitrary method of determining the coefficients must be adopted since only one boundary condition (i.e., at the tip) is known. It was decided to set values for the usually less prominent coefficients C, D, and E and compute a value for B. This decision was influenced by the fact that assigning a value of zero to C, D, and E results in a free-vortex type velocity distribution.

The program commences by defining conditions at the rotor inlet—hub-to-tip radius ratio, tip speed, tip axial velocity, and the absolute tangential velocity distribution. Assuming stagnation pressure and temperature to be uniform radially, the axial velocity distribution is determined by integrating the radial equilibrium equation. The mass flow is determined by integrating the flow derivative in the radial direction. Having determined the axial velocity distribution at the rotor inlet, all other aerodynamic quantities may be readily calculated.

To determine rotor outlet conditions, values must be assigned to the rotor tip diffusion factor and tip axial velocity ratio. Further, to define the axial location of the rotor exit station an aspect ratio is required. This aspect ratio is interpreted as the result of dividing the difference of the tip and hub radii at the rotor inlet station by the axial projected distance between inlet and exit stations.

To account for nonisentropic compression, a rotor efficiency is required. This is assumed constant radially.

The rotor outlet conditions are determined by an iterative procedure which commences by setting the exit hub and tip radii equal to the inlet. From the rotor tip diffusion factor, tip solidity, and axial velocity ratio, the tip absolute tangential velocity is established and from this boundary condition, the tangential velocity distribution across the annulus may be established. The energy transfer and stagnation pressure rise may now be calculated.

Since all the radial variables in the equilibrium equation are now known, this equation may be numerically integrated and, from the boundary condition of a defined tip axial velocity, a constant of integration evaluated. This results in an axial velocity distribution across the annulus at the rotor exit station. From the radial distribution of axial velocity, the rate of change of flow with respect to radius may be established and integrated numerically to give the flow through the rotor exit station. If this flow does not coincide with the rotor inlet flow, the hub radius is increased (or decreased) and the calculation repeated until convergence occurs.

Once the calculation converges on mass flow, the rotor hub ramp angle is calculated and checked against an assigned limit. If the hub ramp angle violates the assigned limit, the rotor exit hub radius is then set at a value for which the limit is attained and the rotor exit tip radius reduced to the point which satisfies the flow requirements. Should the reduction of the rotor exit tip radius cause a violation of the assigned tip ramp angle limit, then the aspect ratio is reduced with hub and tip ramp angles set at their assigned limits and the calculation is repeated until continuity of flow is obtained.

Having satisfied ramp angle tests and continuity of flow, the program now tests the absolute Mach number and relative flow angle at the exit of the rotor hub. If either of these parameters (in this stated order) violates its assigned limit, the program then reduces the rotor tip diffusion factor and repeats the calculation until these limit tests are satisfied.

The calculation now proceeds to establish stator exit conditions. To determine the stator exit annulus, the coefficients in a polynomial identical to the one defining absolute tangential velocity at the rotor exit, Equation (4), are required. An overall stage efficiency, stator hub solidity, tip axial velocity ratio, and aspect ratio are also required.

The stator exit calculations commence similar to those for the rotor by setting the exit hub and tip radius equal to the inlet values. The hub and tip ramp angles are then tested in the same order as the rotor and the aspect ratio relaxed if necessary to satisfy the geometric limits. When the assigned geometric limits have been satisfied, the stator hub diffusion factor

is checked against its assigned limit. If this limit is violated, the rotor tip diffusion factor is reduced and the calculation repeated for the current stage.

When a stage configuration, satisfying all limits, is achieved, the pressure ratio and energy addition are mass averaged to give stage performance. Successive stages are added until some predetermined limit in overall pressure ratio is achieved. If the limit in overall pressure ratio cannot be exceeded in a predetermined maximum number of stages, the calculation is terminated and the values calculated up to this point are printed out.

The logic of the program is restricted to consider only tip radii at any station which is equal to or less than the inlet blade tip radii. Positive tip ramp angles cannot occur.

A detailed description of the program logic development and additional program capabilities and limitations are given in Reference 1.

ANALYTICAL APPROACH

PARAMETRIC COMPRESSOR STUDY OBJECTIVES

The objectives of this parametric compressor study, based on simple-radial-equilibrium with constant efficiency radially, are to (1) delineate the interrelating effects of the aerodynamic parameters and independent parameters on stage pressure ratio and overall length, (2) relate the parameters with present state of the art, and (3) indicate productive areas for compressor aerodynamic research and development. The productive areas of research and development are to be aimed at increasing average stage pressure ratio capability and reducing length for a multistage compressor.

The aerodynamic parameters, which can be controlled by limiting values, are defined as stator hub Mach number, rotor relative hub exit flow angle and stator hub diffusion factor. Independent parameters are tip speed, rotor tip diffusion factor, axial inlet velocity, axial velocity ratio, polytropic stage efficiency, inlet hub-to-tip radius ratio, hub ramp angle, and tip ramp angle.

Because of the many parameters involved and their interdependence, it is desirable to define an area of study which considers a reduced number of parameters that delineates the major effects. Additional areas may then be considered to show the secondary effects. These areas are divided into classes as follows:

Class I. The objective of this class is to determine the effect of varying tip speed, axial inlet velocity, and rotor tip diffusion factors. Aerodynamic parameter limits were not imposed. Hence, each compressor flow path represents a maximum average stage pressure for each rotor tip diffusion factor distribution, and the aerodynamic parameters will not be limiting. The resultant plots of average stage pressure ratio versus tip speed show the effects of various levels of independent parameter limits and permit superposition of curves for selected values of aerodynamic parameter limits.

Class II. The objective of this class is to determine the effect of varying tip speed and rotor axial velocity ratio. The stage axial velocity ratio was held constant at a value near unity. A single level of aerodynamic parameter limits was imposed.

Class III. The objective of this class is to determine the effect of varying tip speed and rotor inlet hub-to-tip radius ratio. Larger values of hub and tip ramp angle limits were permitted to assess their effect on the aerodynamic parameters and compressor length. A single level of aerodynamic parameter limits was imposed.

METHOD OF ANALYSIS

The method of approach used to accomplish the study objectives was to select a compressor design application requiring an overall pressure ratio of 9.0:1 with an inlet tip radius of 12.0 in. Inlet guide vanes were not used in this study and the flow has zero whirl at the inlet of each rotor. Each compressor design was computed on the basis of free-vortex energy addition and radially constant efficiency which results in a constant axial velocity radially for the simple-radial-equilibrium calculation.

Compressor flow paths were then computed for various combinations of independent parameters while limiting the flow path ramp angles with hub and tip ramp angle limits. For Classes II and III, stage energy addition was also limited by imposing aerodynamic parameter limits. Stage energy addition is specified through the rotor tip diffusion factor, which is reduced if necessary by a specific level of aerodynamic parameter limit until that level of aerodynamic parameter limit was identically satisfied. Flow path geometry is specified through blade aspect ratio, which is reduced if necessary when the tip ramp angle limit is exceeded. The aspect ratio was reduced until continuity was satisfied with the hub and tip ramp angle identically equal to their limit values. The tip ramp angle was reduced from zero only after the hub ramp angle attained its limit value.

Throughout this study the input value of rotor tip diffusion factor for each stage is described by a set of three numbers (D_{RT_1}, D_{RT_2}, $D_{RT_{3-N}}$) which are defined as:

D_{RT_1}	first stage rotor
D_{RT_2}	second stage rotor
$D_{RT_{3-N}}$	third to N'th stage rotor

In general, these input values are used as reference values in describing various results, even though they may have been reduced.

The range of independent variable input data for each compressor class is summarized in Table I. Input data that were not varied and are common to all classes are summarized in Table II. Tables III through V summarize the variable input data defining each compressor case considered for the three classes.

The chord was assumed constant with radius, so that solidity varies inversely with radius for all blade rows. It was convenient to express efficiency as polytropic stage efficiency, since then an assumed value could realistically be held constant for all stages of a compressor. In addition to the stage efficiency value, it was necessary to assume or develop an

equivalent value for rotor polytropic efficiency, which reflected the absence of stator losses. An analysis of the effect of stator losses on efficiency for a variety of design conditions and pressure ratios to 1.7 showed that assuming rotor polytropic efficiencies to be 0.02 point higher than stage values gave a good approximation for stator loss effects. The stator total pressure loss would be approximately constant for the range of variables of this study.

Since the overall pressure ratio computed for each case was 9.0:1 or greater, it was necessary to fractionalize the last stage in each calculation to obtain 9.0 to provide a common base for weighing the average stage pressure ratio and comparing compressor length. The fractionalizing of the last stage was done on the basis of energy addition and can be expressed as:

$$n_f = \frac{(T_N)_{(R_c = 9.0)} - (T_{N-1})_{calc}}{(T_N)_{calc} - (T_{N-1})_{calc}} = \frac{\left\{ \frac{9.0}{\left[(R_c)_{N-1}\right]_{calc}} \right\}^{\frac{\gamma - 1}{\gamma \eta_{PS}}} - 1}{\left\{ \frac{(R_c)_{N_{calc}}}{\left[(R_c)_{N-1}\right]_{calc}} \right\}^{\frac{\gamma - 1}{\gamma \eta_{PS}}} - 1} \tag{5}$$

The average stage pressure ratio and compressor length is then computed as follows:

$$R_{c_{avg}} = [9.0]^{\frac{1}{(N-1) + n_f}} \tag{6}$$

$$L = \sum_{i=1}^{N-1} (L_i) + n_f L_N \tag{7}$$

RESULTS AND DISCUSSION

A complete summary of all the compressor performance and aerodynamic parameter output results for this parametric study are given in Tables VI, VII, and VIII for Classes I, II, and III, respectively. The various effects on stage pressure ratio, compressor length, and state-of-the-art technology of the aerodynamic parameters are discussed in the following paragraphs.

EFFECTS OF TIP SPEED AND ROTOR TIP DIFFUSION FACTOR

The compressor performance and aerodynamic parameter results discussed here are taken from the Class I compressor data of Table VI. The Class I results are distinct from Classes II and III in that aerodynamic parameter limits were not imposed. The input rotor tip diffusion factors were not reduced, therefore, and the aerodynamic parameters and average stage pressure ratios obtained are at a maximum value for each tip speed and D_{RT} within the analytical model.

Average Stage Pressure Ratio

Typical results of average stage pressure ratio, as affected by variations in tip speed and variations in rotor tip diffusion factor, are shown in Figures 2 and 3, respectively. Figure 2 shows that average stage pressure ratio increases with increasing tip speed with constant D_{RT}, V_{z1} and η_{PS}. Figure 3 shows that average stage pressure ratio increases with increasing rotor tip diffusion factor at constant U_{T1}, V_{z1} and η_{PS}.

The average stage pressure ratios indicated at the combinations of tip speeds and rotor tip diffusion factor levels considered, yield a significant increase above present production engine compressor average stage pressure ratios of about 1.4. Increase in either tip speed or rotor tip diffusion factor will, of course, alter other aerodynamic requirements such as stator Mach number and diffusion factor. This study evaluates the relative change of magnitude of the parameter. However, no attempt will be made to evaluate the complexity of achieving advances in aerodynamic technology.

Aerodynamic Parameters and Relative Inlet Mach Number

The maximum value of aerodynamic parameter or relative inlet Mach number, regardless of the stage number for which it occurs, can be obtained for each Class I compressor case. In general, maximum values of rotor relative inlet tip Mach number, rotor relative exit hub flow angle, and stator hub Mach number occurred in the first stage and stator hub diffusion factor in the third stage. Typical plots of D_{SH}, M_{SH} and β'_{2H} versus stage number for the Class I D_{RT} of 0.5, 0.6, and 0.7 data illustrating the foregoing statement on maximum values at a given stage number are shown in Figure 4. A study of Tables VI through VIII also shows this general

rule. The maximum values obtained were found to correlate and, therefore, establish trends and magnitudes. The correlated results (Figures 5, 6, and 7) are shown superimposed on the pressure ratio versus tip speed plot of Figure 2.

In the previous paragraph the term maximum value was used to describe the level of rotor relative exit hub flow angle. For the conventional system of definition, the relative flow angle decreases toward zero and then to negative values as energy addition increases with all remaining variables constant. Thus, the relative flow angle tends toward a minimum value. For simplicity of discussion, however, when taking the aerodynamic parameters as a group, the term maximum value will be used in the sense that the actual flow angle value results in a maximum flow turning value at the rotor hub.

The rotor tip relative inlet Mach number is a function of only the tip speed for a fixed axial inlet velocity and zero tangential inlet whirl. Hence, the tip relative inlet Mach number values are easily shown on a scale parallel to tip speed in Figures 5 through 7 which show the effect of U_{T1} and D_{RT} on maximum values of M_{SH}, β'_{2H} and D_{SH}. The data shown in Figures 5 through 7 are also typical of all compressor cases studied.

The significant result shown in Figures 4, 5, and 7 are that maximum stator hub Mach number and stator hub diffusion factor are essentially constant for a given rotor tip diffusion factor level (i.e., independent of tip speed). The maximum rotor relative hub exit flow angle is dependent on both U_{T1} and D_{RT}. In addition, as shown by the 0° exit angle line on Figure 6, if turning past the axial direction is to be prevented, an upper limit of D_{RT} level exists for each tip speed. Turning the flow past the axial direction can result in a positive slope pressure ratio versus flow rate characteristic which is an unstable condition in that an attempt to increase pressure ratio leads to a flow decrease which further decreases the pressure ratio capability.

Inlet guide vanes, although not considered in this study, can be employed to reduce the relative inlet Mach number level of the first stage rotor. Assuming that the energy addition across the rotor would be held constant at a given tip speed, the employment of inlet guide vanes would result in greater rotor blade flow turning and higher diffusion factors. Stator vane diffusion factors would also increase if stator outlet conditions are held the same as for the case with no inlet guide vane turning. If the increase in rotor tip diffusion factor is unacceptable, either the energy addition must be reduced or the inlet guide vane turning reduced.

In summarizing, if only tip speeds are increased to obtain higher average stage pressure ratio, only rotor relative inlet Mach number technology need be advanced. If rotor tip diffusion factor technology is

advanced, then M_{SH} and D_{SH} technology as well as the degree of flow turning past the axial direction must be considered.

State-of-the-Art Aerodynamic Technology

For such a study to be useful in indicating areas to concentrate further research efforts, the interrelations and interdependencies of M'_{1T} on U_{T1}, M_{SH} and D_{SH} on D_{RT}, and β'_{2H} on U_{T1} and D_{RT} must be evaluated with respect to present state-of-the-art capabilities.

To indicate the aerodynamic parameter and relative inlet Mach number advances required beyond present technology levels to increase the present average stage pressure ratio capability, a state-of-the-art compressor aerodynamic technology must be defined. For double circular arc blades of positive camber, the following values are selected as representative.

First stage rotor	$M'_{1T} \cong 1.20$ and $D_{RT_1} \cong 0.40$
First stage stator	$M_{SH_1} \cong 0.9$ and $D_{SH_1} \cong 0.45$
Mid stage rotor	$M'_{nT} \lesssim 1.0$ and $D_{RT_n} \cong 0.45$
Mid stage stator	$M_{SH_n} \lesssim 0.9$ and $D_{SH_n} \cong 0.58$

Selection of a limiting value for β'_{2H} to prevent an unstable operating characteristic depends upon the net flow turning past the axial direction behind each rotor and its stagewise averaging effect. Therefore, a selected value of β'_{2H} is somewhat arbitrary. It is known that some turning past axial in the hub region is acceptable since the overall effect for the rotor depends on the average pressure along the radial length. For purposes of discussion and calculation, a limiting value of -15° was selected as representative.

Based on the aforementioned state-of-the-art aerodynamic technology levels, the rotor tip diffusion factor levels, comparable with the Class I compressor cases, would be about 0.3, 0.4, and 0.5. The resultant maximum average stage pressure ratio of 1.416 is found to be obtainable with the present aerodynamic technology as given in Figures 5, 6, and 7. The limiting parameter for this maximum stage pressure ratio is found to be the relative inlet Mach number of 1.2 (U_{T1} = 1140 ft/sec). This state-of-the-art technology is shown as Case A in Table IX.

Effects of Advancements in Technology

Average stage pressure ratio can be increased at this tip speed level of Case A by increasing D_{RT}. Increasing rotor tip diffusion factor to 0.5,

0.6, and 0.7 and $D_{SH_{max}}$ to 0.68 results in an average stage pressure ratio of 1.65, $M_{SH_{max}}$ of 0.91, and $\beta'_{2H} = -15°$ (Case B, Table IX). Thus, no stator hub Mach number technology advance is required. Note also that the flow turning past the axial direction is becoming limiting and further advances in D_{RT} and D_{SH} levels may not be desirable from the standpoint of unstable pressure ratio-flow rate constant speed characteristic.

By increasing tip speed to 1400 ft/sec at a 0.3, 0.4, and 0.5 D_{RT} level, an average stage pressure ratio of 1.565 can be obtained. This procedure requires only a relative inlet Mach number technology advance to about 1.41 (Case C, Table IX). A tip speed of about 1510 ft/sec, which yields an M'_{1T} of about 1.53, would be required to obtain an average stage pressure ratio of 1.65.

Combining the aforementioned technology advances of D_{RT}, D_{SH}, and M'_{1T} would result in an average stage pressure ratio of about 1.885. The maximum stator hub Mach number remains at the state-of-the-art technology level, and the flow turning past the axial is not limiting (Case D, Table IX).

In summarizing the foregoing discussion for the 600 ft/sec axial inlet velocity condition and the Class I input data conditions, it has been shown that rotor tip and stator hub diffusion factors could be advanced to a specific level from present technology to increase stage pressure ratio without advanced technology on stator hub Mach number and relative inlet Mach number. Similarly, relative inlet Mach number can be advanced to a very high level without advancing the aerodynamic parameters as defined in the second paragraph in the section Analytical Approach. At a point where the relative hub exit flow angle becomes limiting, aerodynamic advancement is required on all parameters. Average stage pressure ratio obtainable is found to be about 1.65 by advancing only the rotor tip and stator hub diffusion factor from present technology (Case B, Table IX). To obtain equal average stage pressure ratio by advancing only relative inlet Mach number from present technology, a Mach number advance to about 1.51 is required. For the rotor tip diffusion factors of 0.5, 0.6, and 0.7, maximum stator hub diffusion factor of 0.68 and relative inlet tip Mach number to 1.42 (tip speed of 1400 ft/sec), average stage pressure ratios of 1.9 can be obtained. Based on these results, it is not clear if aerodynamic advancement on diffusion factors or relative Mach number is preferred since the measure of difficulty to obtain these achievements is not known. The advancement of both diffusion factors and tip speed aerodynamic capabilities should be pursued. It should be renoted that these limit parameters are based on simple radial equilibrium and that inclusion of curvature and entropy terms in the solutions might change the absolute number but should not alter the trends appreciably.

EFFECT OF AXIAL INLET VELOCITY LEVEL ON STAGE PRESSURE RATIO AND THE AERODYNAMIC PARAMETERS

Compressor case results from Class I, Table VI, for identical input data, except for the 700 ft/sec inlet velocity, are shown plotted in Figures 8 through 11. Figures 8 through 11 show, in an identical manner as Figures 2 and 5 through 7, the effects of U_{T1} and D_{RT} on average stage pressure ratio, $M_{SH_{max}}$, $\beta'_{2H_{max}}$ and $D_{SH_{max}}$.

The higher axial inlet velocity is desirable primarily on the basis of increasing flow rate per unit frontal area. A cursory study of Figure 8 indicates that greater average stage pressure ratios for a given U_{T1} and D_{RT} can be obtained. Additional study with respect to equal rotor relative inlet Mach number and rotor tip diffusion factor levels shows that essentially no gain in average stage pressure ratio can be experienced in going from 600 to 700 ft/sec. In addition, for the same values of M'_{1T} and D_{RT}, stator hub Mach numbers are greater.

At the state-of-the-art technology level, the limiting aerodynamic technology parameter is the relative inlet Mach number of 1.2. Extrapolating the 0.3, 0.4, and 0.5 D_{RT} curve in Figures 8 through 11 to the 1080 ft/sec tip speed equivalent of $M'_{1T} = 1.2$, the average stage pressure ratio obtainable is found to be about 1.41 (see Case E, Table IX). This average stage pressure ratio value is equivalent to Case A of Table IX. The stator hub Mach number for Case E is 0.78 as compared to 0.72 for Case A.

As a second comparison for the 700 ft/sec axial inlet velocity, Case F in Table IX shows that an average stage pressure ratio of about 1.915 can be obtained for the $M'_{1T} = 1.42$ and D_{RT} of 0.5, 0.6, and 0.7. A comparison with Case B in Table IX shows a gain of 0.03 points in average stage pressure ratio but with an increased stator hub Mach number to 1.01. Case G in Table IX shows that holding to a maximum stator hub Mach number of 0.91 at M'_{1T} of 1.42 results in a maximum average stage pressure ratio of 1.77 at D_{RT} of about 0.42, 0.52, and 0.62.

In summarizing the foregoing discussion for the 700 ft/sec axial velocity condition and the Class I input data, it has been shown that for a given tip speed and rotor tip diffusion factor level without consideration of aerodynamic parameter technology, significant increases in average stage pressure ratio can be experienced. With consideration of equal aerodynamic technology levels on D_{RT}, $D_{SH_{max}}$ and $M'_{1T_{max}}$, the gains in average stage pressure ratio in going from 600 to 700 ft/sec are small. In addition, the maximum stator hub Mach number is appreciably larger for the higher axial inlet velocity. In an actual compressor design, it may be possible to increase

the pressure ratio of the rear stages by axial velocity increase without exceeding aerodynamic parameter limits. An 11.3% increase in equivalent flow per unit annulus area can be realized, however, by increasing the axial velocity from 600 to 700 ft/sec.

EFFECT OF TIP SPEED AND ROTOR TIP DIFFUSION FACTOR ON COMPRESSOR LENGTH

In brief review of the method of analysis, it will be recalled that each compressor case analyzed was initialized with aspect ratios of 4.0, 3.5, and 2.5 for the first, second, and third to N'th stage, respectively. These aspect ratios were reduced (and length increased) only when the tip and hub ramp angles exceeded their limiting values. The overall length results for the Class I compressor case analyses at 600 ft/sec axial inlet velocity are shown in Figure 12. The tip and hub ramp angle limits were -10° and +30°, respectively, and the hub-to-tip radius ratio at the inlet to the first rotor blade row was 0.5 for these compressor cases.

The overall compressor length decreases with increasing tip speed and increasing rotor tip diffusion factor. It can be shown, however, that the average stage lengths for all cases are approximately equal (i.e., compressor length/number of stages). Therefore, the length reduction is due to the number of stages as affected by average stage pressure ratio for the overall pressure ratio of 9.0:1.

An examination of the hub and tip ramp angles row by row as given in Table VI indicates that large hub and tip surface slope inflections occur. In an actual application, these surfaces would require smoothing by either a change in aspect ratio or axial velocity ratio. It is believed, however, that the general trend of the overall length results are valid.

With respect to axial inlet velocity effects, the increase from 600 to 700 ft/sec will have negligible effect on the length results shown in Figure 12. This is based on the fact that overall length was primarily dependent on average stage pressure ratio. On the basis of comparison of average stage pressure ratio with the 600 ft/sec axial inlet velocity at equal M_{1T}' and D_{RT} levels, no significant change in average stage pressure ratio was found.

EFFECTS OF OTHER INDEPENDENT PARAMETERS

Polytropic Stage Efficiency

The effect of polytropic stage efficiency on average stage pressure ratio and the aerodynamic parameters is shown in Figure 13. These data were taken from Table VI. Figure 13 shows that for small efficiency changes

there is essentially no effect on the aerodynamic parameters within the range of rotor tip diffusion factor and tip speeds investigated. The effect of efficiency on average stage pressure ratio is dependent on the reference pressure ratio level in question. Stage pressure ratio increases of 2.2% at D_{RT_1} = 0.3 and U_{T1} = 1000 ft/sec and 4.7% at D_{RT_1} = 0.6 and U_{T1} = 1400 ft/sec were obtained for a stage polytropic efficiency change from 85 to 90%.

Rotor Axial Velocity Ratio

Class II compressor cases were computed for similar parametric conditions as in Class I, except for the addition of rotor axial velocity ratio variations. The stator axial velocity ratio for each case was correspondingly varied to maintain a stage axial velocity ratio of unity. The overall performance and aerodynamic data, summarized in Table VII, is discussed in the following paragraphs.

Average Stage Pressure Ratio

The effects of rotor axial velocity ratio on average stage pressure ratio are shown in Figures 14 and 15 for rotor tip diffusion factor sets of 0.35, 0.4, and 0.45 and 0.5, 0.6, and 0.7, respectively. It is shown in Figures 14 and 15 that average stage pressure ratio increases with rotor axial velocity ratio. An increase of about 10% in pressure ratio can be obtained in going from a rotor axial velocity ratio of 0.85 to 1.4 for a given D_{RT} and U_{T1}.

Aerodynamic Parameters

Aerodynamic parameter limits ($M_{SH_{lim}}$ = 1.0 and $\beta'_{2H_{lim}}$ = -10°) were imposed on the Class II compressor design calculations. These limits resulted in a reduction in rotor tip diffusion factor for some cases (see Table VII). In general, the violations were not severe except for the cases wherein the rotor axial velocity ratio was 1.4 and D_{RT} was 0.5, 0.6, and 0.7. For these cases, the stator hub Mach number limit of 1.0 reduced the tip diffusion factor and hence the stage pressure ratio significantly. This effect is shown clearly in Figure 15a by the crossover of the 1.4 with the 1.2 axial velocity ratio curves and in Figure 15b by the drop in pressure ratio at the 1.4 axial velocity ratio point.

The increase of rotor axial velocity ratio results in a significant increase in maximum stator hub diffusion factor and stator hub Mach number at a given tip speed and rotor tip diffusion factor. The magnitude of these increases is shown in Figure 16. The maximum rotor hub exit relative

flow angle is not strongly affected by rotor axial velocity ratio with the variation being about 6° to 10° over the range of velocity ratios investigated (see Figure 15). The trend toward negative relative hub exit flow angles at the 1.4 velocity ratio is due to the large negative stator hub ramp angle slope (see Table VI).

Overall Compressor Length

The overall length results are shown in Figure 17. It was previously shown in Figure 12 that overall length is primarily dependent on the number of stages and, therefore, the average stage pressure ratio. Since average stage pressure ratio increased with increasing rotor axial velocity ratio, it would be expected that the overall length would decrease with increasing rotor axial velocity ratio.

The overall length variation shown in Figure 17 does not show this trend even though average stage pressure ratio increased with increasing rotor axial velocity ratio (see Figures 14b and 15b). The cause of this difference in trend is due to the large differences in rotor and stator hub ramp angles as affected by the velocity ratio, that is, small rotor and large stator ramp angles for less than unity rotor velocity ratio with a stage velocity ratio of unity. In some cases, the rotor ramp angle was negative (see Table VII). Conversely, for rotor axial velocity ratios greater than unity, the rotor hub ramp angles were large and the stator hub ramp angles small with some cases being negative. The net effect of the ramp angle variations was to increase blade row chord by either decreasing aspect ratio when the hub ramp angle limits were met at greater than unity velocity ratio or increasing annulus height when the ramp angle was small or negative at less than unity velocity ratio.

The hub and tip ramp angles result in large wall slope inflections for the 0.85 rotor axial velocity ratio at low tip speeds and for the 1.4 rotor axial velocity ratio at the D_{RT} of 0.5, 0.6, and 0.7 (see Table VII). In some of these cases, the hub ramp angles are negative, resulting in larger than average stage length. In an actual application, the flow paths would require smoothing by lowering rotor axial velocity ratios and making appropriate changes in aspect ratio. The net effect for the wall contour smoothing operation would most probably be to increase overall compressor length, since lowering the rotor axial velocity ratio results in reducing stage pressure ratio with a given D_{RT} and U_{T1}.

Effects of Advancement in Technology

A study of the Class II data provides interesting results with respect to the effects of rotor axial velocity ratio and tip speed on the average stage

pressure ratio and aerodynamic parameters. To show these effects, typical compressor cases have been selected. See Table X and Figures 14b and 15b. Selected Case No. 2068 represents a state-of-the-art design with respect to the previously described aerodynamic technology levels.

Compressor Case 2068 with a D_{RT} of 0.35, 0.4, and 0.45, U_{T1} = 1200 ft/sec, and $(V_{zo}/V_{zi})_R$ = 1.0 yields an average stage pressure ratio of 1.416. It has been noted previously that decreasing the rotor axial velocity ratio while holding stage axial velocity ratio enables smoothing of the hub and tip wall contours. This rotor axial velocity ratio reduction also results in lowering of the average stage pressure ratio at constant D_{RT} and U_{T1}.

Case 2080 shows that increasing tip speed to 1400 ft/sec at a D_{RT} of 0.35, 0.4, and 0.45 and a rotor axial velocity ratio of 0.85 will yield an average stage pressure ratio of 1.511. The stator hub Mach number and diffusion factor levels have remained essentially constant with respect to Case 2068. To achieve this objective while maintaining stage efficiency, the relative inlet Mach number technology must be extended to 1.4 levels.

To obtain the same average stage pressure ratio as for Case 2080 at the 1200 ft/sec tip speed, a rotor axial velocity ratio of 1.4 is required. This is shown in Table X as Case 2017 wherein the maximum values of D_{SH} and M_{SH} are about 0.65 and 0.98, respectively. Hence, a significant advancement from the state of the art is required for these two aerodynamic parameters to realize the pressure ratio gain at constant tip speed. Case 2025 is shown to indicate the average stage pressure ratio level of 1.636 if relative inlet Mach number, stator hub diffusion factor, and stator hub Mach number technologies were advanced to about 1.4, 0.65, and 0.98, respectively.

Rotor tip diffusion factor technology advances to 0.5, 0.6, and 0.7 and stator hub diffusion factor advances to 0.75 would yield average stage pressure ratios to about 1.80. Similar compressor cases as discussed previously are shown in Table X to illustrate the identical rotor axial velocity ratio reduction effect for the higher rotor tip diffusion factor.

The cases discussed so far indicate that increases in average stage pressure ratio may be obtained by utilization of axial velocity ratios greater than unity across the rotor blade row. This approach, however, will lead to rather severe hub curvatures. Incorporation of these curvature effects in the design of a compressor may lead to more severe limitations on aerodynamic parameters than indicated by the simple methods of calculation used in this study. As stated previously, fairing of the hub shape to obtain

a smooth contour will result in axial velocity ratios across the rotor of less than one and axial velocity ratios across the stator greater than one.

Hub and Tip Ramp Angles

Compressor design calculations were made to determine the effects of the ramp angles on the average stage pressure ratio, aerodynamic parameters, and overall length. The results of these calculations are given in Table VIII and are referred to as Class III. Input data are identical to the unity axial velocity ratio calculations at D_{RT} of 0.35, 0.4, and 0.45 of Class II, except for hub and tip ramp angle limits of 40° and -20°, respectively, in place of the 30° and -10°.

Average Stage Pressure Ratio

The average stage pressure ratio results, presented in Figure 18, show that pressure ratio is increased by 1 to 2% over the range of tip speeds investigated. This is due to the larger rotor exit radii of each stage through larger hub ramp angle limits. The larger exit radii provide greater work capability for a given D_{RT} and U_{T1}.

Aerodynamic Parameters

The effects of higher allowable ramp angle on the aerodynamic parameters are shown in Figure 18. The magnitude of the change in these parameters is very small. The increase of ramp angle values, however, resulted in a slight increase in $M_{SH_{max}}$, a decrease in $D_{SH_{max}}$, and essentially no change in $\beta'_{2H_{max}}$.

Compressor Overall Length

As shown in Figure 18, the increased ramp angle yields about an 8 to 10% reduction in overall length over the range of tip speeds. Since the average stage pressure ratio increase was about 1 to 2% due to the larger ramp angle, the decrease in overall length was due primarily to the stage length decrease, the stage length being less as a result of decreases in annulus height for fixed values of aspect ratio.

Hub-to-Tip Radius Ratio

Compressor design calculations of Class III were made also to determine hub-to-tip radius ratio effect on average stage pressure ratio, aerodynamic variables, and overall length. These results are summarized in Table VIII. Input data were identical to the previously described Class III cases, except that inlet hub-to-tip radius ratio was varied to 0.4 and 0.6 from 0.5.

Average Stage Pressure Ratio

The average stage pressure ratio is increased about 0.5 to 2.0% over the range of tip speeds investigated at a D_{RT} of 0.35, 0.4, and 0.45 and an increase in rotor inlet hub-to-tip radius ratio from 0.4 to 0.6. These results are shown in Figure 19. As in the case of higher hub ramp angle, the increased pressure ratio is a result of greater work capability due to higher rotor exit radii for a given D_{RT} and U_{T1}.

Aerodynamic Parameters

As inlet hub-to-tip radius ratio increases with all other parameters held constant, significant reductions are obtained in the maximum values of D_{SH}, M_{SH}, and β'_{2H}. See Figure 19. These reductions are of the order of 25% and 12% for D_{SH} and M_{SH}, respectively, in going from a hub-to-tip radius ratio of 0.4 to 0.6. Similarly, the maximum rotor relative hub exit flow angle is reduced about 25°, resulting in 25° less flow turning.

The variation of the aerodynamic parameters is linear with hub-to-tip radius ratio in the range investigated. At the 0.4 hub-to-tip radius ratio point, the stator hub diffusion factor was limited to the 0.5 value for the 1200 and 1400 ft/sec tip speeds. Rotor tip diffusion factors for these two cases were reduced from 0.35 to 0.334 and 0.331 for 1200 and 1400 ft/sec, respectively.

Compressor Overall Length

Reductions in overall length with increasing inlet hub-to-tip radius ratio are significant with all other variables held fixed. See Figure 20a. Overall length-radius ratio reductions are about 25% at 1000 ft/sec tip speed and 30% at 1400 ft/sec tip speed for an inlet hub-to-tip radius ratio change from 0.4 to 0.6. Since the average stage pressure ratio increase was only 0.5 to 2.0% with increasing hub-to-tip radius ratio, the primary effect that decreases overall length-radius ratio is the smaller annulus heights which results in a decrease in stage length for a set value of aspect ratio.

An increasing inlet hub-to-tip radius ratio, however, results in a decreased weight flow rate for a given tip radius or an increased tip radius for the same weight flow rate. The larger tip radius will lead to increased compressor length if the same blade row aspect ratios are maintained. The effect of maintaining equal weight flow rate on compressor length is shown in Figure 20c where the inlet tip radii have been corrected for equal weight flow rate for the 0.5 hub-to-tip radius ratio condition (see Figure 20b). Overall length reductions are about 18% at 1000 ft/sec tip speed and 24% at 1400 ft/sec tip speed from a hub-to-tip radius ratio change from 0.4 to 0.6 at constant weight flow.

SUMMARY OF RESULTS

A parametric compressor study was made on the basis of simple-radial-equilibrium compressor design philosophy with free-vortex energy addition, constant efficiency radially, zero tangential velocity at each rotor inlet, and stage axial velocity ratio of unity. Based on the study results for a multistage compressor design of 9.0:1 pressure ratio and 12.0-in. inlet tip radius, the results are summarized for average stage pressure ratio, overall length, and aerodynamic parameters.

1. Significant gains in achieving higher average stage pressure ratio can be made by advancing rotor tip and stator hub diffusion factor technology and employing this capability with state-of-the-art technology of relative inlet Mach number (i.e., tip speed) and stator hub Mach number.

2. Significant gains in achieving higher average stage pressure ratio can be made by advancing rotor relative inlet Mach number technology and employing this capability with state-of-the-art technology of rotor tip diffusion factor, stator hub diffusion factor, and stator hub Mach number.

3. As rotor tip and stator hub diffusion factor technology are increased to higher levels, a condition will be reached wherein state-of-the-art stator hub Mach number technology must also be advanced.

4. As rotor tip and stator hub diffusion factor technology is increased to higher levels, a condition will be reached wherein rotor hub turning past the axis will become critical for state-of-the-art tip speed. Further advances will require increases in tip speed and relative Mach number technology.

5. As rotor axial velocity ratio is increased while maintaining unity stage axial velocity ratio, stator hub diffusion factor and stator hub Mach number are increased significantly while rotor hub turning is approximately constant.

6. Compressor overall length is primarily dependent on the number of stages and hence the average stage pressure ratio level for a given overall pressure ratio.

7. Compressor overall length can be significantly reduced by advancing compressor design technology on radial flow effects as a result of higher hub and tip ramp angles.

REFERENCES

1. Bryans, A. C. and Miller, M. L., Computer Program for Design of Multistage Axial-Flow Compressors, NASA CR-54530, 1967 (Allison Division, GMC, EDR 4575).

2. Aerodynamic Design of Axial-Flow Compressors, NASA-SP-36, Revised, 1965.

Table I.

Summary of independent variable input data for parametric compressor classes.

Variable	Class I	Class II	Class III
U_{T1}, ft/sec	1000, 1200, 1400 & 1600	1000, 1200 & 1400	1000, 1200 & 1400
D_{RT}	(0.3, 0.4, 0.5), (0.4, 0.5, 0.6), (0.5, 0.6, 0.7) & (0.6, 0.7, 0.8)	(0.35, 0.4, 0.45) & (0.5, 0.6, 0.7)	(0.35, 0.4, 0.45)
$(V_{z1})_T$ ft/sec	600 & 700	600	600 & 700
$(V_{zo}/V_{zi})_T$ rotor	1.0	0.85, 1.0, 1.2 & 1.4	1.0
$(V_{zo}/V_{zi})_T$ stator	1.0	1.15, 1.0, 0.833 & 0.707	1.0
$(R_H/R_T)_1$	0.5	0.5	0.4, 0.5 & 0.6
$(\alpha_H)_{max}$, degrees	30	30	40
$(\alpha_T)_{min}$, degrees	-10	-10	-20
η_{PS}	0.85, 0.875 & 0.90	0.85, 0.875 & 0.90	0.85, 0.875 & 0.90
$(D_{SH})_{max}$	—	0.8 & 1.0	0.5
$(M_{SH})_{max}$	—	1.0 & 1.2	0.8
$(\beta'_{2H})_{min}$, degrees	—	-10	-10
Number of cases	72	81	54

Table II.

Summary of input data for all compressor designs.

Ratio of specific heats	$\gamma = 1.4$
Specific heat at constant pressure	$c_p = 0.24$ BTU/lb_m-°R
Gas molecular weight	$M = 28.97$ lb_m/mole
Rotor inlet tip radius	$R_{T1} = 12.0$ in.
Tip blockage factor—each row	$\delta^*_T = 1.0$ (i.e., zero blockage)
Hub blockage factor—each row	$\delta^*_H = 1.0$ (i.e., zero blockage)
Aspect ratio first stage—initial value	$AR_1 = 4.0$
Aspect ratio second stage—initial value	$AR_2 = 3.5$
Aspect ratio third to last stage—initial value	$AR_{3-N} = 2.5$
Rotor tip solidity—each stage	$\sigma_{RT} = 1.3$
Stator hub solidity—each stage	$\sigma_{SH} = 2.0$
Inlet total temperature	$T_1 = 519$°R
Inlet total pressure	$P_1 = 14.7$ psia
Maximum number of stages	$N_{max} = 10$
Minimum overall pressure ratio	$(R_c)_{ov_{min}} = 9.0{:}1$

Table III.

Summary of Class I input data.

Compressor case	U_{T1} (ft/sec)	$\left(R_H/R_T\right)_1$	V_{zT1} (ft/sec)	η_{PR}	η_{PS}	$\left(\frac{V_{zo}}{V_{zi}}\right)_{TR}$	$\left(\frac{V_{zo}}{V_{zi}}\right)_{TS}$	D_{RT} initial, 1st stage	D_{RT} initial, 2nd stage	D_{RT} initial, 3-N stages	M_{SH} (limit)	D_{SH} (limit)	$\epsilon_{RH}=\epsilon_{SH}$ (limit) (degrees)	$\epsilon_{RT}=\epsilon_{ST}$ (limit) (degrees)	β'_{2H} (limit) (degrees)
1001	1000	0.5	600	0.870	0.850	1.0	1.0	0.60	0.70	0.80	10.0	0.8	30	-10	-40
1002	↓	↓	↓	0.895	0.875	↓	↓	↓	↓	↓	↓	↓	↓	↓	↓
1003	↓	↓	↓	0.920	0.900	↓	↓	↓	↓	↓	↓	↓	↓	↓	↓
1004	1200	↓	↓	0.870	0.850	↓	↓	↓	↓	↓	↓	↓	↓	↓	-30
1005	↓	↓	↓	0.895	0.875	↓	↓	↓	↓	↓	↓	↓	↓	↓	↓
1006	↓	↓	↓	0.920	0.900	↓	↓	↓	↓	↓	↓	↓	↓	↓	↓
1007	1400	↓	↓	0.870	0.850	↓	↓	↓	↓	↓	↓	↓	↓	↓	↓
1008	↓	↓	↓	0.895	0.875	↓	↓	↓	↓	↓	↓	↓	↓	↓	↓
1009	↓	↓	↓	0.920	0.900	↓	↓	↓	↓	↓	↓	↓	↓	↓	↓
1010	1000	↓	↓	0.870	0.850	↓	↓	0.50	0.60	0.70	↓	↓	↓	↓	↓
1011	↓	↓	↓	0.895	0.875	↓	↓	↓	↓	↓	↓	↓	↓	↓	↓
1012	↓	↓	↓	0.920	0.900	↓	↓	↓	↓	↓	↓	↓	↓	↓	↓
1013	1200	↓	↓	0.870	0.850	↓	↓	↓	↓	↓	1.0	↓	↓	↓	-20
1014	↓	↓	↓	0.895	0.875	↓	↓	↓	↓	↓	↓	↓	↓	↓	↓
1015	↓	↓	↓	0.920	0.900	↓	↓	↓	↓	↓	↓	↓	↓	↓	-10
1016	1400	↓	↓	0.870	0.850	↓	↓	↓	↓	↓	↓	↓	↓	↓	↓
1017	↓	↓	↓	0.895	0.875	↓	↓	↓	↓	↓	↓	↓	↓	↓	↓
1018	↓	↓	↓	0.920	0.900	↓	↓	↓	↓	↓	↓	↓	↓	↓	↓
1019	1000	↓	↓	0.870	0.850	↓	↓	0.40	0.50	0.60	10.0	↓	↓	↓	-40
1020	↓	↓	↓	0.895	0.875	↓	↓	↓	↓	↓	↓	↓	↓	↓	↓
1021	↓	↓	↓	0.920	0.900	↓	↓	↓	↓	↓	↓	↓	↓	↓	↓
1022	1200	↓	↓	0.870	0.850	↓	↓	↓	↓	↓	↓	↓	↓	↓	↓
1023	↓	↓	↓	0.895	0.875	↓	↓	↓	↓	↓	↓	↓	↓	↓	↓
1024	↓	↓	↓	0.920	0.900	↓	↓	↓	↓	↓	↓	↓	↓	↓	↓
1025	1400	↓	↓	0.870	0.850	↓	↓	↓	↓	↓	↓	↓	↓	↓	↓
1026	↓	↓	↓	0.895	0.875	↓	↓	↓	↓	↓	↓	↓	↓	↓	↓
1027	↓	↓	↓	0.920	0.900	↓	↓	↓	↓	↓	↓	↓	↓	↓	↓
1028	1000	↓	↓	0.870	0.850	↓	↓	0.30	0.40	0.50	↓	↓	↓	↓	↓
1029	↓	↓	↓	0.895	0.875	↓	↓	↓	↓	↓	↓	↓	↓	↓	↓
1030	↓	↓	↓	0.920	0.900	↓	↓	↓	↓	↓	↓	↓	↓	↓	↓
1031	1200	↓	↓	0.870	0.850	↓	↓	↓	↓	↓	↓	↓	↓	↓	↓
1032	↓	↓	↓	0.895	0.875	↓	↓	↓	↓	↓	↓	↓	↓	↓	↓
1033	↓	↓	↓	0.920	0.900	↓	↓	↓	↓	↓	↓	↓	↓	↓	↓
1034	1400	↓	↓	0.870	0.850	↓	↓	↓	↓	↓	↓	↓	↓	↓	↓
1035	↓	↓	↓	0.895	0.875	↓	↓	↓	↓	↓	↓	↓	↓	↓	↓
1036	↓	↓	↓	0.920	0.900	↓	↓	↓	↓	↓	↓	↓	↓	↓	↓
1037	1200	↓	700	0.870	0.850	↓	↓	0.60	0.70	0.80	↓	↓	↓	↓	-30
1038	↓	↓	↓	0.895	0.875	↓	↓	↓	↓	↓	↓	↓	↓	↓	↓
1039	↓	↓	↓	0.920	0.900	↓	↓	↓	↓	↓	↓	↓	↓	↓	↓
1040	1400	↓	↓	0.870	0.850	↓	↓	↓	↓	↓	↓	↓	↓	↓	↓

Table III (cont)

Compressor case	U_{T1} (ft/sec)	$\left(R_H/R_T\right)_1$	V_{zT1} (ft/sec)	η_{PR}	η_{PS}	$\left(\frac{V_{zo}}{V_{zi}}\right)_{TR}$	$\left(\frac{V_{zo}}{V_{zi}}\right)_{TS}$	D_{RT} initial, 1st stage	D_{RT} initial, 2nd stage	D_{RT} initial, 3-N stages	M_{SH} (limit)	D_{SH} (limit)	$\alpha_{RH}=\alpha_{SH}$ (limit) (degrees)	$\alpha_{RT}=\alpha_{ST}$ (limit) (degrees)	β'_{2H} (limit) (degrees)
1041	1400	0.5	700	0.895	0.875	1.0	1.0	0.60	0.70	0.80	10.0	0.8	30	-10	-30
1042				0.920	0.900										
1043	1600			0.870	0.850										
1044	↓			0.895	0.875										
1045				0.920	0.900										
1046	1200			0.870	0.850			0.50	0.60	0.70					
1047	↓			0.895	0.875										
1048				0.920	0.900										
1049	1400			0.870	0.850										
1050	↓			0.895	0.875										
1051				0.920	0.900										
1052	1600			0.870	0.850										
1053	↓			0.895	0.875										
1054				0.920	0.900										
1055	1200			0.870	0.850			0.40	0.50	0.60					
1056	↓			0.895	0.875										
1057				0.920	0.900										
1058	1400			0.870	0.850										
1059	↓			0.895	0.875										
1060				0.920	0.900										
1061	1600			0.870	0.850										
1062	↓			0.895	0.875										
1063				0.920	0.900										
1064	1200			0.870	0.850			0.30	0.40	0.50					
1065	↓			0.895	0.875										
1066				0.920	0.900										
1067	1400			0.870	0.850										
1068	↓			0.895	0.875										
1069				0.920	0.900										
1070	1600			0.870	0.850										
1071	↓	↓	↓	0.895	0.875	↓	↓	↓	↓	↓	↓	↓	↓	↓	↓
1072				0.920	0.900										

Table IV.

Summary of Class II input data.

Case No.	U_{T1} (ft/sec)	$\left(R_H/R_T\right)_1$	V_{zT1} (ft/sec)	η_{PR}	η_{PS}	$\left(\frac{V_{zo}}{V_{zi}}\right)_{TR}$	$\left(\frac{V_{zo}}{V_{zi}}\right)_{TS}$	D_{RT} initial, 1st stage	D_{RT} initial, 2nd stage	D_{RT} initial 3-N stages	M_{SH} (limit)	D_{SH} (limit)	$\alpha_{RH} = \alpha_{SH}$ (limit) (degrees)	$\alpha_{RT} = \alpha_{ST}$ (limit) (degrees)	β'_{2H} (limit) (degrees)
2001	1000	0.5	600	0.870	0.850	1.2	0.833	0.35	0.40	0.45	1.0	0.80	30	-10	-10
2002	1000			0.870	0.850	1.4	0.707				1.0	0.80			
2003	1400			0.920	0.900	1.2	0.833				10.0	1.0			
2004	1400			0.920	0.900	1.4	0.707				10.0				
2005	1000			0.895	0.875	1.2	0.833				1.0				
2006				0.920	0.900	1.2	0.833				1.0				
2007				0.870	0.850	1.4	0.707				1.2				
2008				0.895	0.875	1.4	0.707				1.0				
2009				0.895	0.875	1.4	0.707				1.2				
2010				0.920	0.900	1.4	0.707				1.0				
2011	1000			0.920	0.900	1.4	0.707				1.2				
2012	1200			0.870	0.850	1.2	0.833				1.0				
2013				0.895	0.875	1.2	0.833				1.0				
2014				0.920	0.900	1.2	0.833				1.0				
2015				0.870	0.850	1.4	0.707				1.0				
2016				0.870	0.850	1.4	0.707				1.2				
2017				0.895	0.875	1.4	0.707				1.0				
2018				0.895	0.875	1.4	0.707				1.2				
2019				0.920	0.900	1.4	0.707				1.0				
2020	1200			0.920	0.900	1.4	0.707				1.2				
2021	1400			0.870	0.850	1.2	0.833				1.0				
2022				0.895	0.875	1.2	0.833				1.0				
2023				0.870	0.850	1.4	0.707				1.0				
2024				0.870	0.850	1.4	0.707				1.2				
2025				0.895	0.875	1.4	0.707				1.0				
2026				0.895	0.875	1.4	0.707				1.2				
2027	1400	0.5	600	0.920	0.900	1.4	0.707	0.35	0.40	0.45	1.2	1.0	30	-10	-10
2028	1200	0.5	600	0.870	0.850	1.4	0.707	0.50	0.60	0.70	1.0	0.80	30	-10	-10
2029				0.895	0.875										
2030				0.920	0.900										
2031				0.870	0.850	1.2	0.833								
2032				0.895	0.875										
2033				0.920	0.900										
2034				0.870	0.850	0.85	1.150								
2035				0.895	0.875										
2036				0.920	0.900										
2037	1400			0.870	0.850	1.4	0.707								
2038				0.895	0.875										
2039				0.920	0.900										
2040				0.870	0.850	1.2	0.833								
2041				0.895	0.875										
2042				0.920	0.900										
2043				0.870	0.850	0.85	1.150								
2044				0.895	0.875										
2045				0.920	0.900										

Table IV (cont)

Case No.	U_{T1} (ft/sec)	$\left(R_H/R_T\right)_1$	V_{zT1} (ft/sec)	η_{PR}	η_{PS}	$\left(\frac{V_{zo}}{V_{zi}}\right)_{TR}$	$\left(\frac{V_{zo}}{V_{zi}}\right)_{TS}$	D_{RT} initial, 1st stage	D_{RT} initial, 2nd stage	D_{RT} initial, 3-N stages	M_{SH} (limit)	D_{SH} (limit)	$\alpha_{RH} = \alpha_{SH}$ (limit) (degrees)	$\alpha_{RT} = \alpha_{ST}$ (limit) (degrees)	β'_{2H} (limit) (degrees)
2046	1600	0.5	600	0.870	0.850	1.40	0.707	0.50	0.60	0.70	1.0	0.80	30	-10	-10
2047	1600			0.895	0.875										
2048				0.920	0.900										
2049				0.870	0.850	1.20	0.833								
2050				0.895	0.875										
2051				0.920	0.920										
2052				0.870	0.850	0.85	1.950								
2053				0.895	0.875										
2054				0.920	0.920										
2055	1200			0.870	0.850	1.0	1.0								
2056				0.895	0.875										
2057				0.920	0.900										
2058	1400			0.870	0.850										
2059				0.895	0.875										
2060				0.920	0.900										
2061	1600			0.870	0.850										
2062				0.895	0.895										
2063				0.920	0.900										
2064	1000			0.870	0.850			0.35	0.40	0.45					
2065				0.895	0.875										
2066				0.920	0.900										
2067	1200			0.870	0.850										
2068				0.895	0.875										
2069				0.920	0.900										
2070	1400			0.870	0.850										
2071				0.895	0.875										
2072				0.920	0.900										
2073	1000			0.870	0.850	0.85	1.15								
2074				0.895	0.875										
2075				0.920	0.900										
2076	1200			0.870	0.850										
2077				0.895	0.875										
2078				0.920	0.900										
2079	1400			0.870	0.850										
2080				0.895	0.875										
2081				0.920	0.900										

Table V.

Summary of Class III input data.

Case No.	U_{T1} (ft/sec)	$\left(R_H/R_T\right)_1$	V_{zT1} (ft/sec)	η_{PR}	η_{PS}	$\left(\frac{V_{zo}}{V_{zi}}\right)_{TR}$	$\left(\frac{V_{zo}}{V_{zi}}\right)_{TS}$	D_{RT} Initial 1st stage	D_{RT} Initial 2nd stage	D_{RT} Initial 3-N stages	M_{SH} (limit)	D_{SH} (limit)	$\alpha_{RH} = \alpha_{SH}$ (limit) (degrees)	$\alpha_{RT} = \alpha_{ST}$ (limit) (degrees)	β'_{2H} (limit) (degrees)
3001	1000	0.4	600	0.870	0.850	1.0	1.0	0.35	0.40	0.45	0.80	0.50	40	-20	-10
3002		0.5	600	0.870	0.850										
3003		0.4	600	0.895	0.875										
3004		0.4	600	0.920	0.900										
3005		0.4	700	0.870	0.850										
3006		0.4	700	0.895	0.875										
3007		0.4	700	0.920	0.900										
3008		0.5	600	0.895	0.875										
3009		0.5	600	0.920	0.900										
3010		0.5	700	0.870	0.850										
3011		0.5	700	0.895	0.875										
3012		0.5	700	0.920	0.900										
3013		0.6	600	0.870	0.850										
3014		0.6	600	0.895	0.875										
3015		0.6	600	0.920	0.900										
3016		0.6	700	0.870	0.850										
3017		0.6	700	0.895	0.875										
3018	1000	0.6	700	0.920	0.900										
3019	1200	0.4	600	0.870	0.850										
3020		0.4	600	0.895	0.875										
3021		0.4	600	0.920	0.900										
3022		0.4	700	0.870	0.850										
3023		0.4	700	0.895	0.875										
3024		0.4	700	0.920	0.900										
3025		0.5	600	0.870	0.850										
3026		0.5	600	0.895	0.875										
3027		0.5	600	0.920	0.900										
3028		0.5	700	0.870	0.850										
3029		0.5	700	0.895	0.875										
3030		0.5	700	0.920	0.900										
3031		0.6	600	0.870	0.850										
3032		0.6	600	0.895	0.875										
3033		0.6	600	0.920	0.900										
3034		0.6	700	0.870	0.850										
3035		0.6	700	0.895	0.875										

Table V (cont)

Case No.	U_{T1} (ft/sec)	$\left(R_H/R_T\right)_1$	V_{zT1} (ft/sec)	η_{PR}	η_{PS}	$\left(\frac{V_{zo}}{V_{zi}}\right)_{TR}$	$\left(\frac{V_{zo}}{V_{zi}}\right)_{TS}$	D_{RT} Initial 1st stage	D_{RT} Initial 2nd stage	D_{RT} Initial 3-N stages	M_{SH} (limit)	D_{SH} (limit)	$\alpha_{RH} = \alpha_{SH}$ (limit) (degrees)	$\alpha_{RT} = \alpha_{ST}$ (limit) (degrees)	β'_{2H} (limit) (degrees)
3036	1200	0.6	700	0.920	0.900	1.0	1.0	0.35	0.40	0.45	0.80	0.50	40	-20	-10
3037	1400	0.4	600	0.870	0.850	1.0	1.0	0.35	0.40	0.45	0.80	0.50	40	-20	-10
3038	1400	0.4	600	0.895	0.875	1.0	1.0	0.35	0.40	0.45	0.80	0.50	40	-20	-10
3039	↓	0.4	600	0.920	0.900	↓	↓	↓	↓	↓	↓	↓	↓	↓	↓
3040		0.4	700	0.870	0.850										
3041		0.4	700	0.895	0.875										
3042		0.4	700	0.920	0.900										
3043		0.5	600	0.870	0.850										
3044		0.5	600	0.895	0.875										
3045		0.5	600	0.920	0.900										
3046		0.5	700	0.870	0.850										
3047		0.5	700	0.895	0.875										
3048		0.5	700	0.920	0.900										
3049		0.6	600	0.870	0.850										
3050		0.6	600	0.895	0.875										
3051		0.6	600	0.920	0.900										
3052		0.6	700	0.875	0.850										
3053		0.6	700	0.895	0.875										
3054	↓	0.6	700	0.920	0.900	↓	↓	↓	↓	↓	↓	↓	↓	↓	↓

Table VI.

Summary of computed Class I aerodynamic, performance, and geometric results.

Case No.	Stator hub diffusion factor, Stage No. 1	2	3	4	5	6	7	8	Stator hub Mach number, Stage No. 1	2	3	4	5	6	7	8	Relative flow angle (degrees), Stage No. 1	2	3	4	5	6	7	8	N	$(R_c)_{ov}$	η_{ad}	N_f	R_{cave}
1001	0.719	0.724	0.783	0.752	0.735				1.103	0.999	1.019	0.865	0.771				-38.27	-31.37	-37.37	-27.53	-20.99				5	12.2017	0.7916	4.240	1.678
1002	0.714	0.720	0.782	0.752	0.735				1.091	0.993	1.019	0.866	0.773				-37.49	-30.80	-37.30	-27.57	-21.15				5	13.0137	0.8247	4.115	1.705
1003	0.707	0.714	0.780	0.750					1.077	0.982	1.015	0.864					-36.19	-29.60	-36.66	-27.01					4	9.0349	0.8658	3.991	1.734
1004	0.720	0.716	0.757	0.729					1.079	0.946	0.915	0.784					-29.14	-17.83	-19.35	-7.00					4	10.5174	0.7953	3.670	1.619
1005	0.713	0.710	0.752	0.726					1.063	0.936	0.908	0.780					-27.24	-16.02	-17.80	-5.78					4	11.1861	0.8279	3.558	1.854
1006	0.708	0.705	0.748	0.722					1.048	0.928	0.901	0.778					-25.39	-14.13	-16.10	-4.45					4	11.9280	0.8611	3.448	1.891
1007	0.726	0.722	0.759	0.736					1.064	0.915	0.869	0.747					-17.88	-2.65	-2.71	8.83					4	14.6930	0.7869	3.091	2.035
1008	0.719	0.716	0.754						1.047	0.905	0.861						-15.38	-0.46	-0.88						3	9.0022	0.8325	3.000	2.080
1009	0.712	0.711	0.749						1.032	0.897	0.854						-12.97	1.58	0.78						3	9.4999	0.8649	2.914	2.125
1010	0.619	0.638	0.681	0.647	0.629	0.617			0.928	0.877	0.862	0.751	0.681	0.630			-23.62	-16.86	-17.15	-5.36	1.44	5.71			6	11.8175	0.7924	5.153	1.531
1011	0.614	0.633	0.677	0.644	0.625	0.614			0.921	0.871	0.858	0.749	0.679	0.628			-22.77	-16.11	-16.43	-4.71	1.97	6.13			6	12.3533	0.8255	5.002	1.551
1012	0.608	0.628	0.674	0.641	0.623				0.913	0.863	0.854	0.745	0.677				-21.61	-14.87	-15.34	-3.79	2.72				5	9.5060	0.8649	4.850	1.573
1013	0.628	0.641	0.683	0.654	0.638				0.923	0.851	0.828	0.719	0.650				-13.13	-3.42	-2.11	9.80	15.99				5	11.9509	0.7921	4.280	1.670
1014	0.621	0.635	0.679	0.650	0.635				0.914	0.843	0.820	0.715	0.647				-11.46	-1.57	-0.42	11.06	16.96				5	12.7922	0.8251	4.140	1.700
1015	0.615	0.630	0.674	0.647	0.632				0.905	0.836	0.814	0.711	0.645				-9.86	0.18	1.14	12.13	17.77				5	13.6722	0.8588	4.014	1.728
1016	0.639	0.653	0.695	0.671					0.921	0.835	0.800	0.697					-1.03	10.92	12.63	22.67					4	11.1300	0.7959	3.586	1.851
1017	0.633	0.647	0.690	0.668					0.911	0.827	0.794	0.693					1.01	12.84	14.12	23.53					4	11.8326	0.8267	3.461	1.886
1018	0.626	0.642	0.685	0.664					0.901	0.820	0.788	0.691					2.94	14.62	15.51	24.31					4	12.5763	0.8602	3.362	1.921
1019	0.508	0.551	0.601	0.566	0.546	0.533	0.524		0.797	0.787	0.784	0.694	0.635	0.591	0.556		-7.68	-4.03	-4.04	7.20	13.61	17.63	20.33		7	11.1767	0.7938	6.189	1.426
1020	0.503	0.546	0.597	0.563	0.543	0.530	0.521		0.792	0.783	0.781	0.692	0.633	0.590	0.556		-7.05	-3.48	-3.48	7.72	14.05	17.99	20.82		7	11.8394	0.8267	6.009	1.441
1021	0.498	0.542	0.594	0.560	0.540	0.527			0.788	0.780	0.778	0.690	0.632	0.589			-6.36	-3.05	-3.02	8.15	14.40	18.27			6	9.4291	0.8851	5.844	1.456
1022	0.521	0.560	0.613	0.581	0.563	0.551			0.799	0.775	0.766	0.674	0.613	0.569			2.74	8.26	9.37	20.34	26.00	29.34			6	12.2236	0.7916	5.069	1.542
1023	0.515	0.554	0.609	0.577	0.559				0.793	0.769	0.761	0.670	0.611				4.02	9.64	10.64	21.28	26.72				5	9.2973	0.8318	4.910	1.564
1024	0.510	0.549	0.603	0.573	0.556				0.788	0.764	0.755	0.668	0.609				5.27	10.96	11.86	22.00	27.25				5	9.8153	0.8644	4.767	1.585
1025	0.536	0.575	0.628	0.602	0.587				0.802	0.765	0.748	0.657	0.596				14.12	21.52	22.71	31.58	36.04				5	12.4845	0.7910	4.195	1.688
1026	0.530	0.569	0.622	0.598	0.583				0.796	0.759	0.742	0.654	0.594				15.53	22.89	23.86	32.21	32.11				5	13.2836	0.8245	4.075	1.714
1027	0.524	0.564	0.617	0.594					0.789	0.754	0.737	0.651					16.86	24.18	24.93	32.79					4	9.1505	0.8656	3.984	1.740
1028	0.383	0.455	0.518	0.484	0.463	0.448	0.439	0.431	0.696	0.713	0.722	0.650	0.601	0.563	0.533	0.508	7.89	7.78	6.90	16.88	22.63	26.29	28.77	30.56	8	9.9946	0.7966	7.528	1.338
1029	0.379	0.451	0.515	0.480	0.459	0.445	0.436	0.428	0.693	0.710	0.720	0.648	0.599	0.562	0.532	0.507	8.32	8.24	7.45	17.41	23.09	26.68	29.10	30.85	8	10.5775	0.8291	7.298	1.351
1030	0.375	0.447	0.512	0.477	0.456	0.442	0.433	0.426	0.690	0.707	0.718	0.647	0.598	0.561	0.531	0.506	8.82	8.58	7.90	17.85	23.48	27.00	29.38	31.07	8	11.1789	0.8622	7.089	1.363
1031	0.397	0.470	0.538	0.503	0.483	0.470	0.461		0.699	0.710	0.718	0.637	0.584	0.545	0.513		16.77	17.73	18.13	28.02	33.17	36.26	38.27		7	11.4069	0.7933	6.134	1.430
1032	0.392	0.464	0.534	0.499	0.480	0.467			0.695	0.705	0.713	0.635	0.583	0.543			17.64	18.61	18.96	28.67	33.68	36.67			6	9.1375	0.8322	5.948	1.446
1033	0.387	0.458	0.529	0.496	0.476	0.464			0.692	0.701	0.708	0.633	0.581	0.542			18.44	10.48	19.78	29.14	34.05	36.96			6	9.6158	0.8647	5.784	1.462
1034	0.413	0.484	0.555	0.526	0.508	0.496			0.702	0.703	0.704	0.624	0.569	0.528			26.47	29.04	29.62	37.70	41.85	44.24			6	12.3015	0.7914	5.070	1.542
1035	0.408	0.479	0.549	0.522	0.504				0.698	0.699	0.699	0.622	0.568				27.32	30.04	30.59	38.24	42.25				5	9.2539	0.8319	4.824	1.582
1036	0.403	0.474	0.543	0.517	0.500				0.695	0.695	0.694	0.619	0.566				28.13	31.02	31.49	38.74	42.37				5	9.1465	0.8645	4.790	1.581
1037	0.691	0.693	0.761	0.736					1.217	1.062	1.071	0.906					-31.45	-22.55	-30.29	-21.45					4	13.3214	0.7894	3.270	1.957
1038	0.683	0.687	0.758	0.734					1.197	1.050	1.065	0.904					-29.66	-21.04	-29.38	-20.72					4	14.2833	0.8228	3.174	1.998
1039	0.675	0.681	0.754	0.731					1.179	1.039	1.057	0.889					-27.91	-19.40	-28.13	-19.65					4	15.3511	0.8568	3.081	2.040
1040	0.686	0.686	0.736						1.171	1.004	0.964						-19.96	-7.73	-11.58						3	9.7674	0.7972	2.872	2.148
1041	0.674	0.681	0.732						1.153	0.994	0.957						-17.70	-5.83	-10.03						3	10.3704	0.8295	2.787	2.200
1042	0.670	0.675	0.727						1.137	0.985	0.950						-15.60	-4.04	-8.67						3	10.9873	0.8625	2.710	2.249
1043	0.688	0.692	0.736						1.143	0.970	0.913						-7.60	6.05	3.11						3	12.9030	0.7902	2.494	2.412
1044	0.680	0.687	0.732						1.125	0.962	0.907						-4.95	7.94	4.54						3	13.7746	0.8235	2.424	2.475
1045	0.672	0.682	0.728						1.109	0.954	0.901						-2.46	9.67	5.87						3	14.7084	0.8575	2.357	2.539
1046	0.591	0.609	0.660	0.630					1.033	0.949	0.928	0.789					-15.88	-8.83	-10.57	0.31					4	9.1960	0.7987	3.953	1.743
1047	0.584	0.603	0.656	0.627					1.022	0.940	0.918	0.794					-14.33	-7.15	-8.96	1.54					4	9.7741	0.8308	3.825	1.775
1048	0.577	0.597	0.651	0.623					1.012	0.932	0.912	0.790					-12.83	-5.50	-7.44	2.68					4	10.3953	0.8634	3.706	1.809
1049	0.593	0.611	0.659	0.635					1.014	0.915	0.878	0.760					-4.15	5.25	4.71	14.16					4	12.4745	0.7911	3.367	1.920
1050	0.586	0.605	0.654	0.632					1.003	0.908	0.871	0.757					-2.30	7.02	6.17	15.01					4	13.3216	0.8242	3.268	1.958
1051	0.579	0.600	0.649	0.629					0.993	0.900	0.864	0.755					-0.54	8.66	7.53	15.78					4	14.2250	0.8581	3.174	1.997
1052	0.600	0.621	0.668						1.001	0.894	0.847						7.93	17.74	17.08						3	9.5928	0.7978	2.900	2.133
1053	0.592	0.615	0.664						0.989	0.887	0.841						9.92	19.40	18.42						3	10.1665	0.8289	2.815	2.182
1054	0.585	0.611	0.659						0.979	0.880	0.835						11.71	20.85	19.62						3	10.7727	0.8628	2.736	2.231
1055	0.481	0.520	0.578	0.547	0.530				0.897	0.861	0.847	0.743	0.675				-0.86	4.04	3.71	13.77	18.98				5	10.0627	0.7964	4.700	1.595
1056	0.475	0.515	0.574	0.543	0.526				0.891	0.855	0.842	0.740	0.673				0.31	5.28	4.93	14.66	19.87				5	10.7046	0.8289	4.551	1.620
1057	0.469	0.510	0.568	0.540	0.524				0.885	0.850	0.837	0.737	0.671				1.49	6.47	5.98	15.21	20.07				5	11.3365	0.8619	4.422	1.643
1058	0.488	0.528	0.585	0.560					0.890	0.841	0.817	0.717					10.12	16.68	16.78	25.08					4	9.1383	0.7888	3.966	1.740
1059	0.482	0.522	0.579	0.556					0.883	0.835	0.811	0.714					11.43	17.94	17.83	25.65					4	9.6494	0.8310	3.853	1.768
1060	0.476	0.517	0.574	0.552					0.877	0.830	0.806	0.712					12.68	19.13	18.81	26.17					4	10.1794	0.8638	3.749	1.796
1061	0.497	0.541	0.597	0.578					0.883	0.826	0.794	0.697					20.69	27.63	27.48	33.88					4	12.3121	0.7914	3.401	1.907
1062	0.490	0.535	0.592	0.574					0.876	0.821	0.789	0.694					22.03	28.74	28.42	34.37					4	13.0822	0.8246	3.308	1.942
1063	0.484	0.530	0.587	0.570					0.870	0.816	0.784	0.691					23.28	29.80	29.32	34.85					4	13.9177	0.8584	3.218	1.979
1064	0.358	0.428	0.499	0.465	0.448	0.434			0.792	0.794	0.795	0.706	0.647	0.602			12.63	13.16	12.65	22.04	26.96	29.92			6	9.7336	0.7972	5.742	1.466
1065	0.353	0.423	0.494	0.461	0.443	0.431			0.789	0.790	0.791	0.704	0.645	0.601			13.42	14.03	13.51	22.63	27.43	30.29			6	10.3080	0.8296	5.569	1.483
1066	0.350	0.418	0.489	0.458	0.440	0.428			0.786	0.786	0.787	0.702	0.644	0.600			14.09	15.03	14.43	23.18	27.85	30.62			6	10.9168	0.8626	5.407	1.501
1067	0.368	0.436	0.507	0.480	0.463				0.789	0.780	0.773	0.686	0.625				21.97	24.30	24.18	31.90	35.97				5	9.6220	0.7975	4.820	1.577
1068	0.363	0.432	0.501	0.477	0.460				0.786	0.776	0.768	0.684	0.624				22.79	25.25	25.10	32.41	36.34				5	10.1769	0.8299	4.682	1.598
1069	0.358	0.427	0.496	0.472	0.457				0.782	0.772	0.763	0.681	0.623				23.57	26.18	25.95	32.88	36.60				5	10.7387	0.8629	4.557	1.619
1070	0.378	0.449	0.520	0.499	0.485				0.787	0.769	0.754	0.668	0.607				30.61	33.85	33.79	39.73	42.87				5	13.0700	0.7899	4.124	1.703
1071	0.372	0.444	0.514	0.494	0.481				0.782	0.765	0.749	0.666	0.606				31.50	34.73	34.60	40.11	43.09				5	13.8878	0.8234	4.015	1.728
1072	0.367	0.439	0.508	0.490					0.778	0.761	0.745	0.663					32.29	35.56	35.33	40.51					4	9.3971	0.8651	3.911	1.753

Table VI. (cont)

Case No.	Rotor hub ramp angle (degrees) Stage No. 1	2	3	4	5	6	7	8	Stator hub ramp angle (degrees) Stage No. 1	2	3	4	5	6	7	8	Rotor tip ramp angle (degrees) Stage No. 1	2	3	4-N	Stator tip ramp angle (degrees) Stage No. 1	2	3	4-N	Rotor aspect ratio Stage No. 1	2	3-N	Stator aspect ratio Stage No. 1	2	3-N
1001	30.000	28.782	15.404	14.401	13.201				30.000	30.000	30.000	28.169	23.918				-7.789	0.000	0.000	0.000	-10.000	-10.000	-5.128	0.000	4.0000	3.5000	2.5000	3.5294	3.4189	2.5000
1002		30.000	17.300	15.944	14.524						30.000	28.311	24.060				-9.914	-1.913				-10.000	-5.308		4.0000	3.5000		3.5892	3.4578	
1003			19.379	17.837							30.000	28.274					-10.000	-4.176				-9.797	-5.340		3.7056	3.5000		3.6501	3.5000	
1004			24.199	21.249							29.799	24.028						-8.805				-8.358	0.000		3.0567	3.5000		3.5245		
1005			26.157	22.898							29.531	23.818						-10.000				-7.838			2.8565	3.3772		3.5923		
1006			28.044	24.507							29.243	23.185										-7.392			2.6975	3.1508		3.6554		
1007			29.523	25.274							28.058	22.550										-7.587			2.5771	2.8925		3.4532		
1008			30.000								27.844											-7.084			2.2478	2.7155		3.5282		
1009			30.000								27.374											-6.609			2.1368	2.564		3.5979		
1010			21.584	19.434	17.473	15.807					25.135	20.276	17.156	14.941			-8.564	-2.824				-2.756	-0.733		4.0000	3.5000		4.0000		
1011			23.173	20.800	18.690	16.910					24.985	20.193	17.043	14.882			-10.000	-4.434				-2.305	-0.510		3.9807	3.5000				
1012			24.805	22.166	19.910						24.772	20.019	16.963					-6.198				-2.016	0.000		3.7346	3.5000				
1013			27.233	23.804	21.045					29.969	23.865	19.092	16.054					-10.000			-3.218	0.000			3.1328	3.4760				
1014			28.862	25.238	22.339					29.598	23.590	18.904	15.920								-2.740				2.9634	3.2897				
1015			30.000	26.583	23.566					29.228	23.242	18.737	15.801						-0.484		-2.278				2.8162	3.0904				
1016			30.000	27.158						30.000	25.081	19.570							-1.805		-4.035				2.6953	2.8484				
1017			30.000	28.514						29.624	22.854	18.419							-5.527		-3.480				2.3781	2.6053				
1018			30.000	29.802						29.209	22.550	18.259							-5.219		-2.949				2.2753	2.5811				
1019			23.309	20.669	18.818	17.107	15.562		22.755	23.185	19.401	15.804	13.185	11.479	10.313		-7.189	-3.150	0.000		0.000				4.0000	3.5000				
1020			24.621	23.032	19.875	18.080	16.466		22.474	22.905	19.266	15.493	13.098	11.411	10.261		-8.447	-4.518	0.000						4.0000	3.5000				
1021			25.864	23.141	20.880	19.019			21.853	22.859	19.147	15.334	13.021	11.352			-9.851	-5.851	0.000						4.0000	3.5000				
1022			28.270	24.804	22.083	19.849			23.254	23.159	19.183	15.210	12.752	11.034			-10.000	-6.589	0.000						3.6985	3.5000				
1023			29.844	26.044	23.200				22.790	22.657	18.917	15.052	12.635					-10.000	0.000						3.2449	3.3560				
1024			30.000	27.195	24.288				22.306	22.3217	18.504	14.911	12.531					-10.000	-1.050						3.0987	3.1857				
1025			30.000	28.039	24.706				24.178	23.265	18.897	15.083	12.577					-10.000	-2.804						2.7502	2.9090				
1026			30.000	29.241	25.832				25.751	23.854	18.599	14.935	12.471					-10.000	-4.077						2.4348	2.7114				
1027			30.000	30.000					23.346	22.443	18.322	14.746						-10.000	-5.509	-0.467					2.5321	2.6489				
1028			23.769	21.297	19.292	17.631	16.130	14.967	13.576	16.157	14.541	11.703	9.895	8.622	7.784	7.000	-6.155	-2.140	0.000	0.000					4.0000	3.5000				
1029			24.922	22.331	20.241	18.513	16.955	15.742	13.432	15.948	14.420	11.599	9.810	8.553	7.728	6.953	-5.098	-3.238	0.000						4.0000	3.5000				
1030			26.019	23.322	21.155	19.365	17.755	16.495	12.874	15.768	14.313	11.506	9.734	8.490	7.678	6.912	-5.196	-4.296	0.000						4.0000	3.5000				
1031			28.438	25.060	22.422	20.261	18.436		13.955	16.416	14.861	11.748	9.824	8.498	7.815		-10.000	-7.779	0.000						4.0000	3.5000				
1032			29.628	26.148	23.431	21.232			13.459	16.064	14.695	11.623	9.728	8.417				-9.058	0.000						3.8160	3.5000				
1033			30.000	27.164	24.381	22.124			13.087	15.795	14.326	11.510	9.641	8.350				-10.000	-0.817						3.658	3.4565				
1034			30.000	28.277	25.074	22.519			14.593	16.592	14.925	11.855	9.843	8.463				-10.000	-2.520						3.2367	3.1215				
1035			30.000	29.372	26.105				14.345	16.470	14.664	11.724	9.747					-10.000	-3.762						3.1128	2.9965				
a 1036			30.000	30.000	27.086				14.114	16.208	14.424	11.537	9.657					-10.000	-4.973						3.0010	2.7773				
1037			20.777	17.904					30.000	30.000	30.000	30.000						-8.172	0.000		-10.000	-10.000	-8.440	-0.196	3.0073	3.5000		2.9896	3.0663	
1038			23.114	19.827							30.000	30.000						-10.000	0.000				-8.312	0.000	2.7947	3.4133		3.0482	3.1110	
1039			25.448	21.779							30.000	28.898							0.000				-8.027		2.6177	3.1587		3.1062	3.1557	
1040			28.322								30.000								0.000				-2.540		2.3004	2.8685		3.0858	3.2856	
1041			30.000								30.000								-0.849				-2.140		2.1758	2.6851		3.1298	3.3773	
1042			30.000								30.000								-2.841				-1.711		2.0673	2.5260		3.1806	3.3891	
1043			30.000								29.942								-3.553				0.000		1.9033	2.4150		3.0662	3.3742	
1044			30.000								29.731								-5.708				0.000		1.8141	2.2799		3.1341	3.4160	
1045			30.000								29.466								-7.881				0.000		1.7369	2.1634		3.2002	3.4556	
1046			28.305	22.943							27.803	22.290							0.000		-7.321	-4.338	0.000		3.0056	3.4458		4.0000	3.5000	
1047			28.156	24.531							27.531	22.090							0.000		-6.783	-3.944	0.000		2.8385	3.2287				
1048			29.890	26.044							27.250	21.905							0.000		-6.264	-3.377	0.000		2.6939	3.0308				
1049			30.000	26.798							25.889	20.803							-1.597		-7.311	-3.218	0.000		2.3947	2.7881				
1050			30.000	28.246							25.814	20.652							-3.431		-6.707	-2.747	0.000		2.282	2.6341				
1051			30.000	29.620					30.000	30.000	25.304	20.513							-5.275	0.000	-6.150	-2.304	0.000		2.1852	2.5006	2.5000	4.0000		
1052			30.000						30.000	30.000	24.982								-5.855		-7.580	-2.858			2.0082	2.3857				
1053			30.000						30.000	30.000	24.683								-7.839		-6.928	-2.406			1.9257	2.2673				
1054			30.000						30.000	30.000	24.410								-9.748		-6.495	-2.129			1.8558	2.1680				
1055			28.800	24.987	22.088				26.449	25.976	21.826	17.337	14.522						0.000		0.000	0.000			3.2251	3.4011				
1056			30.000	28.270	25.388				25.962	25.637	21.523	17.175	14.406						-0.114						3.0797	3.3242				
1057				27.474	24.394				25.457	25.298	21.121	17.048	14.318						-1.610						2.9411	3.0680				
1058				28.276					26.595	25.632	20.892	16.696							-3.153						2.6220	2.8085				
1059				29.520					26.137	25.225	20.593	16.559							-4.713						2.5134	2.6794				
1060				30.000					25.703	24.819	20.317	16.354							-5.240	-0.654					2.4185	2.5570				
1061				30.000					26.933	25.494	20.449	16.325							-7.199	-1.085					2.2157	2.4117				
1062				30.000					26.457	25.268	20.163	16.072							-8.872	-2.620					2.1334	2.3123				
b 1063				30.000					26.012	24.935	19.856	16.035							-10.000	-4.009					2.0596	2.2198				
1064			29.103	25.539	22.754	20.511			15.874	16.535	16.803	13.315	11.113	9.592				-9.114	0.000	0.000					3.7428	3.5000				
1065			30.000	26.962	23.796	21.482			15.2801	16.222	16.596	13.190	11.020	9.521				-10.000	-0.386						3.5609	3.4459				
1066				27.732	24.795	22.420			15.334	17.907	16.377	13.068	10.930	9.454					-1.556						3.4566	3.3945				
1067				28.744	25.395				16.216	18.321	16.433	13.075	10.844						-3.280						3.0705	2.9899				
1068				29.866	26.454				15.943	18.201	16.163	12.947	10.752						-4.593						2.9555	2.8715				
c 1069				30.000	27.445				15.689	17.924	15.918	12.686	10.568						-5.876						2.8514	2.7581				
d 1070				30.000	27.525				15.701	18.686	16.240	12.812	10.739						-7.130						2.6030	2.5775				
e 1071				30.000	28.576				16.108	18.395	15.836	12.780	10.553						-8.844						2.5064	2.4763				
1072				30.000					15.772	18.120	15.659	12.624						-10.000	-10.000	-4.183					2.4244	2.3850				

a. Rotor tip ramp angle =-0.489 in Stage 4
b. Rotor aspect ratio = 3.4820 in Stage 3
c. Rotor tip ramp angle = -1.104 in Stage 4
d. Rotor tip ramp angle = -1.658 in Stage 4
e. Rotor tip ramp angle = -2.869 in Stage 4

Table VII.

Summary of computed Class II aerodynamic, performance, and geometric results.

Case No.	η_{PS}	U_{T1}	$\left(\frac{V_{zo}}{V_{zi}}\right)_{TR}$	$\left(\frac{V_{zo}}{V_{zi}}\right)_{TS}$	Rotor tip diffusion factor, Stage No. 1	2	3	4	5-N	N	$(R_c)_{ov}$	η_{ad}	N_f	$R_{c_{avg}}$	Aerodynamic limit violation, Stage No. 1	2	3	4	5-N
2001	0.850	1000	1.2	0.833	0.350	0.400	0.450	0.450	0.450	8	10.6740	0.7950	7.226	1.356					
2002	0.850	1000	1.4	0.707	0.325					7	10.8228	0.7946	6.247	1.421	M_{SH}				
2003	0.900	1400	1.2	0.833	0.350					5	9.8251	0.8644	4.752	1.588					
2004	0.900	1000	1.4	0.707						5	11.6799	0.8614	4.292	1.668					
2005	0.875		1.2	0.833						7	9.0208	0.8324	7.000	1.368					
2006	0.900		1.2	0.833						7	9.5267	0.8649	6.771	1.383					
2007	0.850		1.4	0.707						7	10.9904	0.7942	6.180	1.427					
2008	0.875		1.4	0.707	0.329					6	9.0100	0.8324	6.000	1.442	M_{SH}				
2009	0.875		1.4	0.707	0.350					6	9.1414	0.8321	5.943	1.448					
2010	0.900		1.4	0.707	0.332					6	9.604	0.8647	5.768	1.463	M_{SH}				
2011	0.900		1.4	0.707	0.350					6	9.7249	0.8645	5.723	1.468					
2012	0.850	1200	1.2	0.833						7	11.4353	0.7932	6.081	1.435					
2013	0.875		1.2	0.833						6	9.3156	0.8318	5.880	1.453					
2014	0.900		1.2	0.833						6	9.8673	0.8643	5.680	1.473					
2015	0.850		1.4	0.707						6	10.7238	0.7948	5.390	1.504					
2016	0.850		1.4	0.707						6	10.7238	0.7948	5.390	1.504					
2017	0.875		1.4	0.707						6	11.4796	0.8274	5.180	1.528					
2018	0.875		1.4	0.707						6	11.4796	0.8274	5.180	1.528					
2019	0.900		1.4	0.707						5	9.0137	0.8658	5.000	1.552					
2020	0.900		1.4	0.707						5	9.0137	0.8658	5.000	1.552					
2021	0.850	1400	1.2	0.833						6	11.9194	0.7922	5.097	1.539					
2022	0.875		1.2	0.833						5	9.2627	0.8319	4.915	1.563					
2023	0.850		1.4	0.707						5	10.2320	0.7960	4.726	1.593					
2024	0.850		1.4	0.707						5	10.2320	0.7960	4.627	1.607					
2025	0.875		1.4	0.707						5	10.9323	0.8284	4.457	1.636					
2026	0.875		1.4	0.707						5	10.9323	0.8284	4.457	1.636					
2027	0.900		1.4	0.707						5	11.6799	0.8614	4.300	1.666					
2028	0.850	1200	1.4	0.707	0.366	0.494	0.608	0.646	0.667	5	13.9733	0.7882	4.053	1.721	M_{SH}	M_{SH}	β'_{2H}	β'_{2H}	β'_{2H}
2029	0.875		1.4	0.707	0.370	0.501	0.614	0.651		4	9.5250	0.8313	3.891	1.760	M_{SH}	M_{SH}	M_{SH}	β'_{2H}	
2030	0.900		1.4	0.707	0.375	0.507	0.620	0.656		4	10.3576	0.8635	3.735	1.802	M_{SH}	M_{SH}	M_{SH}	β'_{2H}	
2031	0.850		1.2	0.833	0.486	0.600	0.692	0.700		4	9.4397	0.7980	3.898	1.758	M_{SH}		β_{2H}		
2032	0.875		1.2	0.833	0.492	0.600	0.698	0.700		4	10.1297	0.8300	3.753	1.797	M_{SH}		β_{2H}		
2033	0.900		1.2	0.833	0.497	0.600	0.700	0.700		4	10.8294	0.8627	3.629	1.833	M_{SH}				
2034	0.850		0.85	1.15	0.437	0.600	0.700	0.700	0.700	5	10.0012	0.7966	4.705	1.596	β_{2H}				
2035	0.875		0.85	1.15	0.450	0.600	0.700	0.700	0.700	5	10.7685	0.8287	4.516	1.626	β_{2H}				
2036	0.900		0.85	1.15	0.457	0.600	0.700	0.700	0.700	5	11.4231	0.8618	4.378	1.652	β_{2H}				
2037	0.850	1400	1.4	0.707	0.395	0.546	0.678	0.700		4	13.2752	0.7895	3.316	1.942	M_{SH}	M_{SH}	M_{SH}		
2038	0.875		1.4	0.707	0.400	0.553	0.684	0.700		4	14.5276	0.8224	3.188	1.993	M_{SH}	M_{SH}	M_{SH}		
2039	0.900		1.4	0.707	0.405	0.560	0.690	0.700		4	15.9005	0.8562	3.068	2.047	M_{SH}	M_{SH}	M_{SH}		
2040	0.850		1.2	0.833	0.500	0.600	0.700	0.700		4	12.7125	0.7406	3.328	1.935					
2041	0.875		1.2	0.833	0.500	0.600	0.700	0.700		4	13.6202	0.8238	3.226	1.977					
2042	0.900		1.2	0.833	0.500	0.600	0.700	0.700		4	14.5942	0.8576	3.131	2.020					
2043	0.850		0.85	1.15	0.486	0.600	0.700	0.700		4	9.9548	0.7967	3.778	1.790	β_{2H}				
2044	0.875		0.85	1.15	0.498	0.600	0.700	0.700		4	10.5487	0.8292	3.659	1.822	β_{2H}				
2045	0.900		0.85	1.15	0.500	0.600	0.700	0.700		4	11.1453	0.8622	3.556	1.857					
2046	0.850	1600	1.4	0.707	0.417	0.585	0.693			3	10.0367	0.7965	2.838	2.187	M_{SH}	M_{SH}	D_{SH}		
2047	0.875		1.4	0.707	0.423	0.593	0.697			3	10.9073	0.8285	2.730	2.238	M_{SH}	M_{SH}	D_{SH}		
2048	0.900		1.4	0.707	0.429	0.599	0.700			3	11.8383	0.8612	2.631	2.310	M_{SH}	M_{SH}			
2049	0.850		1.2	0.833	0.500	0.600	0.700			3	9.7761	0.7971	2.869	2.152					
2050	0.875		1.2	0.833	0.500	0.600	0.700			3	10.3890	0.8295	2.786	2.200					
2051	0.900		1.2	0.833	0.500	0.600	0.700			3	11.0409	0.8624	2.703	2.255					
2052	0.850		0.85	1.15	0.500	0.600	0.700	0.700		4	14.0712	0.7880	3.145	2.013					
2053	0.875		0.85	1.15	0.500	0.600	0.700	0.700		4	14.9564	0.8218	3.060	2.052					
2054	0.900		0.85	1.15	0.500	0.600	0.700			3	9.1412	0.8656	2.974	2.095					
2055	0.850	1200	1.0	1.0	0.481	0.600	0.700	0.700	0.700	5	11.8889	0.7923	4.298	1.667	β'_{2H}				
2056	0.875	1200			0.491					5	12.7616	0.8252	4.148	1.699	β'_{2H}				
2057	0.900	1200			0.500					5	13.6722	0.8588	4.015	1.729					
2058	0.850	1400								4	11.1300	0.7939	3.571	1.851					
2059	0.875	1400								4	11.8326	0.8267	3.460	1.888					
2060	0.900	1400								4	12.5763	0.8602	3.362	1.925					
2061	0.050	1600								4	15.4885	0.7856	3.029	2.067					
2062	0.875	1600								3	9.3418	0.8317	2.940	2.113					
2063	0.900	1600								3	9.8693	0.8643	2.860	2.158					
2064	0.850	1000			0.350	0.400	0.450	0.450	0.450	9	10.6365	0.7950	8.137	1.311					
2065	0.875	1000								8	9.2161	0.8320	7.891	1.322					
2066	0.900	1000								8	9.6970	0.8646	7.650	1.333					
2067	0.850	1200								7	10.1337	0.7962	6.529	1.400					
2068	0.875	1200								7	10.7325	0.8288	6.317	1.416					
2069	0.900	1200								7	11.3769	0.8619	6.120	1.432					
2070	0.850	1400								6	11.1349	0.7939	5.304	1.515					
2071	0.875	1400								6	11.8255	0.8268	5.143	1.535					
2072	0.900	1400								5	9.0364	0.8658	4.988	1.554					
2073	0.850	1000	0.85	1.15						10	9.4692	0.7979	9.679	1.256					
2074	0.875	1000								10	10.1531	0.8300	9.284	1.268					
2075	0.900	1000								9	9.1567	0.8655	8.902	1.280					
2076	0.850	1200								8	10.9705	0.7943	7.087	1.364					
2077	0.875	1200								7	9.4317	0.8315	6.801	1.382					
2078	0.900	1200								7	10.0876	0.8639	6.536	1.401					
2079	0.850	1400								6	10.3815	0.7956	5.508	1.490					
2080	0.875	1400								6	11.0081	0.8283	5.331	1.511					
2081	0.900	1400								6	11.6720	0.8615	5.164	1.531					

Table VII. (cont)

Case No.	Stator hub diffusion factor, Stage No.										Stator hub Mach number, Stage No.										Relative exit flow angle (degrees), Stage No.									
	1	2	3	4	5	6	7	8	9	10	1	2	3	4	5	6	7	8	9	10	1	2	3	4	5	6	7	8	9	10
2001	0.535	0.548	0.570	0.549	0.536	0.526	0.519	0.514			0.864	0.823	0.793	0.727	0.677	0.637	0.605	0.577			-1.36	1.614	2.83	9.05	13.16	16.02	18.14	19.75		
2002	0.613	0.850	0.672	0.658	0.649	0.642	0.637				1.00	0.965	0.913	0.824	0.758	0.705	0.661				-3.92	-5.60	-5.78	-0.95	2.22	4.50	6.26			
2003	0.525	0.539	0.559	0.544	0.534						0.830	0.772	0.729	0.663	0.615						2.243	27.59	29.35	33.29	35.55					
2004	0.599	0.616	0.638	0.629	0.623						0.949	0.870	0.809	0.730	0.670						18.61	22.2	22.98	26.61	28.87					
2005	0.531	0.544	0.566	0.546	0.533	0.524	0.517				0.861	0.820	0.790	0.724	0.675	0.636	0.604				-0.69	2.45	3.64	9.61	13.55	16.28	18.30			
2006	0.529	0.541	0.562	0.593	0.531	0.522	0.516				0.858	0.816	0.786	0.722	0.674	0.635	0.603				-0.013	3.27	4.43	10.16	13.92	16.56	18.47			
2007	0.635	0.648	0.670	0.656	0.648	0.641	0.637				1.029	0.957	0.907	0.819	0.754	0.702	0.659				-7.11	-4.83	-5.21	-0.519	2.58	4.82	6.55			
2008	0.613	0.647	0.669	0.655	0.646	0.640					1.00	0.960	0.908	0.820	0.755	0.703					-3.74	-4.71	-4.89	-0.14	2.98	5.23				
2009	0.632	0.645	0.667	0.654	0.646	0.639					1.024	0.953	0.903	0.817	0.752	0.700					-6.44	-4.06	-4.40	2.30	3.28	5.49				
2010	0.614	0.644	0.666	0.653	0.644	0.638					1.00	0.955	0.904	0.817	0.752	0.700					-3.55	-3.86	-4.05	0.63	3.70	5.90				
2011	0.629	0.643	0.665	0.652	0.644	0.635					1.020	0.948	0.899	0.814	0.750	0.698					-5.79	-3.32	-3.24	0.93	3.44	5.12				
2012	0.530	0.512	0.562	0.545	0.533	0.525	0.520				0.848	0.797	0.758	0.694	0.645	0.606	0.574				10.34	14.79	16.42	21.57	24.86	27.13	28.77			
2013	0.527	0.538	0.558	0.541	0.530	0.523					0.844	0.743	0.755	0.691	0.645	0.605					11.11	15.68	17.27	22.18	25.30	27.44				
2014	0.523	0.535	0.554	0.538	0.528	0.520					0.841	0.790	0.752	0.689	0.642	0.604					11.86	16.49	18.12	22.86	25.81	27.83				
2015	0.614	0.628	0.649	0.637	0.629	0.624					0.984	0.907	0.851	0.768	0.706	0.657					6.05	9.19	9.64	14.02	16.83	18.32				
2016	0.614	0.628	0.649	0.637	0.629	0.624					0.984	0.907	0.851	0.768	0.706	0.657					6.05	9.19	9.64	14.02	16.83	18.82				
2017	0.611	0.625	0.646	0.634	0.627	0.622					0.979	0.904	0.847	0.766	0.704	0.656					6.78	9.99	10.46	14.75	17.50	19.45				
2018	0.611	0.625	0.646	0.634	0.627	0.622					0.979	0.904	0.847	0.766	0.704	0.656					6.78	9.99	10.46	14.75	17.50	19.45				
2019	0.608	0.623	0.644	0.632	0.625						0.976	0.900	0.844	0.764	0.703						7.47	10.74	11.23	15.44	18.12					
2020	0.608	0.623	0.644	0.632	0.625						0.976	0.900	0.844	0.764	0.703						7.47	10.74	11.23	15.44	18.12					
2021	0.533	0.546	0.566	0.549	0.510	0.533					0.838	0.779	0.604	0.667	0.618	0.580					20.83	25.97	27.79	32.03	34.50	36.18				
2022	0.529	0.542	0.562	0.547	0.537						0.834	0.775	0.731	0.665	0.617						21.65	26.80	28.60	32.68	35.05					
2023	0.605	0.622	0.643	0.633	0.626						0.957	0.876	0.815	0.733	0.672						17.16	20.74	21.51	25.35	27.76					
2024	0.605	0.622	0.643	0.633	0.626						0.957	0.876	0.815	0.733	0.672						17.16	20.74	21.51	25.35	27.76					
2025	0.602	0.619	0.641	0.631	0.625						0.953	0.873	0.812	0.731	0.671						17.90	21.48	22.28	26.00	28.34					
2026	0.602	0.619	0.641	0.631	0.625						0.953	0.873	0.812	0.731	0.671						17.90	21.48	22.28	26.00	28.34					
2027	0.594	0.616	0.638	0.629	0.623						0.949	0.870	0.809	0.730	0.670						18.61	22.20	22.99	26.61	28.87					
2028	0.627	0.699	0.764	0.780	0.790						1.00	1.00	0.999	0.921	0.850						4.18	-1.93	-10.0	-10.0	-10.0					
2029	0.621	0.700	0.766	0.782							1.00	1.00	1.00	0.922							4.44	-1.65	9.77	-10.0						
2030	0.628	0.701	0.767	0.785							1.00	1.00	1.00	0.923							4.70	-1.38	-9.52	-10.0						
2031	0.657	0.699	0.742	0.730							1.00	0.981	0.931	0.826							-7.89	-6.97	-10.0	-3.13						
2032	0.657	0.694	0.744	0.727							1.00	0.952	0.934	0.820							-7.50	-5.43	-10.0	-2.82						
2033	0.658	0.690	0.742	0.724							1.00	0.943	0.930	0.816							-7.09	-3.98	-9.05	-1.91						
2034	0.571	0.649	0.678	0.646	0.632						0.813	0.814	0.759	0.647	0.376						-10.0	-7.77	-1.48	15.31	24.96					
2035	0.578	0.639	0.670	0.640	0.627						0.819	0.799	0.748	0.640	0.511						-10.0	-4.15	1.90	17.90	26.86					
2036	0.578	0.633	0.664	0.635	0.622						0.819	0.791	0.741	0.635	0.568						-10.0	-2.37	3.81	17.38	27.95					
2037	0.641	0.725	0.796	0.799							1.00	1.00	1.00	0.885							12.45	5.57	-4.18	-1.02						
2038	0.641	0.726	0.797	0.796							1.00	1.00	1.00	0.878							12.78	5.97	-3.92	0.04						
2039	0.642	0.727	0.799	0.794							1.00	1.00	1.00	0.872							13.11	6.35	-3.67	0.99						
2040	0.669	0.698	0.743	0.726							0.988	0.820	0.886	0.774							2.35	7.55	4.17	11.15						
2041	0.664	0.694	0.739	0.724							0.989	0.914	0.881	0.772							3.84	8.88	5.38	11.99						
2042	0.659	0.690	0.736	0.722							0.981	0.908	0.877	0.764							5.25	10.12	6.48	12.77						
2043	0.646	0.666	0.696	0.672							0.893	0.801	0.741	0.633							10.0	8.05	15.10	29.31						
2044	0.649	0.656	0.690	0.666							0.897	0.788	0.733	0.628							-10.0	10.57	16.95	30.51						
2045	0.642	0.648	0.685	0.662							0.886	0.778	0.727	0.624							-7.561	12.81	18.64	31.64						
2046	0.656	0.750	0.800								1.00	1.00	0.949								20.49	13.19	8.04							
2047	0.657	0.751	0.800								1.00	1.00	0.946								20.87	13.62	8.66							
2048	0.657	0.752	0.799								1.00	1.00	0.942								21.23	14.03	9.38							
2049	0.674	0.706	0.750								0.984	0.898	0.854								14.11	19.58	16.73							
2050	0.669	0.702	0.747								0.975	0.892	0.850								15.64	20.82	17.80							
2051	0.664	0.098	0.744								0.967	0.887	0.846								17.08	21.96	18.79							
2052	0.674	0.680	0.719	0.700							0.916	0.788	0.732	0.625							1.08	22.96	28.13	39.34						
2053	0.664	0.672	0.714	0.695							0.900	0.778	0.727	0.621							4.58	25.12	29.61	40.27						
2054	0.655	0.664	0.709								0.886	0.769	0.721								7.69	27.24	31.26							
2055	0.608	0.643	0.684	0.655	0.639						0.897	0.856	0.829	0.720	0.651						-10.000	-3.677	-2.083	9.966	16.193					
2056	0.612	0.636	0.679	0.651	0.635						0.902	0.846	0.821	0.715	0.648						-10.000	-1.704	-0.390	11.155	17.069					
2057	0.615	0.630	0.674	0.647	0.632						0.905	0.836	0.814	0.711	0.645						-8.841	0.175	1.137	12.130	17.766					
2058	0.639	0.653	0.695	0.671							0.921	0.835	0.800	0.697							-1.027	10.915	12.626	22.667						
2059	0.633	0.647	0.690	0.668							0.911	0.827	0.794	0.693							1.010	12.837	14.115	23.533						
2060	0.626	0.642	0.685	0.664							0.901	0.820	0.788	0.691							2.944	14.618	15.509	24.312						
2061	0.652	0.669	0.711	0.693							0.919	0.824	0.782	0.682							11.736	23.670	24.618	32.384						
2062	0.645	0.664	0.706								0.908	0.817	0.776								13.886	25.442	25.489							
2063	0.638	0.659	0.702								0.898	0.810	0.771								15.945	27.033	27.213							
2064	0.447	0.450	0.464	0.434	0.415	0.402	0.392	0.385	0.380		0.743	0.704	0.674	0.617	0.576	0.543	0.517	0.495	0.475		0.271	9.004	14.088	21.997	26.775	29.923	32.120	33.741	34.970	
2065	0.442	0.446	0.460	0.431	0.412	0.399	0.389	0.383			0.740	0.701	0.672	0.616	0.575	0.543	0.516	0.494			0.803	9.426	14.493	22.401	27.139	30.242	32.397	33.979		
2066	0.438	0.442	0.458	0.428	0.409	0.396	0.387	0.380			0.736	0.699	0.671	0.615	0.574	0.542	0.516	0.494			1.409	9.729	14.803	22.724	27.432	30.496	32.613	34.161		
2067	0.461	0.464	0.484	0.454	0.436	0.424	0.415				0.746	0.698	0.666	0.604	0.559	0.525	0.497				10.104	19.676	25.103	32.635	36.823	39.444	41.211			
2068	0.456	0.457	0.480	0.450	0.432	0.420	0.412				0.742	0.693	0.664	0.602	0.558	0.524	0.497				11.156	20.593	25.739	33.150	37.243	39.790	41.499			
2069	0.451	0.451	0.476	0.446	0.429	0.417	0.409				0.738	0.689	0.661	0.600	0.557	0.523	0.496				12.042	21.458	26.407	33.679	37.668	40.138	41.787			
2070	0.477	0.477	0.503	0.477	0.466	0.450					0.750	0.690	0.656	0.591	0.544	0.508					20.681	30.851	35.526	41.702	45.030	47.035				
2071	0.472	0.472	0.498	0.473	0.457	0.446					0.745	0.686	0.652	0.589	0.543	0.507					21.773	31.803	36.298	42.168	45.386	47.317				
2072	0.466	0.467	0.492	0.469	0.453						0.740	0.682	0.648	0.587	0.542						22.828	32.721	36.995	42.588	45.704					
2073	0.426	0.428	0.443	0.406	0.385	0.373	0.366	0.363	0.362	0.363	0.691	0.642	0.606	0.541	0.495	0.460	0.431	0.406	0.384	0.365	-7.726	1.920	9.369	21.886	29.674	34.996	38.911	41.956	44.427	46.501
2074	0.420	0.420	0.434	0.399	0.378	0.367	0.360	0.357	0.357	0.358	0.685	0.636	0.600	0.537	0.492	0.457	0.428	0.403	0.382	0.363	-6.183	4.115	11.805	23.894	31.348	36.427	40.160	43.065	45.425	47.409
2075	0.414	0.412	0.427	0.392	0.372	0.361	0.355	0.353	0.352		0.681	0.630	0.594	0.533	0.488	0.454	0.425	0.401	0.380		-4.782	6.227	14.050	25.720	32.861	37.715	41.280	44.056	46.315	
2076	0.460	0.449	0.483	0.433	0.417	0.409	0.406	0.406			0.708	0.637	0.594	0.528	0.481	0.445	0.416	0.391			4.467	19.499	28.063	38.159	43.940	47.130	50.490	52.622		
2077	0.453	0.441	0.456	0.427	0.412	0.404	0.402				0.702	0.631	0.588	0.524	0.478	0.442	0.413				6.328	21.686	30.122	39.656	45.115	48.698	51.317	52.051		
2078	0.447	0.434	0.449	0.421	0.406	0.400	0.397				0.696	0.626	0.583	0.520	0.475	0.440	0.411				8.105	23.696	31.973	40.996	46.164	49.573	52.051			
2079	0.487	0.477	0.992	0.466	0.454	0.450					0.720	0.638	0.588	0.519	0.472	0.435					16.465	33.058	40.953	48.625	52.865	55.626				
2080	0.478	0.471	0.486	0.461	0.449	0.445					0.713	0.635	0.584	0.517	0.470	0.433					17.599	34.017	41.915	49.316	53.402	56.062				
2081	0.471	0.466	0.480	0.455	0.444	0.440					0.707	0.631	0.581	0.514	0.468	0.432					18.536	34.929	42.799	49.962	53.884	56.450				

Table VII. (cont)

Case No.	Rotor hub ramp angle (degrees) Stage No. 1	2	3	4	5	6	7	8	9	10	Stator hub ramp angle (degrees) Stage No. 1	2	3	4	5	6	7	8	9	10
2001	30.000	30.000	30.000	30.000	30.000	30.000	30.000	30.000			-11.325	-8.796	-5.551	-8.694	-11.068	-12.708	-14.023	-15.013		
2002	30.000	30.000	30.000	30.000	30.000	30.000	30.000				-28.425	-22.828	-17.569	-22.857	-26.616	-24 378	-31.499			
2003	30.000	30.000	30.000	30.000	30.000						-13.012	-11.463	-8.491	-11.362	-13.374					
2004	30.000	30.000	30.000	30.000							-31.763	-30.452	-24.348	-28.480						
2005	30.000	30.000	30.000	30.000	30.000	30.000	30.000				-11.545	-8.985	-5.716	-8.768	-11.137	-12.730	-14.017			
2006	30.000	30.000	30.000	30.000	30.000	30.000	30.000				-11.539	-9.181	-5.870	-8.839	-10.943	-12.756	-14.015			
2007	30.000	30.000	30.000	30.000	30.000	30.000	30.000				-24.314	-23.378	-17.926	-23.101	-26.794	-29.514	-31.608			
2008	30.000	30.000	30.000	30.000	30.000	30.000					-28.064	-23.040	-17.682	-22.872	-26.595	-29.339				
2009	30.000	30.000	30.000	30.000	30.000	30.000					-24.574	-23.499	-17.982	-23.080	-26.745	-29.456				
2010	30.000	30.000	30.000	30.000	30.000	30.000					-27.713	-23.236	-17 786	-22 889	-26.578	-29.305				
2011	30.000	30.000	30.000	30.000	30.000	30.000					-24.822	-23.611	-18.033	-23.061	-26.704	-29.403				
2012	30.000	30.000	30.000	30.000	30.000	30.000	30.000				-12.401	-10.635	-7.363	-10.308	-12.418	-14.016	-15.360			
2013	30.000	30.000	30.000	30.000	30.000	30.000					-12.633	-10.894	-7.583	-10.377	-12.445	-14.018				
2014	30.000	30.000	30.000	30.000	30.000	30.000					-12.8512	-10.890	-7.673	-10.448	-12.477	-14.027				
2015	30.000	30.000	30.000	30.000	30.000	30.000					-29.196	-28.114	-22.029	-26.635	-29.785	-32.089				
2016	30.000	30.000	30.000	30.000	30.000	30.000					-29.196	-28.114	-22.029	-26.635	-29.785	-32.089				
2017	30.000	30.000	30.000	30.000	30.000	30.000					-29.392	-28.175	-22.060	-26.606	-29.731	-32.025				
2018	30.000	30.000	30.000	30.000	30.000	30.000					-29.392	-28.175	-22.060	-26.606	-29.731	-32.025				
2019	30.000	30.000	30.000	30.000	30.000						-29.576	-28.230	-22.094	-26.581	-29.681					
2020	30.000	30.000	30.000	30.000	30.000						-29.576	-28.230	-22.094	-26.581	-29.681					
2021	30.000	30.000	30.000	30.000	30.000	30.000					-12.553	-11.184	-8.281	-11.286	13.322	-14.886				
2022	30.000	30.000	30.000	30.000	30.000						-12.793	-11.330	-8.386	-11.324	-13.350					
2023	30.000	30.000	30.000	30.000	30.000						-31.461	-30.539	-24.277	-28.540	-31.437					
2024	30.000	30.000	30.000	30.000	30.000						-31.461	-30.539	-24.277	-28.540	-31.437					
2025	30.000	30.000	30.000	30.000	30.000						-31.619	-30.428	-24.312	-28.508	-31.381					
2026	30.000	30.000	30.000	30.000	30.000						-31.619	-30.428	-24.312	-28.508	-31.381					
2027	30.000	30.000	30.000	30.000	30.000						-31.763	-30.452	-24.348	-28.480	-31.330					
2028	30.000	30.000	30.000	30.000	30.000						-26.770	-15.285	-5.484	-9.723	-14.221					
2029	30.000	30.000	30.000	30.000							-26.349	-14.586	-4.940	-9.161						
2030	30.000	30.000	30.000	30.000							-25.934	-13.905	-4.453	-8.646						
2031	30.000	30.000	30.000	30.000							9.606	12.799	11.201	4.749						
2032	30.000	30.000	30.000	30.000							10.064	12.162	11.696	4.558						
2033	30.000	30.000	30.000	30.000							10.495	11.567	11.628	4.313						
2034	27.215	20.690	10.108	5.338	1.771						30.000	30.000	30.000	29.928	27.769					
2035	30.000	23.646	12.449	7.393	3.508						30.000	30.000	30.000	29.572	27.575					
2036	30.000	26.173	14.505	9.210	5.102						30.000	30.000	30.000	29.378	27.433					
2037	30.000	30.000	30.000	30.000							-25.116	-12.242	-3.059	-11.395						
2038	30.000	30.000	30.000	30.000							-24.632	-11.570	-2.565	-11.764						
2039	30.000	30.000	30.000	30.000							-24.154	-10.936	-2.110	-12.098						
2040	30.000	30.000	30.000	30.000							11.019	9.973	8.658	1.385						
2041	30.000	30.000	30.000	30.000							10.280	9.541	8.302	1.285						
2042	30.000	30.000	30.000	30.000							9.583	9.138	8.088	1.191						
2043	30.000	29.379	15.752	9.569							30.000	30.000	30.000	29.786						
2044	30.000	30.000	17.776	11.411							30.000	30.000	30.000	29.577						
2045	30.000	30.000	19.819	13.275							30.000	30.000	30.000	29.407						
2046	30.000	30.000	30.000								-23.483	-9.683	-6.7143							
2047	30.000	30.000	30.000								-22.900	-9.041	-6.612							
2048	30.000	30.000	30.000								-22.368	-8.440	-6.659							
2049	30.000	30.000	30.000								10.707	8.929	6.861							
2050	30.000	30.000	30.000								9.945	9.525	6.656							
2051	30.000	30.000	30.000								9.235	8.152	6.471							
2052	30.000	30.000	20.450	13.071							30.000	30.000	30.000	30.000						
2053	30.000	30.000	22.623	15.082							30.000	30.000	30.000	29.751						
2054	30.000	30.000	24.727								30.000	30.000	30.000							
2055	30.000	30.000	27.454	23.978	21.184						30.000	30.000	19.172	16.106						
2056	30.000	30.000	28.974	25.326	22.410						30.000	29.723	23.654	18.942	15.944					
2057	30.000	30.000	30.000	26.583	23.566						30.000	29.228	23.242	18.737	15.801					
2058	30.000	30.000	30.000	27.158							30.000	30.000	23.081	18.570						
2059	30.000	30.000	30.000	28.514							30.000	29.624	22.854	18.401						
2060	30.000	30.000	30.000	28.802							30.000	29.209	22.550	18.259						
2061	30.000	30.000	30.000	29.705							30.000	30.000	22.885	18.390						
2062	30.000	30.000	30.000								30.000	29.828	22.585							
2063	30.000	30.000	30.000								30.000	29.380	22.310							
2064	30.000	30.000	22.591	20.369	18.567	17.086	15.703	14.635	13.701		17.965	15.723	11.503	9.434	8.066	7.082	6.438	5.815	5.312	
2065	30.000	30.000	23.817	21.301	19.429	17.871	16.460	15.240			17.756	15.522	11.409	9.351	7.996	7.023	6.389	5.773		
2066	30.000	30.000	24.598	22.196	20.259	18.649	17.194	16.043			17.139	15.349	11.326	9.276	7.933	6.971	6.345	5.736		
2067	30.000	30.000	26.923	23.925	21.562	19.835	17.946				18.270	16.109	11.781	9.505	8.042	7.006	6.326			
2068	30.000	30.000	28.002	24.919	22.489	20.503	18.765				17.850	15.525	11.650	9.403	7.961	6.942	6.272			
2069	30.000	30.000	29.042	25.883	23.391	21.352	19.569				17.822	15.194	11.520	9.302	7.883	6.880	6.221			
2070	30.000	30.000	30.000	27.025	24.148	21.724					19.266	16.003	11.846	9.624	8.086	7.143				
2071	30.000	30.000	30.000	28.049	25.115	22.640					18.928	15.864	11.787	9.514	8.003	7.077				
2072	30.000	30.000	30.000	29.030	26.046						18.610	15.614	11.571	9.411	7.928					
2073	3.936	1.993	0.478	-1.636	-3.543	-5.210	-6.659	-7.823	-8.029	-10.005	30.000	30.000	25.697	23.969	22.899	22.169	21.645	21.250	20.943	20.686
2074	6.958	4.287	2.110	-0.203	-2.256	-4.038	-5.582	-6.923	-8.101	-9.136	30.000	30.000	25.461	23.765	22.717	22.009	21.501	21.119	20.823	20.586
2075	9.618	6.768	3.693	1.194	-0.997	-2.890	-4.525	-5.946	-7.189		30.000	30.000	25.242	23.575	22.551	21.862	21.369	21.000	20.714	
2076	20.715	14.091	7.840	4.133	1.237	-1.175	-3.185	-4.910			18.928	15.864	11.787	9.514	8.003	7.077				
2077	23.557	16.578	9.639	5.702	2.651	0.000	-2.016				30.000	30.000	25.310	23.739	22.884	22.064	21.482			
2078	26.210	18.929	11.365	7.222	4.028	1.372	-0.859				30.000	30.000	25.081	23.569	22.541	21.859	21.374			
2079	30.000	24.077	13.956	8.909	5.121	2.047					30.000	30.000	25.711	24.071	22.952	22.212				
2080	30.000	26.318	15.705	10.482	6.557	3.363					30.000	30.000	25.536	23.937	22.836	22.110				
2081	30.000	28.416	17.364	12.138	7.946	4.642					30.000	30.000	25.367	23.892	22.725	22.015				

Table VIII.

Summary of computed Class III aerodynamic, performance, and geometric results.

Case No.	U_{T1} (ft/sec)	$(R_H/R_T)_1$	$(V_zT)_i$	η_{PS}	Rotor tip diffusion factor, Stage No. 1	2	3	4-N	N	$(R_c)_{ov}$	η_{ad}	N_f	$R_{e_{avg}}$	Aerodynamic limit violation, Stage No. 1	2	3	4-N
3001	1000	0.4	600	0.85	0.336	0.400	0.450	0.450	8	9.055	0.799	8.00	1.316	β'_{2H}			
3002		0.5	600	0.85	0.350				8	9.115	0.799	7.94	1.319				
3003		0.4	600	0.875	0.342				8	9.641	0.831	7.67	1.332	β'_{2H}			
3004			600	0.90	0.346	0.400			8	10.22	0.864	7.42	1.344	β'_{2H}			
3005			700	0.85	0.258	0.356			8	9.958	0.797	7.55	1.338	M_{SH}	M_{SH}		
3006			700	0.875	0.261	0.362			8	10.71	0.829	7.25	1.354	M_{SH}	M_{SH}		
3007		0.4	700	0.90	0.264	0.367			7	9.034	0.866	7.00	1.369	M_{SH}	M_{SH}		
3008		0.5	600	0.875	0.350	0.400			8	9.728	0.831	7.64	1.334				
3009			600	0.90	0.350				8	10.32	0.864	7.38	1.347				
3010			700	0.85	0.303				8	10.41	0.795	7.34	1.349	M_{SH}			
3011			700	0.875	0.305				8	11.17	0.828	7.05	1.366	M_{SH}			
3012		0.5	700	0.90	0.308				7	9.42	0.865	6.83	1.380	M_{SH}			
3013		0.6	600	0.85	0.350				8	9.115	0.799	7.94	1.319				
3014			600	0.875	0.350				8	9.728	0.831	7.63	1.334				
3015			600	0.90	0.350				8	10.38	0.863	7.35	1.349				
3016			700	0.85	0.348				8	10.65	0.795	7.23	1.356	M_{SH}			
3017			700	0.875	0.350				7	9.081	0.832	7.00	1.369				
3018	1000	0.6	700	0.90	0.350				7	9.618	0.865	6.76	1.384				
3019	1200	0.4	600	0.85	0.334				7	10.74	0.795	6.31	1.416	D_{SH}			
3020		0.4	600	0.875	0.339				7	11.38	0.828	6.11	1.432	D_{SH}			
3021			600	0.90	0.344	0.400			6	9.154	0.866	5.94	1.447	D_{SH}			
3022			700	0.85	0.262	0.370			7	11.58	0.793	6.08	1.435	M_{SH}	M_{SH}		
3023			700	0.875	0.266	0.375			6	9.269	0.832	5.89	1.452	M_{SH}	M_{SH}		
3024		0.4	700	0.90	0.269	0.380			6	9.776	0.864	5.72	1.468	M_{SH}	M_{SH}		
3025		0.5	600	0.85	0.350	0.400			7	10.92	0.794	6.24	1.422				
3026			600	0.875	0.350				7	11.61	0.827	6.04	1.439				
3027			600	0.90	0.350				6	9.341	0.865	5.87	1.454				
3028			700	0.85	0.306				6	9.209	0.799	5.92	1.449	M_{SH}			
3029			700	0.875	0.310				6	9.715	0.831	5.74	1.466	M_{SH}			
3030	1200	0.5	700	0.90	0.314	0.400	0.450	0.450	6	10.24	0.864	5.57	1.483	M_{SH}			
3031		0.6	600	0.85	0.350	0.400	0.450	0.450	7	11.04	0.794	6.20	1.425				
3032			600	0.875					6	9.004	0.833	6.00	1.442				
3033			600	0.90					6	9.495	0.865	5.82	1.459				
3034			700	0.85					6	9.474	0.798	5.82	1.459				
3035			700	0.875					6	10.02	0.830	5.63	1.478				
3036	1200	0.6	700	0.90	0.350	0.400	0.450		6	10.57	0.863	5.47	1.494				
3037	1400	0.4	600	0.85	0.325	0.387	0.429		6	11.12	0.794	5.32	1.511	D_{SH}	D_{SH}	D_{SH}	
3038			600	0.875	0.331	0.393	0.434		6	11.81	0.827	5.16	1.530	D_{SH}	D_{SH}	D_{SH}	
3039			600	0.90	0.337	0.399	0.439		6	12.52	0.860	5.00	1.552	D_{SH}	D_{SH}	D_{SH}	
3040			700	0.85	0.266	0.380	0.450		6	11.97	0.792	5.14	1.535	M_{SH}	M_{SH}		
3041			700	0.875	0.271	0.386	0.450		5	9.029	0.832	5.00	1.552	M_{SH}	M_{SH}		
3042		0.4	700	0.90	0.276	0.392	0.450		5	9.497	0.865	4.85	1.574	M_{SH}	M_{SH}		
3043		0.5	600	0.85	0.350	0.400	0.447		6	11.73	0.793	5.15	1.533			D_{SH}	
3044			600	0.875	0.350		0.450		6	12.39	0.826	5.00	1.552				
3045			600	0.90	0.350				5	9.379	0.865	4.88	1.569				
3046			700	0.85	0.310				5	9.058	0.799	5.00	1.552	M_{SH}			
3047			700	0.875	0.315				5	9.523	0.831	4.82	1.578	M_{SH}			
3048		0.5	700	0.90	0.320				5	10.01	0.864	4.71	1.594	M_{SH}			
3049		0.6	600	0.85	0.350				6	12.03	0.792	5.08	1.541				
3050			600	0.875					5	9.194	0.832	4.94	1.560				
3051			600	0.90					5	9.641	0.865	4.80	1.580				
3052			700	0.85					5	9.459	0.798	4.86	1.571				
3053			700	0.875					5	9.947	0.830	4.72	1.593				
3054	1400	0.6	700	0.90	0.350	0.400	0.450	0.450	5	10.46	0.863	4.59	1.614				

Table VIII. (cont)

Case No.	Rotor hub ramp angle (degrees) Stage No.								Stator hub ramp angle (degrees) Stage No.								Rotor tip ramp angle (degrees) Stage No.			Stator tip ramp angle (degrees) Stage No.
	1	2	3	4	5	6	7	8	1	2	3	4	5	6	7	8	1	2	3-N	1-N
3001	39.2	32.9	23.1	20.8	18.9	17.4	15.9	14.8	20.1	17.3	12.1	9.7	8.2	7.2	6.5	5.9	0	0	0	0
3002	38.1	32.3	22.9	20.6	18.8	17.3	15.9	14.8	18.4	15.5	11.2	9.3	7.9	7.0	6.4	5.7	0			
3003	40.0	34.2	24.2	21.8	19.8	18.2	16.7	15.6	20.3	17.0	11.9	9.6	8.1	7.1	6.5	5.8	-0.72			
3004	40.0	35.4	25.2	22.6	20.7	19.0	17.5	16.3	20.3	16.7	11.7	9.5	8.0	7.0	6.4	5.7	-1.9			
3005	37.4	33.8	24.7	22.0	19.9	18.2	16.6	15.4	15.1	17.3	15.1	11.9	10.0	8.6	7.8	7.0	0			
3006	38.9	35.3	25.9	23.1	20.9	19.1	17.4	16.2	15.2	17.4	14.8	11.7	9.8	8.5	7.7	6.9	0			
3007	40.0	36.7	27.0	24.1	21.8	19.9	18.2		15.1	17.7	14.5	11.5	9.7	8.4	7.6		-0.33			
3008	39.6	33.7	24.0	21.6	19.7	18.0	16.7	15.6	18.2	15.2	11.1	9.1	7.8	7.0	6.3	5.7	0			
3009	40.0	34.9	25.0	22.6	20.6	18.8	17.5	16.3	17.5	15.1	10.9	9.0	7.8	7.0	6.2	5.6	-1.0			
3010	38.0	34.1	24.0	21.5	19.5	17.8	16.3	15.1	16.7	18.7	13.5	11.0	9.4	8.2	7.4	6.7	0			
3011	39.5	35.5	25.2	22.6	20.5	18.7	17.2	15.9	16.8	18.4	13.2	10.8	9.2	8.1	7.3	6.6	0			
3012	40.0	36.7	26.2	23.5	21.4	19.6	18.0		16.6	18.2	13.1	10.7	9.2	8.0	7.3		-0.89			
3013	37.0	31.9	22.7	20.5	18.7	17.1	15.9	14.8	15.5	13.9	10.4	8.8	7.6	6.9	6.2	5.6	0			
3014	38.4	33.2	23.8	21.5	19.6	18.0	16.7	15.5	15.4	13.8	10.3	8.7	7.5	6.8	6.1	5.6	0			
3015	39.6	34.4	24.9	22.5	20.5	18.8	17.5	16.3	15.2	13.6	10.2	8.6	7.5	6.7	6.1	5.5	0			
3016	38.8	33.3	23.6	21.2	19.2	17.5	16.2	15.0	18.2	16.4	12.3	10.3	8.9	8.0	7.2	6.5	0			
3017	40.0	34.6	24.7	22.2	20.2	18.4	17.0		18.1	16.2	12.2	10.2	8.8	7.9	7.1		-0.37			
3018	40.0	35.8	25.8	23.2	21.1	19.3	17.8		18.0	16.1	12.1	10.1	8.8	7.9	7.1		-1.6			
3019	40.0	39.2	27.7	24.5	22.1	20.0	18.3		20.4	18.0	12.2	9.7	8.2	7.1	6.4		-5.4			
3020	40.0	40.0	28.7	25.5	22.9	20.9	19.1		20.5	17.5	12.0	9.7	8.1	7.0	6.3		-6.8	-0.50		
3021	40.0	40.0	29.7	26.4	23.8	21.7			20.5	17.3	11.9	9.5	8.0	6.9			-8.1	-1.5		
3022	40.0	40.0	29.4	25.8	23.1	20.9	19.0		15.1	18.3	14.5	11.3	9.5	8.1	7.3		-3.8	-0.50		
3023	40.0	40.0	30.5	26.8	24.0	21.7			15.1	18.4	14.3	11.2	9.4	8.1			-5.0	-1.9		
3024	40.0	40.0	31.4	27.7	24.9	22.6			15.4	18.4	14.1	11.1	9.3	8.0			-6.1	-3.3		
3025	40.0	38.4	27.4	24.3	21.9	19.8	18.2		18.9	16.2	11.4	9.3	7.9	7.0	6.2		-5.4	0		
3026	40.0	39.6	28.5	25.4	22.9	20.7	19.1		18.5	16.0	11.3	9.2	7.8	7.0	6.2		-6.7	0		
3027	40.0	40.0	29.5	26.3	23.8	21.6			18.0	15.8	11.2	9.1	7.8	6.9			-8.0	-1.0		
3028	40.0	40.0	28.5	25.2	22.6	20.5			16.8	18.6	13.2	10.6	9.0	7.8			-5.1	-0.35		
3029	40.0	40.0	29.6	26.2	23.5	21.3			17.0	18.5	13.0	10.5	8.9	7.8			-6.4	-1.8		
3030	40.0	40.0	30.6	27.2	24.4	22.2			17.1	18.2	12.9	10.4	8.8	7.7			-7.8	-2.9		
3031	40.0	38.0	27.2	24.2	21.9	19.8	18.2		16.4	14.7	10.7	8.9	7.6	6.8	6.1		-4.7	0	0	
3032	40.0	39.2	28.3	25.3	22.8	20.7			16.0	14.6	10.6	8.8	7.6	6.8			-6.2	0		
3033	40.0	40.0	29.3	26.2	23.7	21.6			15.7	14.3	10.5	8.7	7.5	6.7			-7.6	-0.48		
3034	40.0	39.2	28.0	24.8	22.3	20.2			18.5	16.7	12.2	10.0	8.6	7.7			-6.7	0		
3035	40.0	40.0	29.1	25.9	23.3	21.1			18.2	16.4	12.1	10.0	8.5	7.6			-8.2	-0.57		
3036	40.0	40.0	30.2	26.8	24.2	21.9			17.8	16.4	12.0	9.9	8.5	7.6			-8.7	-1.9		
3037	40.0	40.0	31.0	27.8	24.8	22.3			19.9	17.2	11.7	10.1	8.4	7.2			-10.8	-4.2		
3038	40.0	40.0	32.0	28.7	25.6	23.2			20.0	17.5	11.8	10.0	8.3	7.1			-12.3	-5.5		
3039	40.0	40.0	33.1	29.5	26.4	23.9			20.0	17.5	11.8	9.8	8.2	7.0			-13.8	-7.0		
3040	40.0	40.0	33.1	28.8	25.5	22.9			15.6	19.2	14.6	11.3	9.3	8.0			-9.0	-6.1		
3041	40.0	40.0	34.0	29.7	26.4				15.6	18.3	14.4	11.2	9.2				-10.3	-7.6		
3042	40.0	40.0	34.9	30.6	27.3				15.7	19.3	14.2	11.0	9.1				-11.7	-9.1		
3043	40.0	40.0	31.0	27.3	24.4	21.9			19.5	16.9	11.7	9.5	8.0	7.1			-11.9	-3.8		
3044	40.0	40.0	32.1	28.3	25.3	22.9			19.1	16.3	11.7	9.4	7.9	7.0			-13.3	-5.4		
3045	40.0	40.0	33.1	29.3	26.3				18.7	16.0	11.7	9.4	7.9				-14.6	-6.8		
3046	40.0	40.0	32.2	28.1	25.0				17.4	18.7	13.4	10.6	8.9				-11.4	-6.0		
3047	40.0	40.0	33.2	29.1	25.9				17.4	18.3	13.2	10.5	8.8				-13.0	-7.4		
3048	40.0	40.0	34.2	30.1	26.9				17.4	17.9	13.1	10.4	8.8				-14.5	-8.7		
3049	40.0	40.0	30.9	27.3	24.4	22.0			17.1	15.5	11.2	9.1	7.8	6.9			-12.0	-3.6		
3050	40.0	40.0	32.0	28.3	25.3				16.8	15.3	11.1	9.1	7.7				-13.5	-5.1		
3051	40.0	40.0	33.0	29.3	26.3				16.4	14.8	11.0	9.0	7.7				-15.0	-6.7		
3052	40.0	40.0	31.6	27.8	24.8				18.9	17.1	12.4	10.1	8.6				-14.0	-5.0		
3053	40.0	40.0	32.7	28.8	25.7				18.5	16.7	12.3	10.0	8.5				-15.5	-6.7		
3054	40.0	40.0	33.7	29.8	26.7				18.2	16.4	12.2	10.0	8.5				-17.0	-8.2	0	0

Table IX.

Effects of the aerodynamic parameters, relative tip Mach number, and axial velocity on stage pressure ratio.

$(V_{zo}/V_{zi})_R = 1.0$, $(R_H/R_T)_1 = 0.5$, $\eta_{PS} = 0.875$

Case No.	V_{z1} (ft/sec)	U_{T1} (ft/sec)	$R_{c_{avg}}$	$M_{SH_{max}}$	$D_{SH_{max}}$	M'_{1T}	$\beta'_{2H_{max}}$ (degrees)	D_{RT}
A	600	1140	1.42	0.72	0.53	1.20	+15	0.3, 0.4, 0.5
B	600	1140	1.65	0.91	0.68	1.20	-15	0.5, 0.6, 0.7
C	600	1400	1.565	0.70	0.55	1.42	+27	0.3, 0.4, 0.5
D	600	1400	1.885	0.91	0.69	1.42	+1	0.5, 0.6, 0.7
E	700	1080	1.41	0.78	0.48	1.2	+9	0.3, 0.4, 0.5
F	700	1352	1.915	1.01	0.66	1.42	-5	0.5, 0.6, 0.7
G	700	1352	1.77	0.91	0.60	1.42	+6	0.42, 0.52, 0.62

Table X.

Effects of rotor axial velocity ratio, aerodynamic parameters, and relative Mach number on stage pressure ratio.

Case No.	D_{RT_1}	U_{T1} (fps)	$(V_{zo}/V_{zi})_R$	$M_{SH_{max}}$	$D_{SH_{max}}$	$\beta'_{2H_{max}}$ (degrees)	M'_{1T}	$R_{c_{avg}}$
2068	0.35	1200	1.0	0.742	0.480	11.0	1.24	1.416
2080	0.35	1400	0.85	0.713	0.486	17.6	1.41	1 511
2017	0.35	1200	1.40	0.979	0.646	6.8	1.24	1.528
2025	0.35	1400	1.40	0.953	0.641	17.9	1.41	1.636
2056	0.50	1200	1.0	0.902	0.679	-10.0	1.24	1.70
2044	0.50	1400	0.85	0.897	0.690	-10.0	1.41	1.822
2032	0.50	1200	1.20	1.0	0.744	-10.0	1.24	1.797
2041	0.50	1400	1.20	0.989	0.739	3.8	1.41	1.977

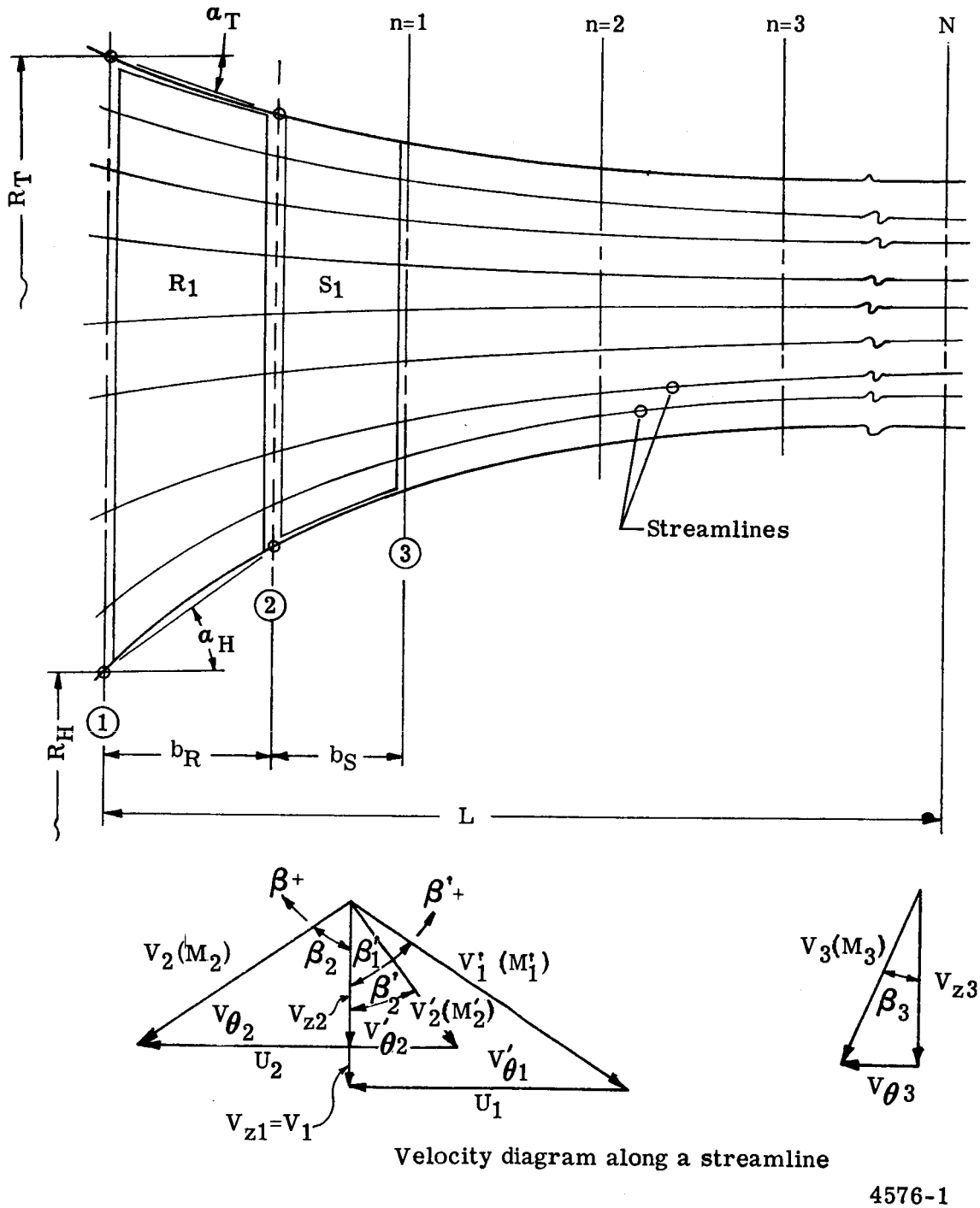

Figure 1. Schematic presentation of symbols.

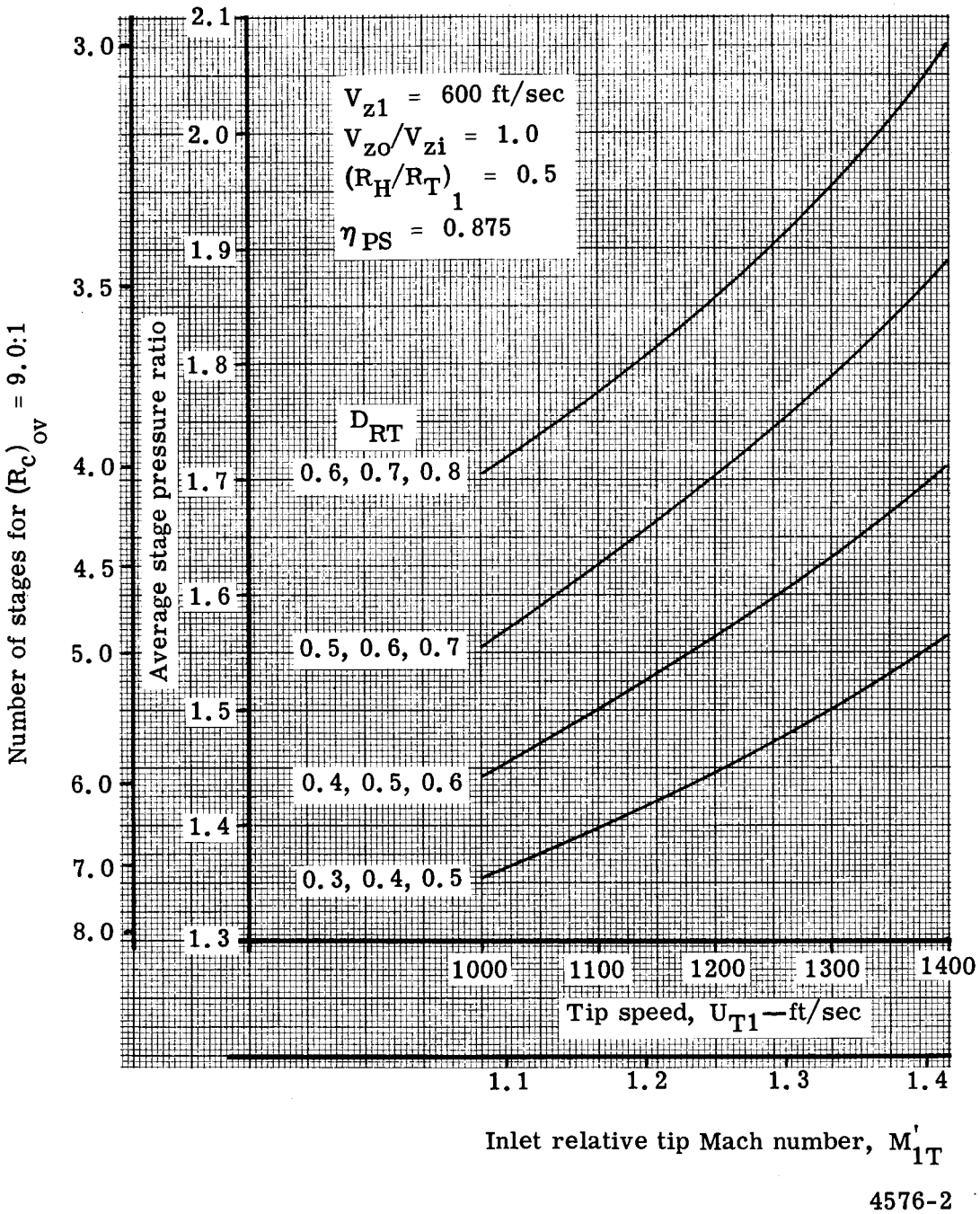

Figure 2. Effect of tip speed on average stage pressure ratio.

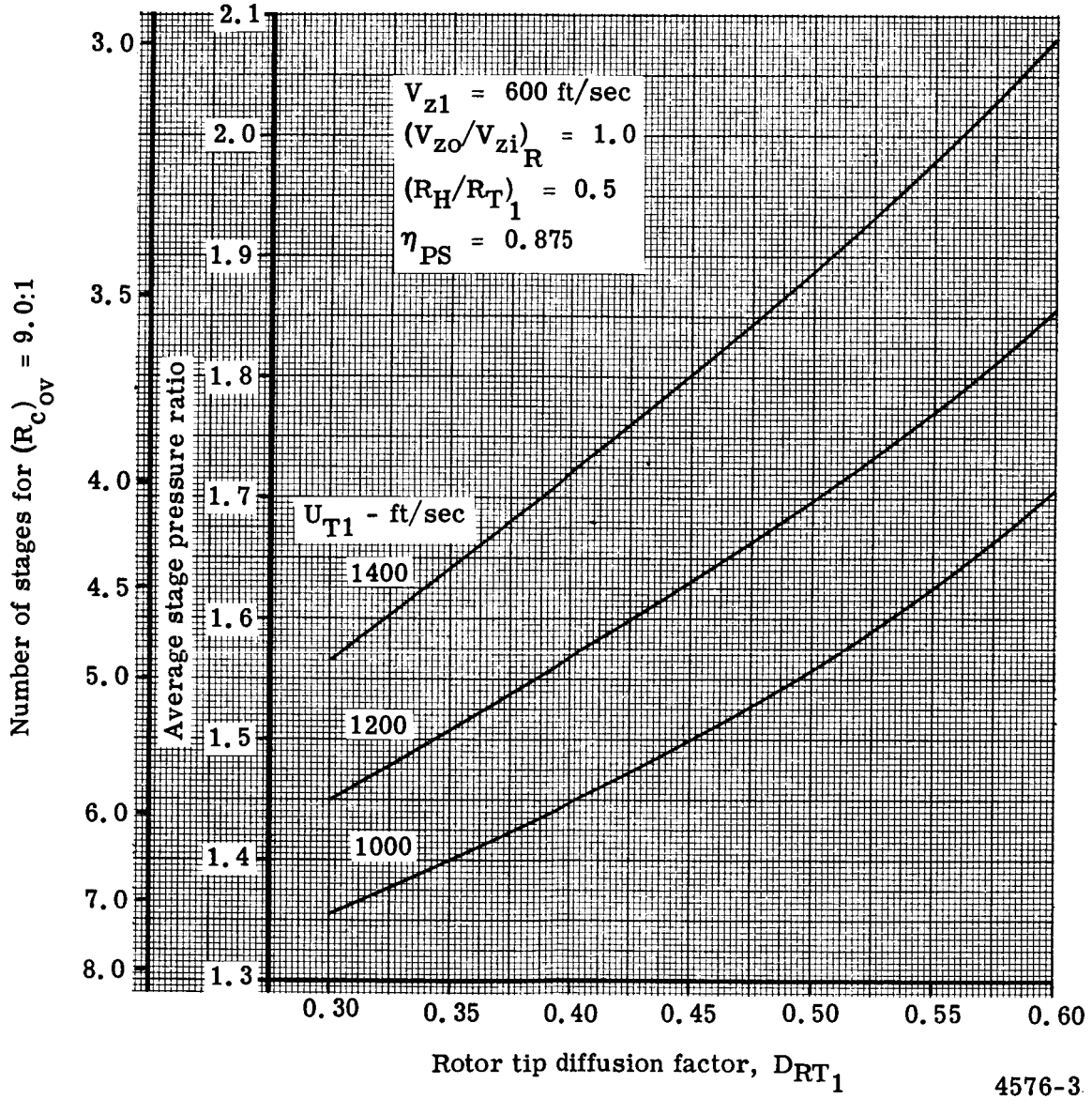

Figure 3. Effect of rotor tip diffusion factor on average stage pressure ratio.

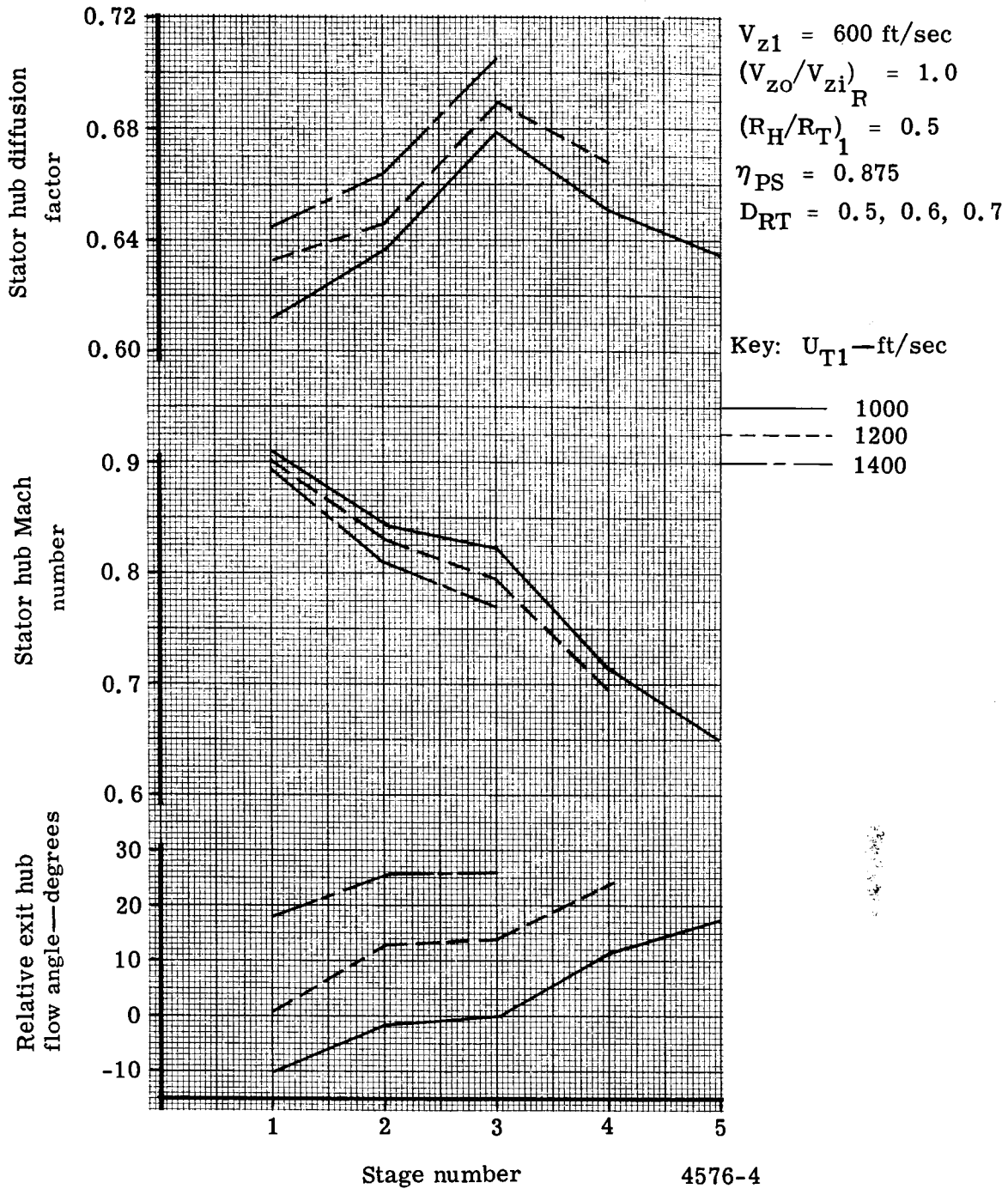

Figure 4. Typical aerodynamic parameter variations with compressor stage number.

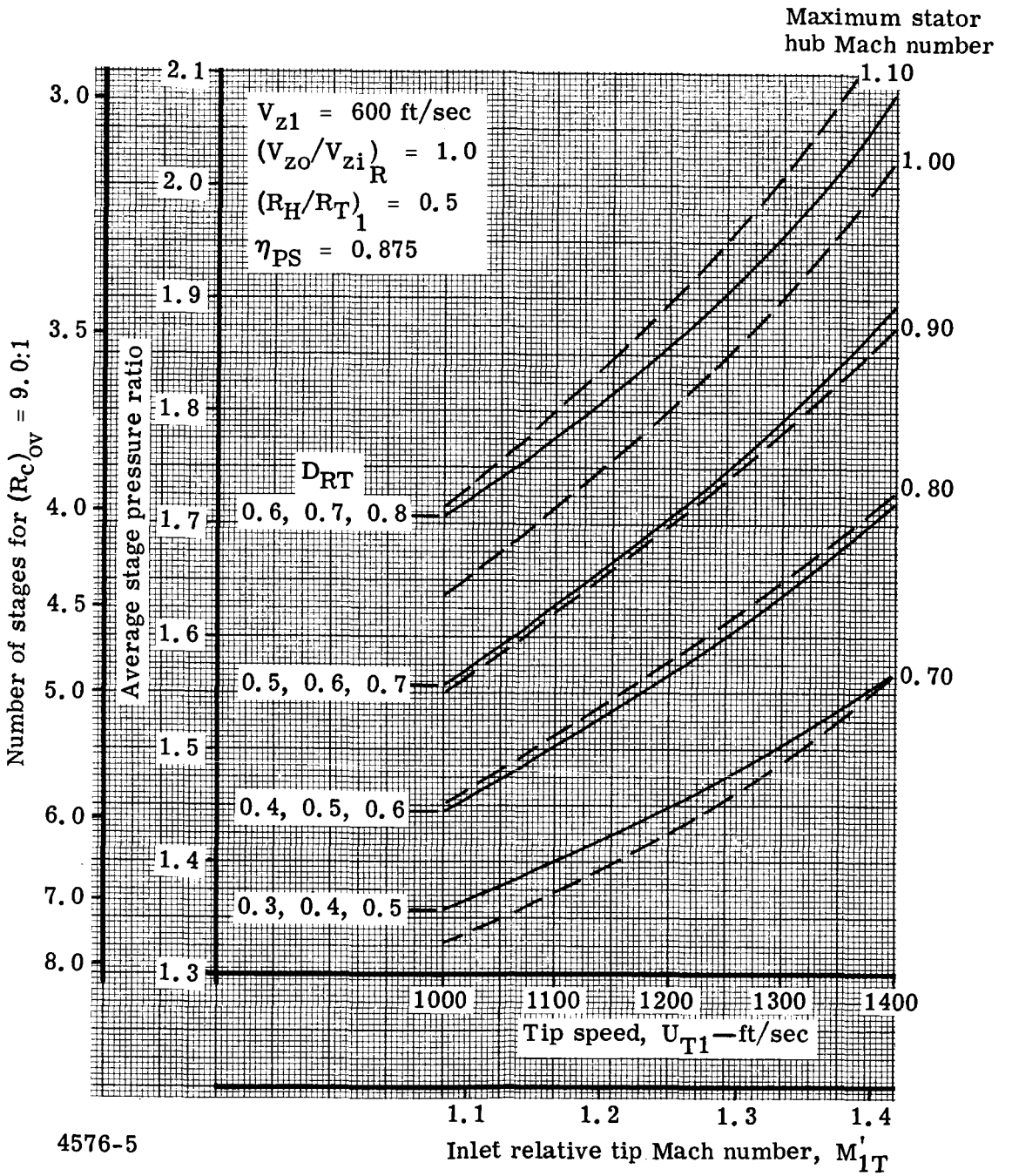

Figure 5. Effect of tip speed and rotor tip diffusion factor on maximum stator hub Mach number.

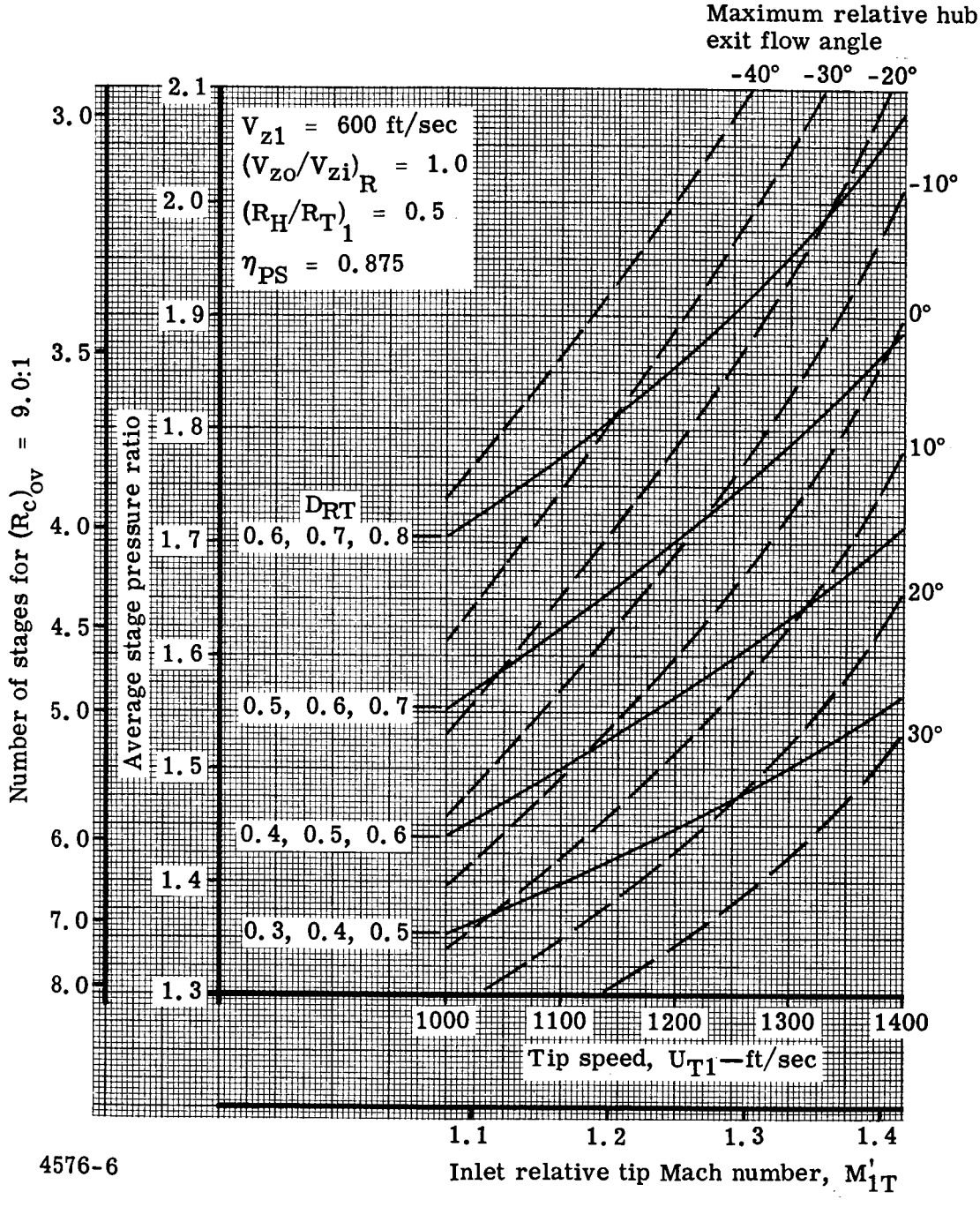

Figure 6. Effect of tip speed and rotor tip diffusion factor on maximum relative hub exit flow angle.

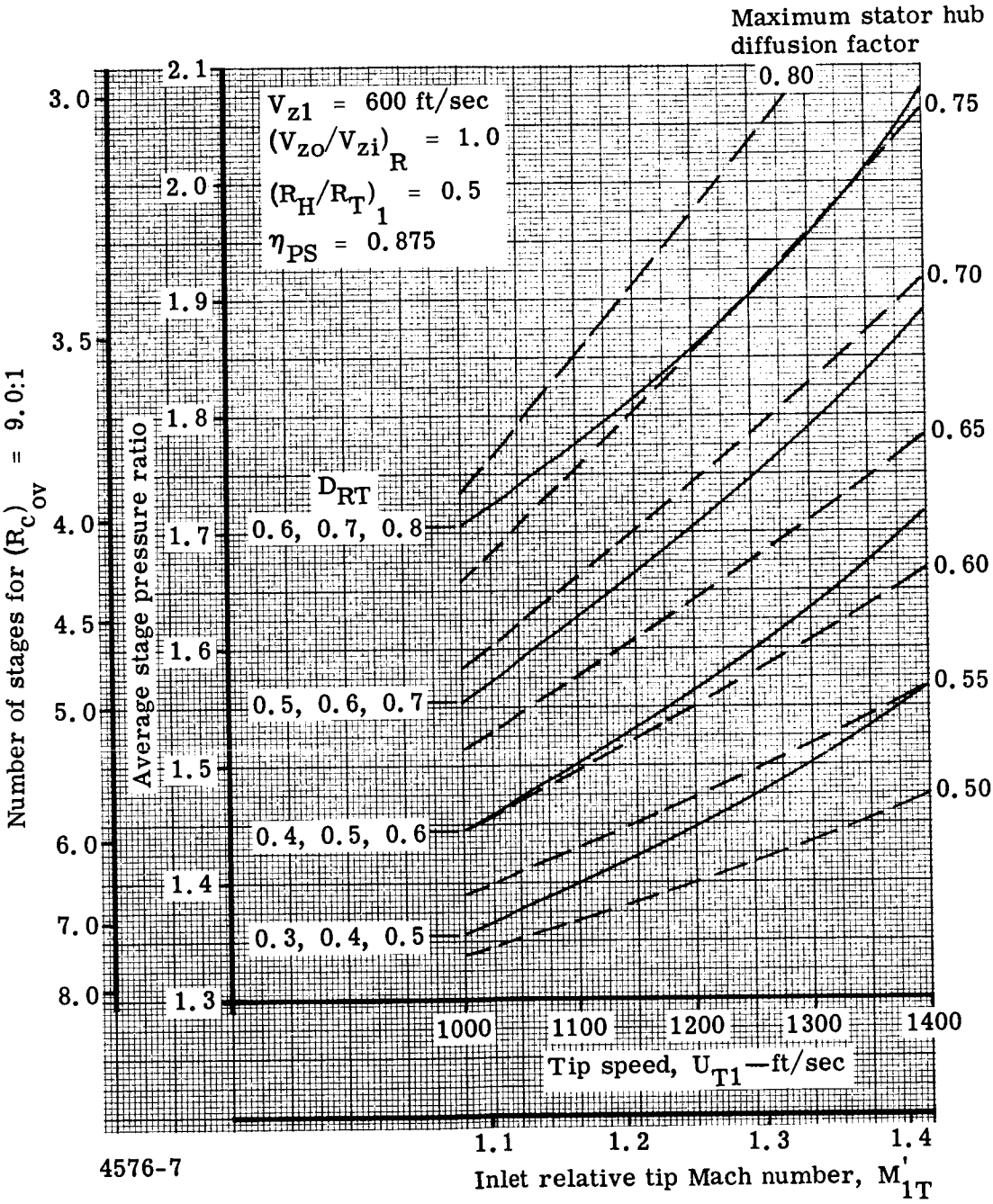

Figure 7. Effect of tip speed and rotor tip diffusion factor on maximum stator hub diffusion factor.

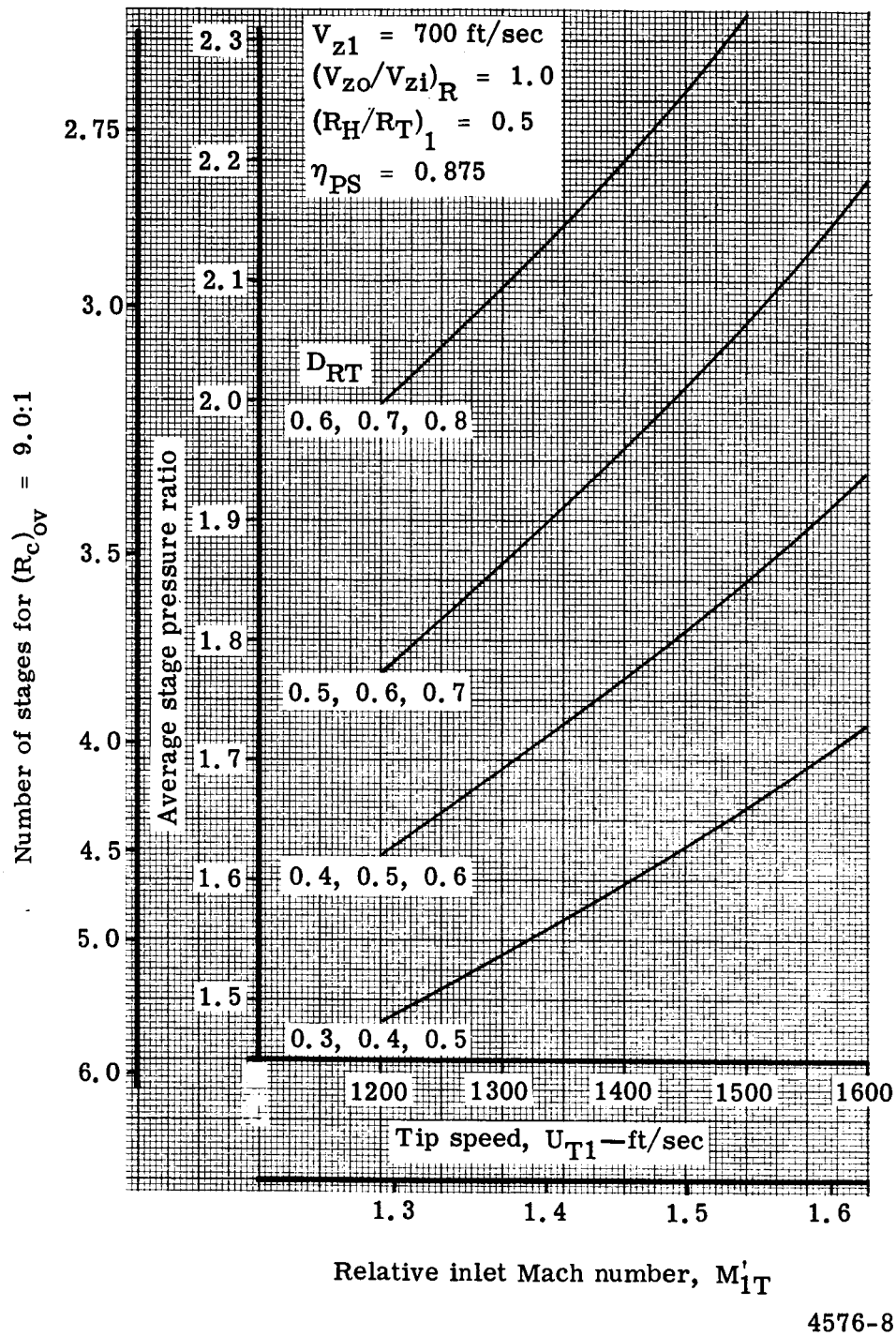

Figure 8. Effect of tip speed on average stage pressure ratio.

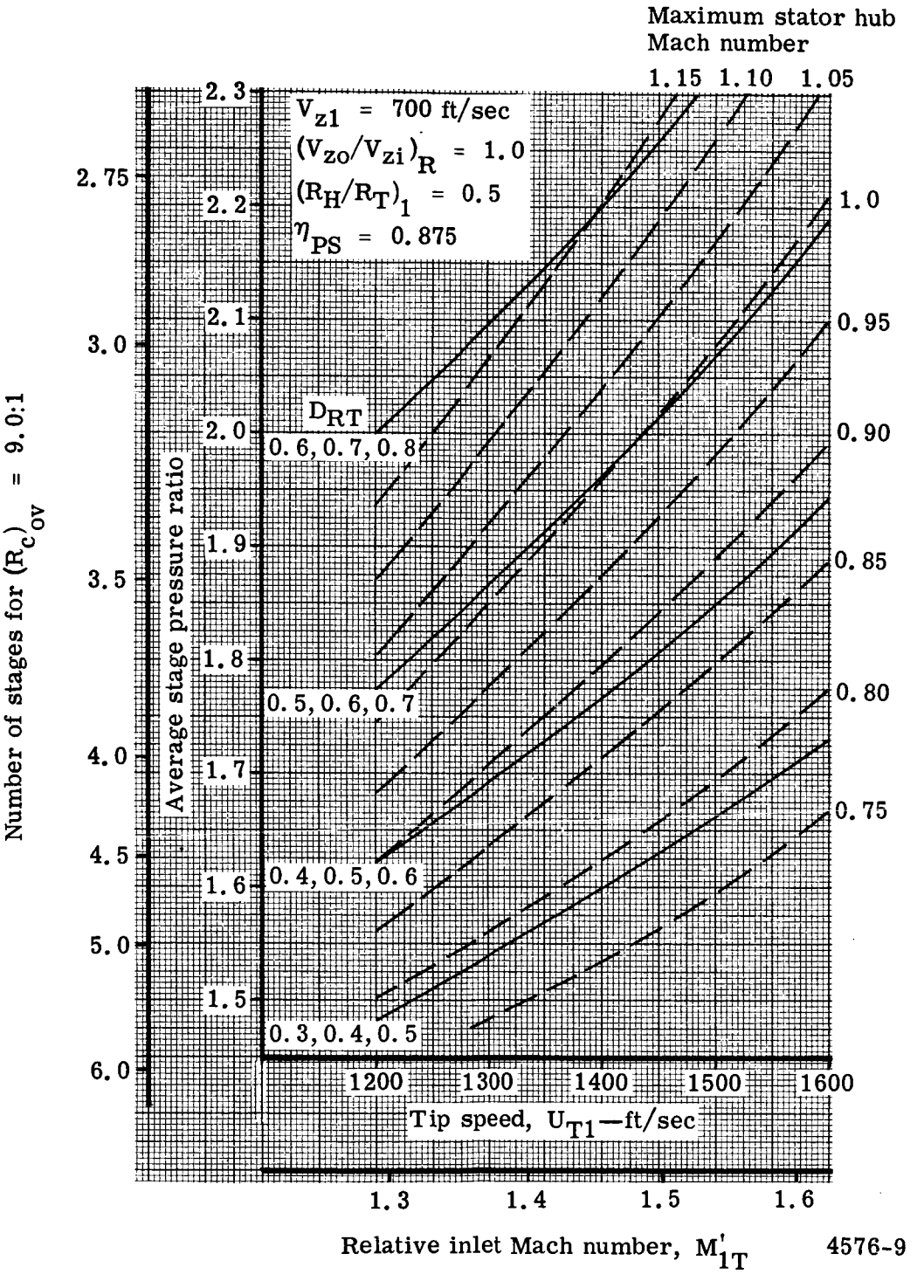

Figure 9. Effect of tip speed and rotor tip diffusion factor on maximum stator hub Mach number.

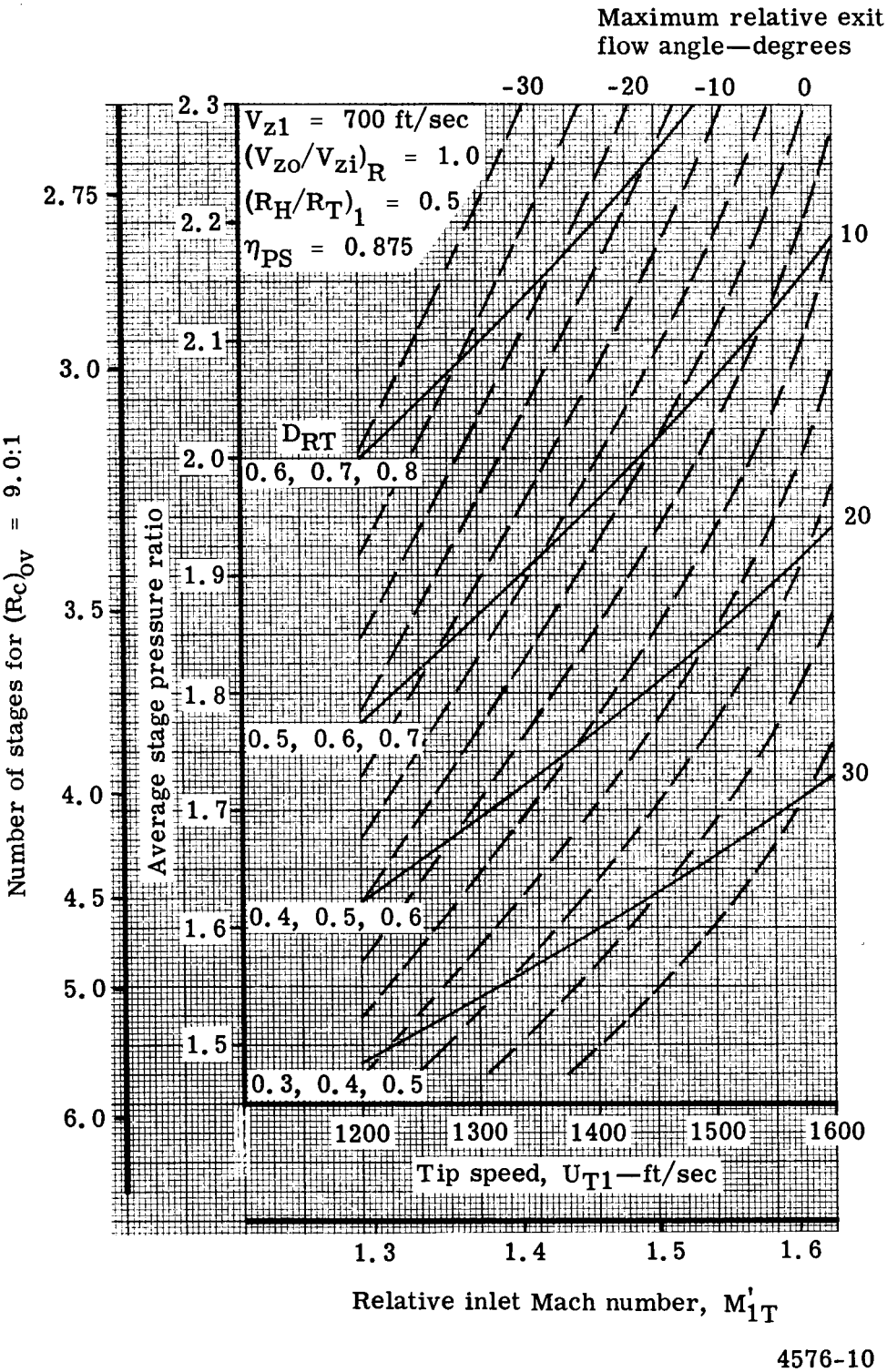

Figure 10. Effect of tip speed and rotor tip diffusion factor on maximum relative exit flow angle.

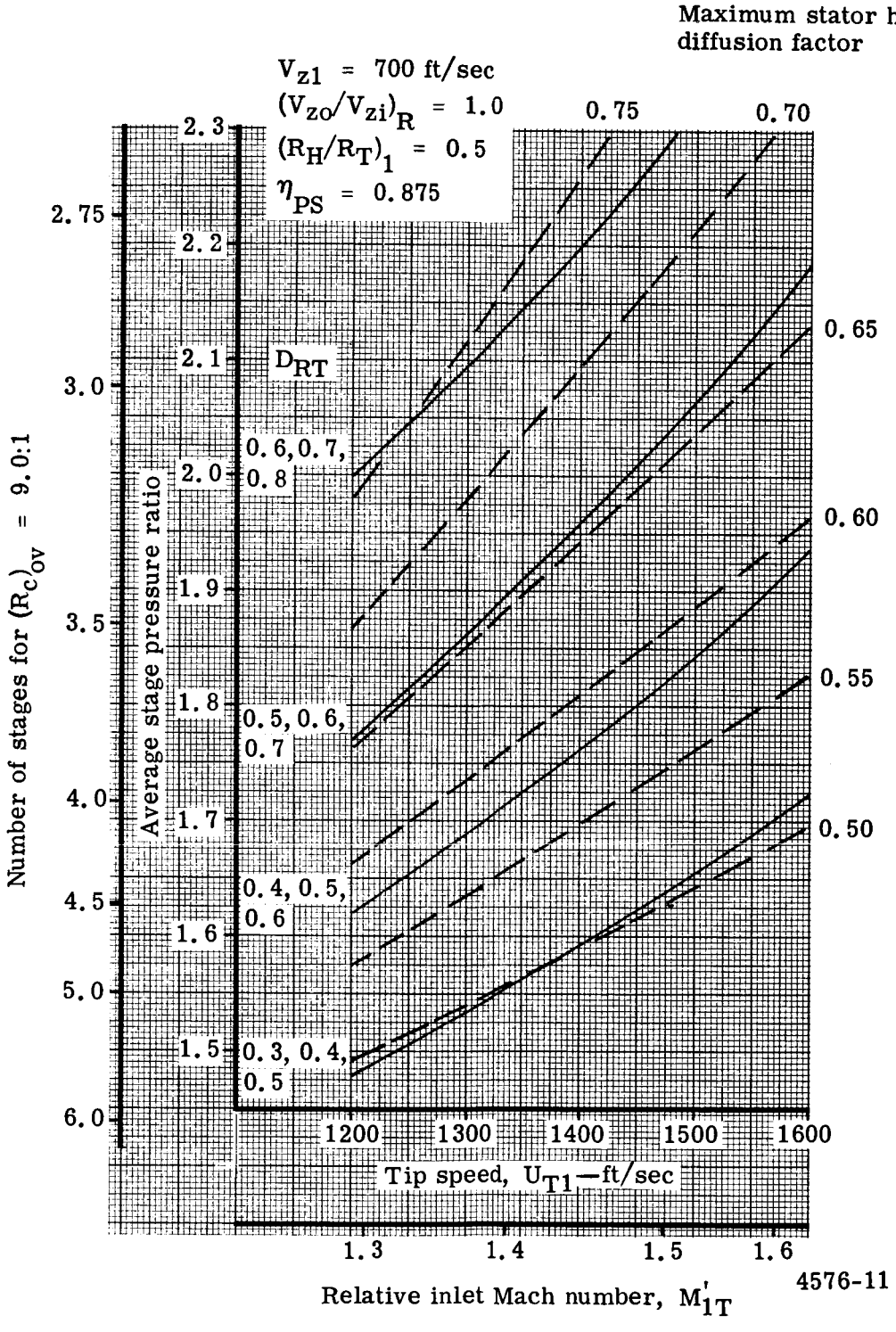

Figure 11. Effect of tip speed and rotor tip diffusion factor on maximum stator hub diffusion factor.

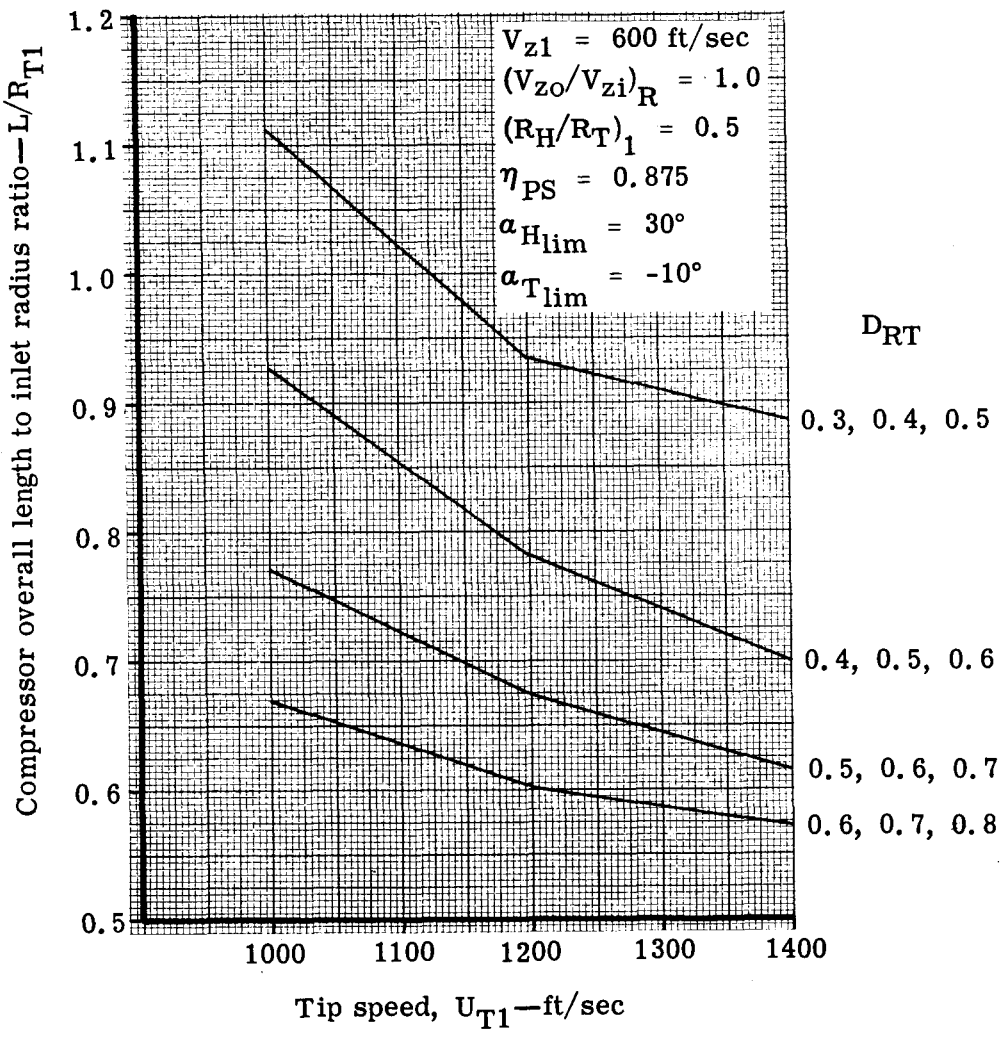

Figure 12. Effect of tip speed and rotor tip diffusion factor on compressor overall length.

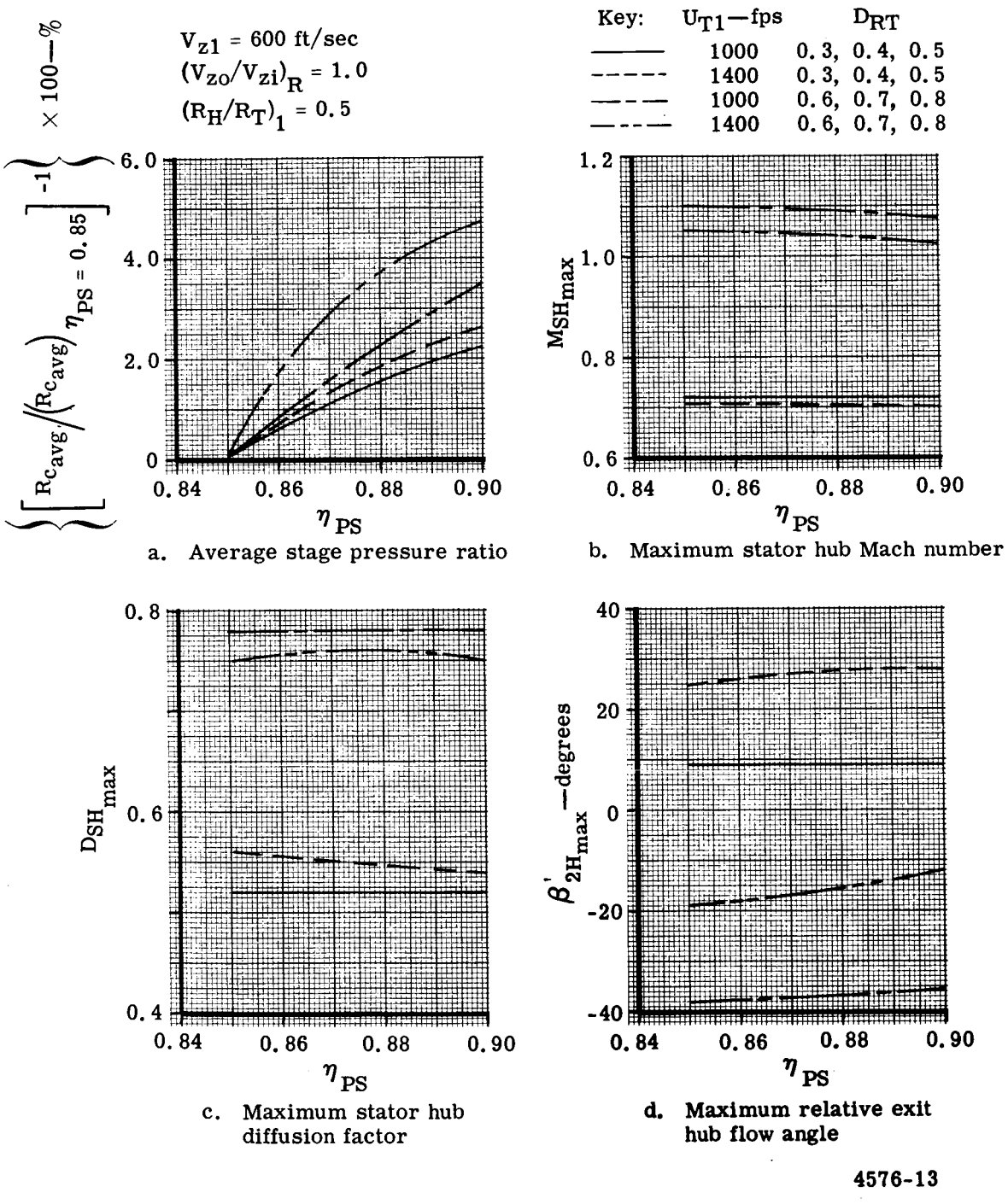

a. Average stage pressure ratio

b. Maximum stator hub Mach number

c. Maximum stator hub diffusion factor

d. Maximum relative exit hub flow angle

4576-13

Figure 13. Effect of polytropic stage efficiency on average stage pressure ratio and aerodynamic parameters.

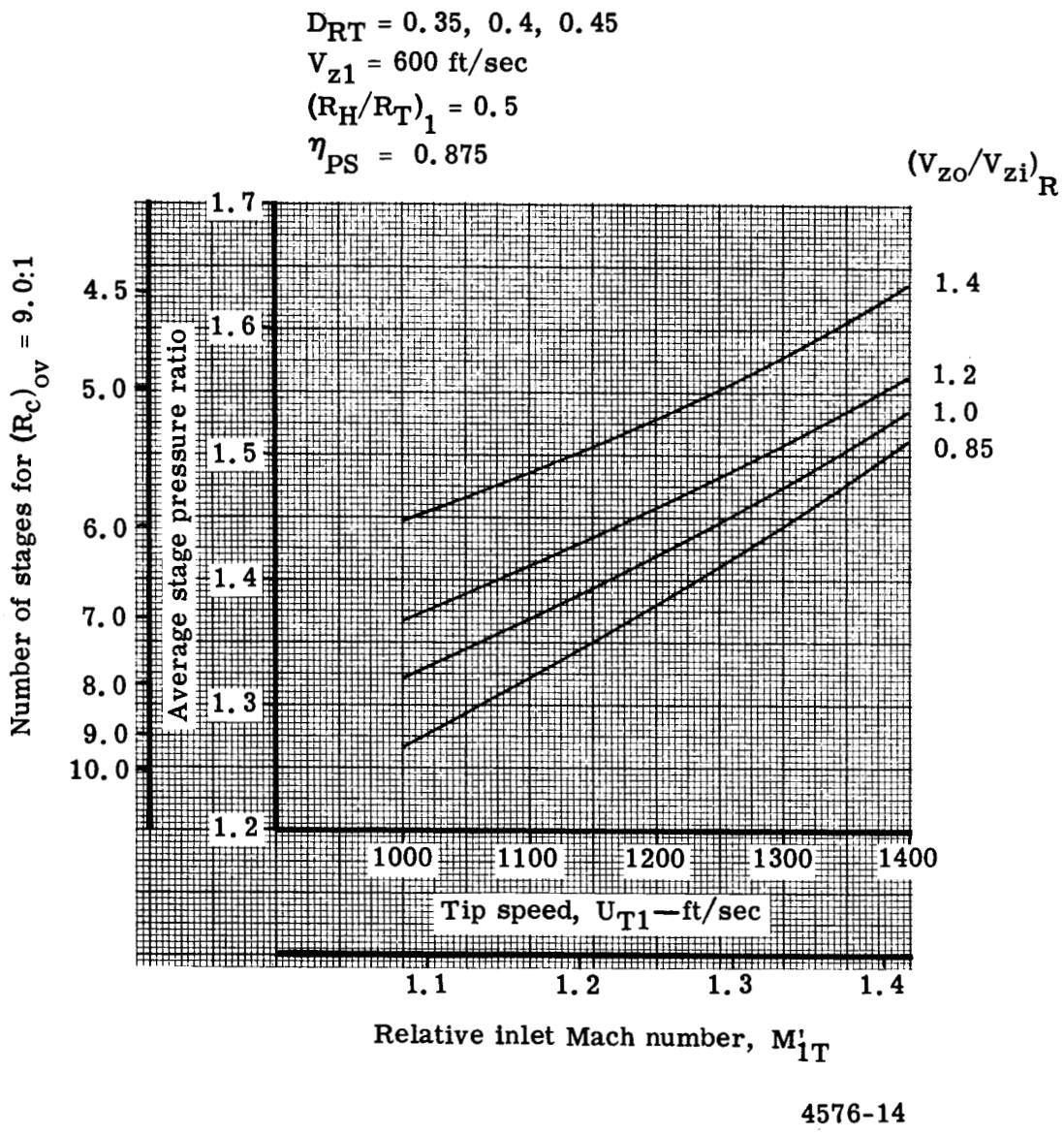

Figure 14a. Effect of tip speed and rotor axial velocity ratio on average stage pressure ratio.

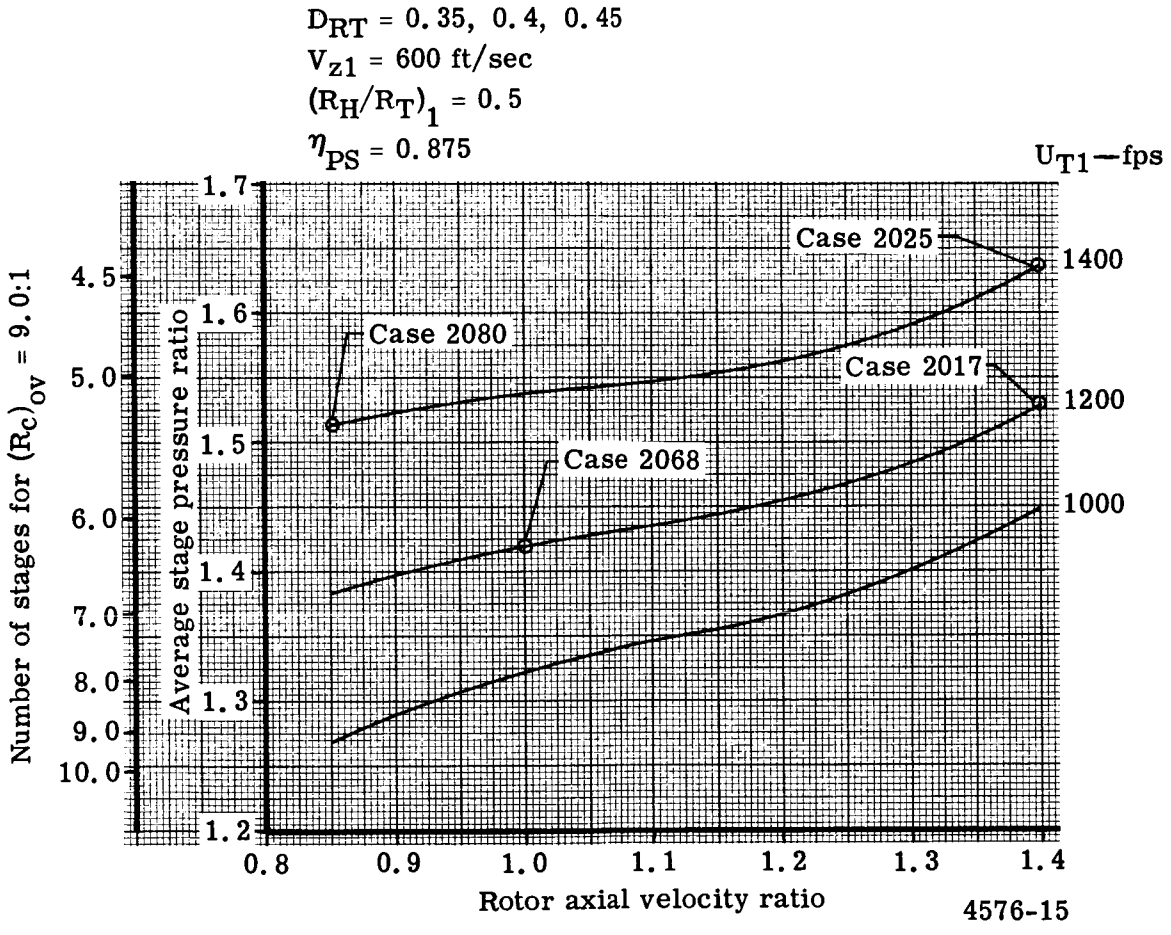

Figure 14b. Effect of tip speed and rotor axial velocity ratio on average stage pressure ratio.

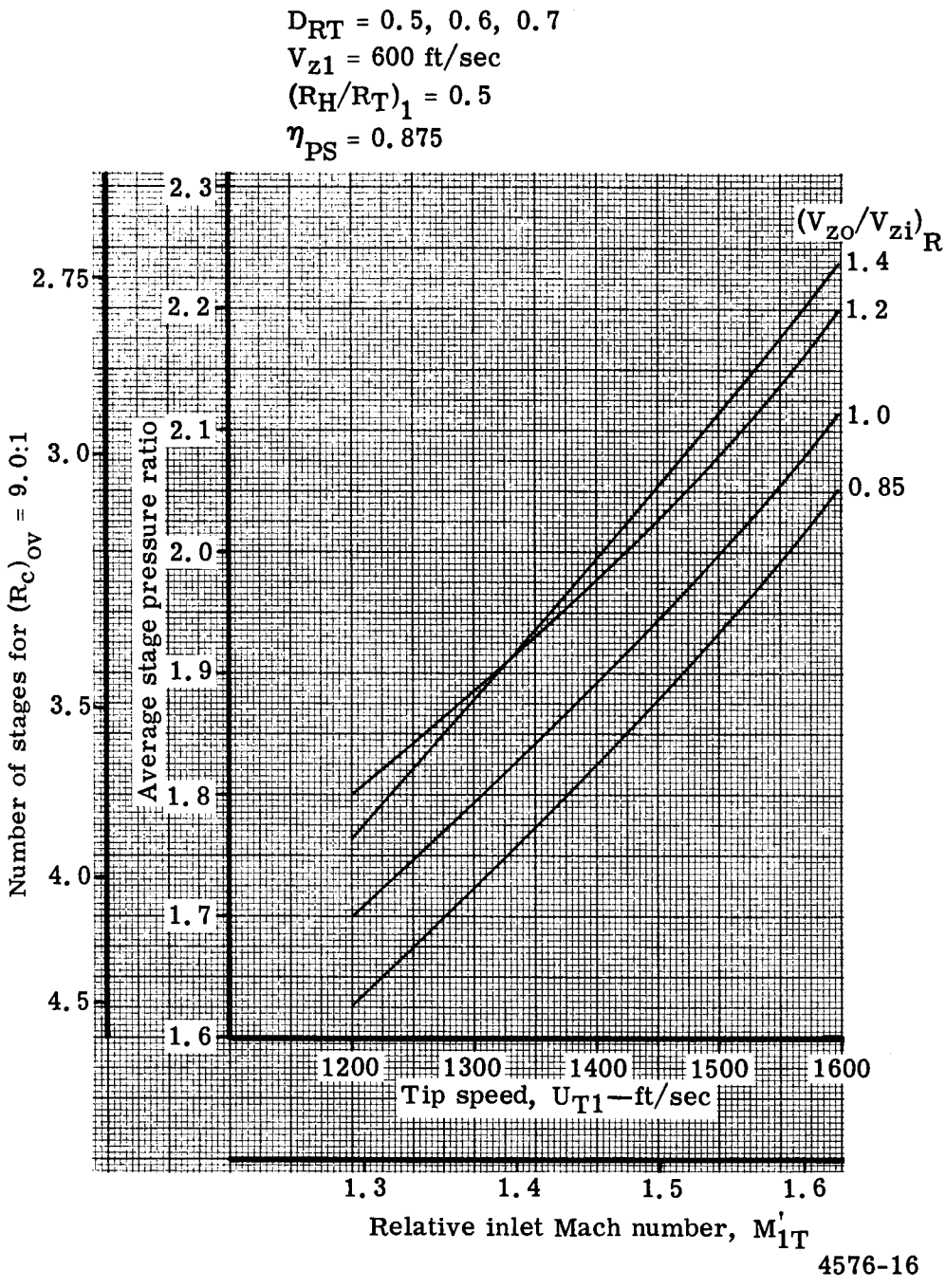

Figure 15a. Effect of tip speed and rotor axial velocity ratio on average stage pressure ratio for specified aerodynamic parameter limits ($M_{SH_{lim}}$ = 1.0 and $\beta'_{2H_{lim}}$ = -10°).

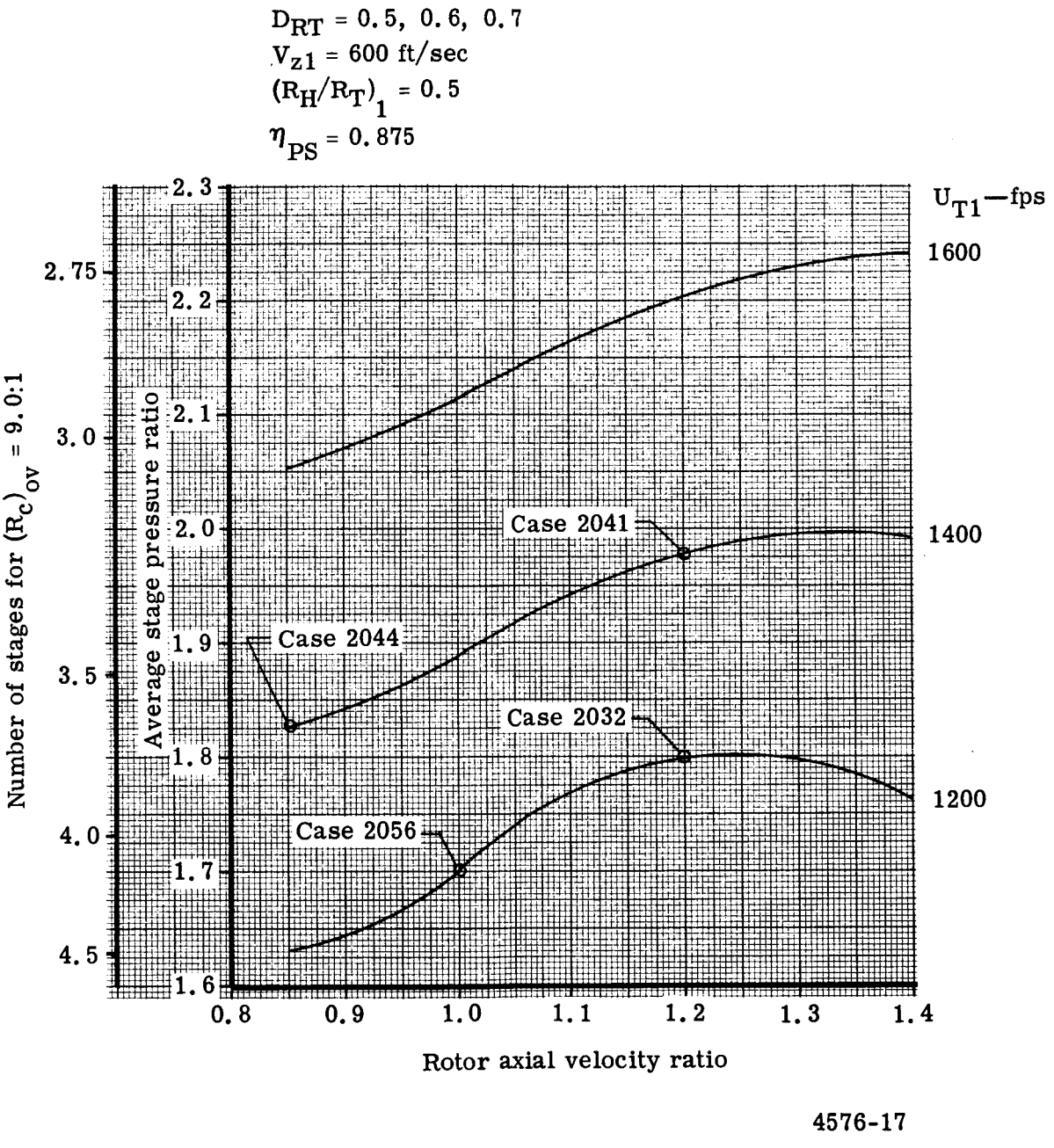

Figure 15b. Effect of tip speed and rotor axial velocity ratio on average stage pressure ratio for specified aerodynamic parameter limits ($M_{SH_{lim}}$ = 1.0 and $\beta'_{2H_{lim}}$ = -10°).

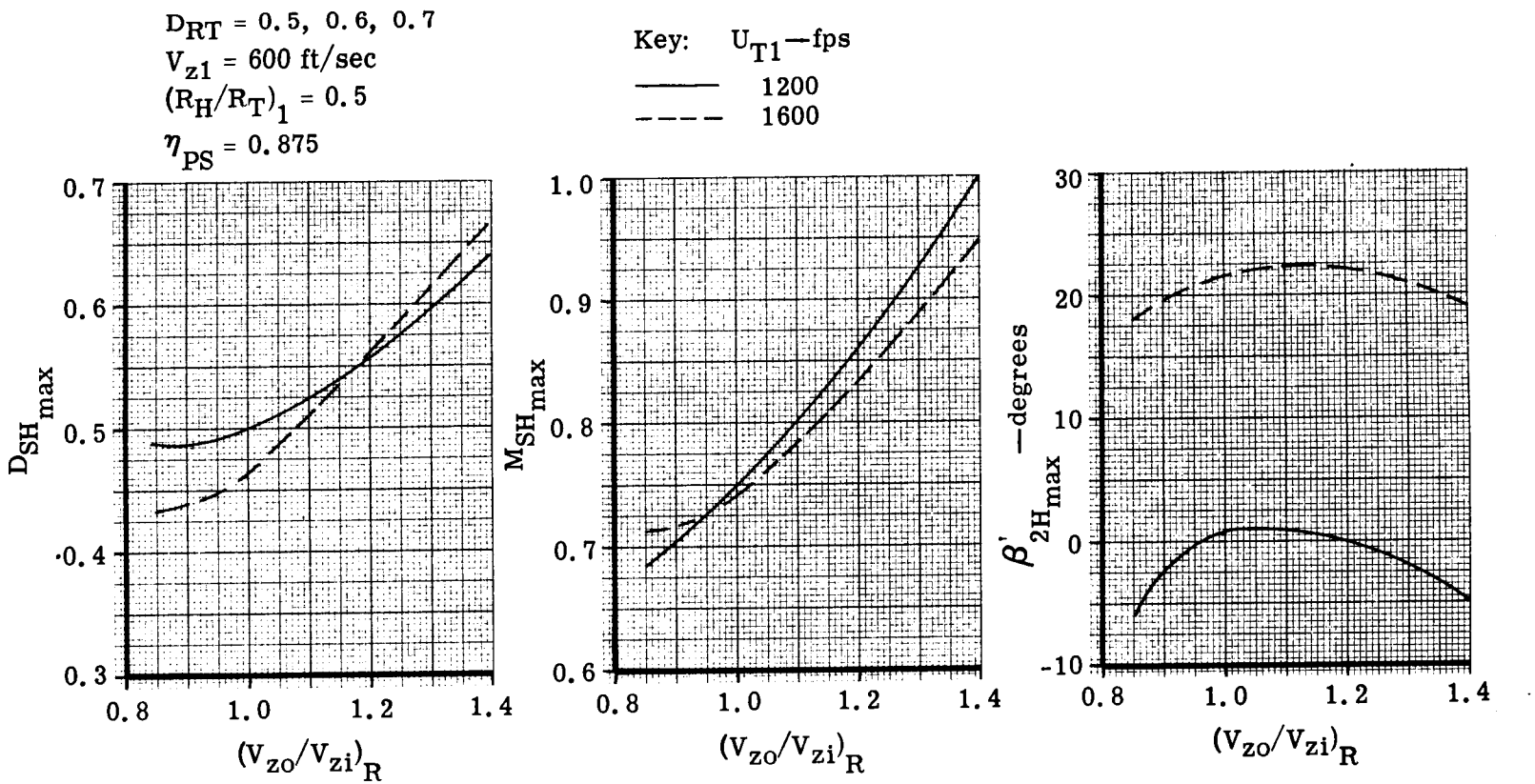

a. Maximum stator hub diffusion factor

b. Maximum stator hub Mach number

c. Maximum relative exit hub flow angle

4576-18

Figure 16. Effect of rotor axial velocity ratio on the aerodynamic parameters.

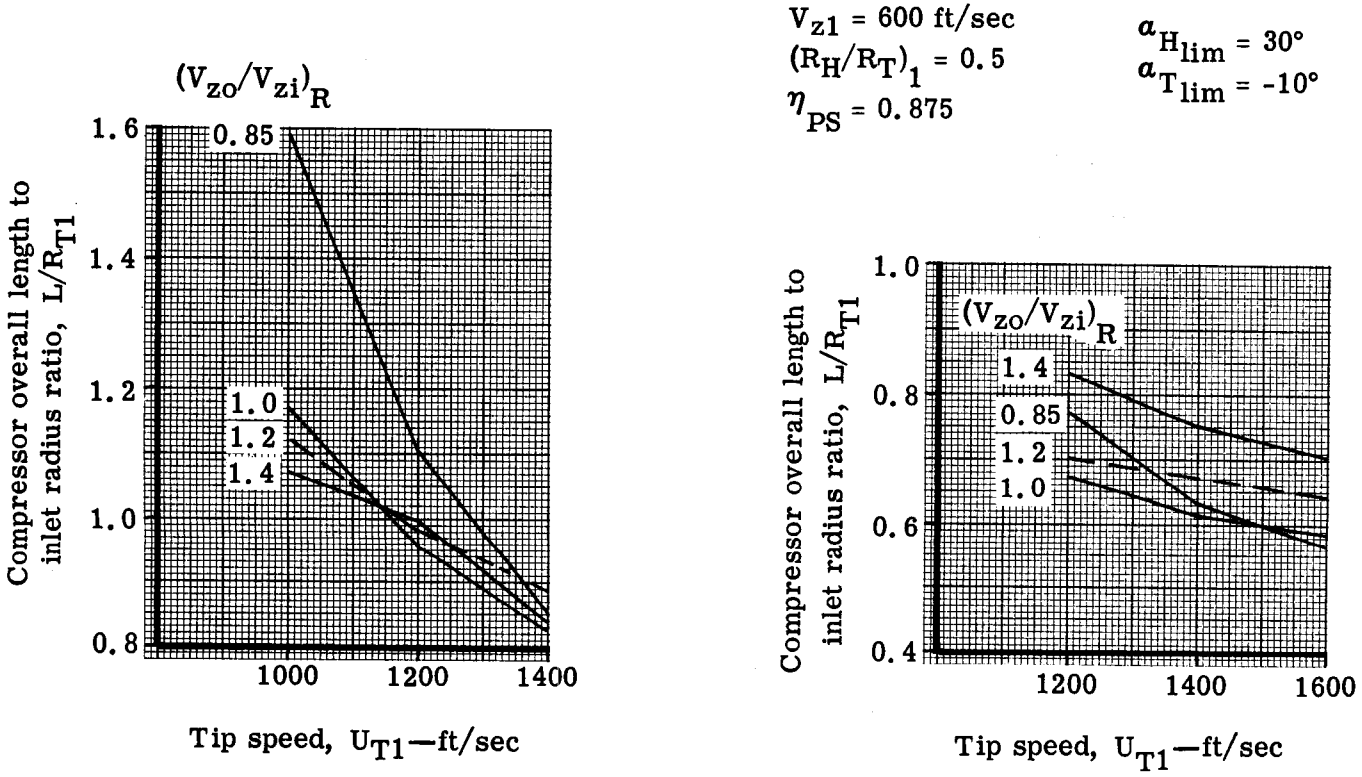

Figure 17. Effect of rotor axial velocity ratio on compressor overall length.

D_{RT} = 0.35, 0.4, 0.45
V_{z1} = 600 ft/sec
$(V_{zo}/V_{zi})_R$ = 1.0
$(R_H/R_T)_1$ = 0.5
η_{PS} = 0.875

Key: $\alpha_{H_{lim}}$ $\alpha_{T_{lim}}$
——— 40° -20°
– – – – 30° -10°

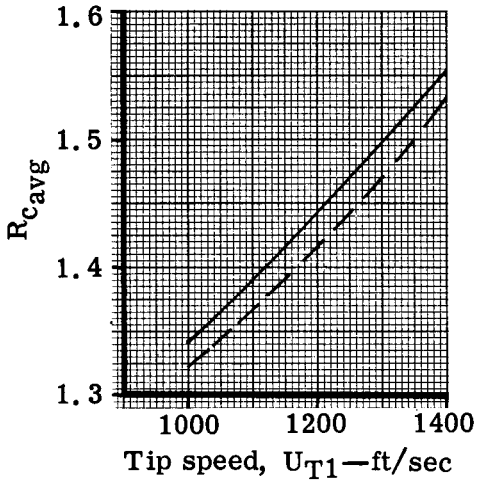

a. Average stage pressure ratio

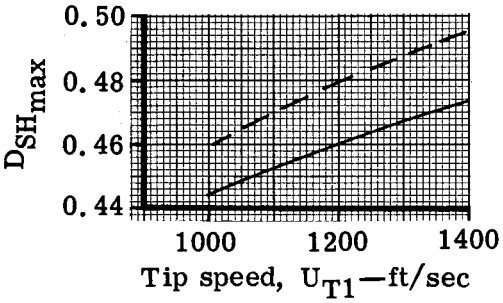

c. Maximum stator hub diffusion factor

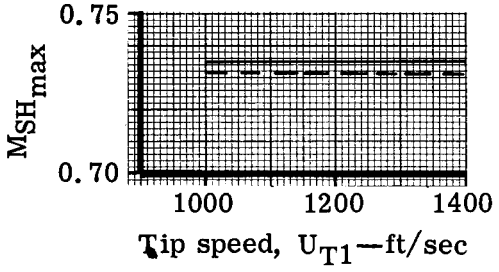

d. Maximum stator hub Mach number

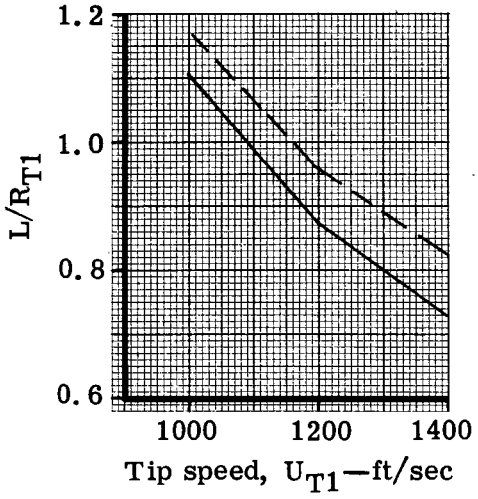

b. Compressor overall length to inlet radius ratio

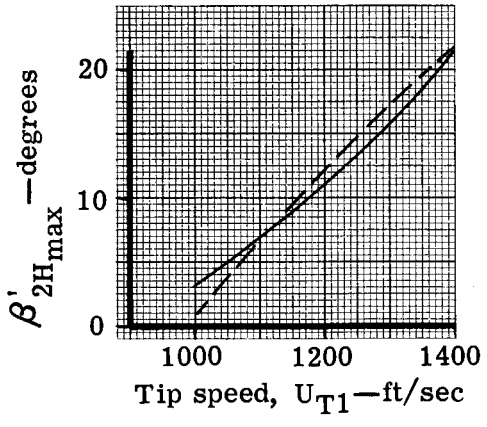

e. Maximum relative exit hub flow angle

4576-20

Figure 18. Effect of hub and tip ramp angle on average stage pressure ratio, overall length, and aerodynamic parameters.

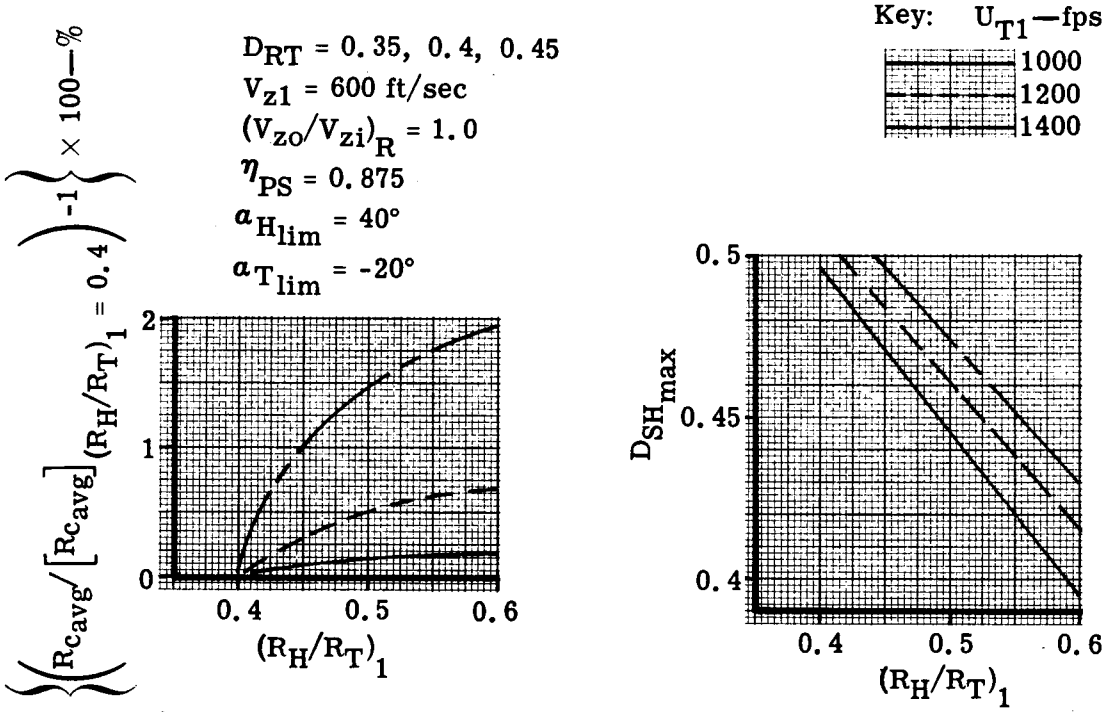

a. Average stage pressure ratio

b. Maximum stator hub Mach number

c. Maximum stator hub diffusion factor

d. Maximum relative exit hub flow angle

4576-21

Figure 19. Effect of inlet hub-tip radius ratio on average stage pressure ratio and aerodynamic parameters.

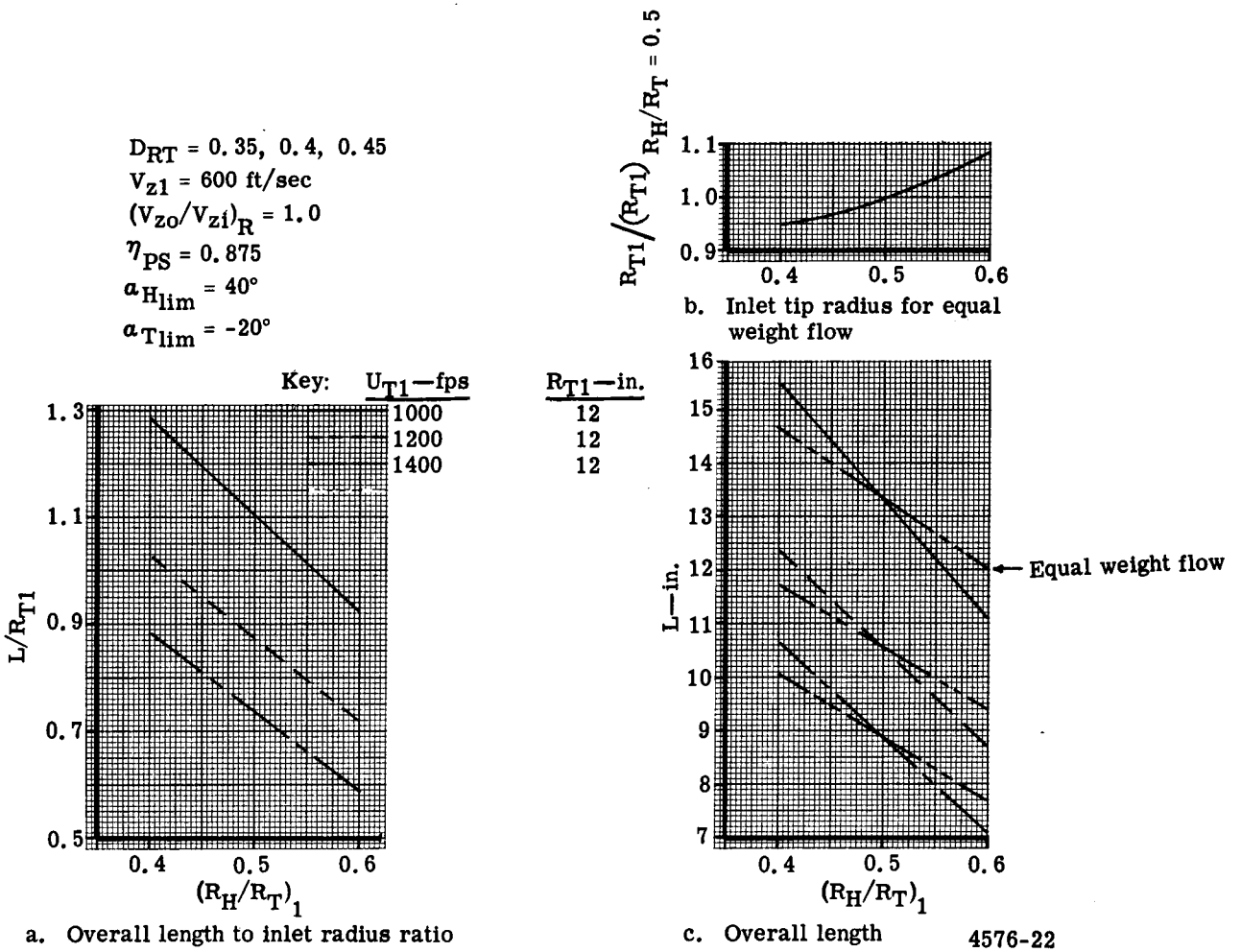

Figure 20. Effect of inlet hub-tip radius ratio on compressor overall length.